1,25-DIHYDROXYVITAMIN D_3-INDUCED GENES IN OSTEOBLASTS: UNCOVERING NEW FUNCTIONS FOR MENINGIOMA 1 AND SEMAPHORIN 3B IN SKELETAL PHYSIOLOGY

by

XIAOXUE ZHANG

Submitted in partial fulfillment of the requirements

for the Degree of Doctor of Philosophy

Thesis advisor: Paul N. MacDonald

Department of Pharmacology

CASE WESTERN RESERVE UNIVERSITY

May 2009

CASE WESTERN RESERVE UNIVERSITY

SCHOOL OF GRADUATE STUDIES

We hereby approve the thesis/dissertation of

Xiaoxue Zhang

candidate for the Ph.D. degree *.

(signed) Ruth Keri
(chair of the committee)

Paul N. MacDonald

Diane Dowd

Yu-Chung Yang

David Danielpour

(date) 2/19/2009

*We also certify that written approval has been obtained for any proprietary material contained therein.

I dedicate this thesis to my mother and father for their lifelong love,

encouragement and sacrifice

TABLE OF CONTENTS

LIST OF TABLES

LIST OF FIGURES

Acknowledgements

I would like to acknowledge my advisor, Dr. Paul MacDonald, for the continuous support and encouragement during the graduate study. Being patient and knowledgeable, he gave me step-by-step instruction and guidance on science. I would like to thank Dr. Diane Dowd, our lab member and my thesis committee member, who provided a lot of expertise on experiments and assistance on scientific writing. I would like to acknowledge my thesis committee members, Dr. Ruth Keri, Dr. David Danielpour, and Dr. Yu-Chung Yang, for their valuable inputs on my projects, especially when I was in difficult times and needed discussions and suggestions.

I would like to thank my previous and current lab members for their help on experiments, classes, and presentation practice. Dr. Amelia Sutton identified MN1 and SEMA3B and started excellent studies about these two genes. She generated SEMA3B transgenic animals, performed bone imaging analysis, and set up protocols for animal handling and bone cell analysis. Ms. Meika Moore gave plenty of assistance on animal experiments, including the maintenance, breeding, and genotyping of experimental mice. Dr. Tara Ellison made nuclear receptor expression constructs, gave valuable suggestions on molecular biology, and provided useful discussions on troubleshooting. Dr. Chi Zhang taught me a lot about graduate studies and assisted me to settle down in Cleveland. I am also grateful to other laboratories for generously sharing various equipments and

providing valuable experimental instructions, especially to the laboratories of Drs. Ruth Keri, Ruth Siegel, Monica Montano, and Yu-Chung Yang. I would like to acknowledge the previous and current departmental members, including Dr. Erin Milliken, Dr. Yu Chen, Dr. Hui Wang, Dr. Yiping Rong, Dr. Gang Zheng, for their help on classes, experiments, presentations, preliminary exams, and career choice. I would also like to thank the Pharmacology Department for providing this great training program.

I would like to acknowledge Dr. Ellen C. Zwarthoff (Erasmus Medical Center, Rotterdam, The Netherlands) and Dr. Gerard Grosveld (St. Jude Children's Research Hospital, Memphis, TN) for providing MN1 knockout mice breeding pairs. I would also like to thank Dr. Benoit de Crombrugghe for providing the 2300*lacZ* plasmid, Dr. John D. Minna for providing the pcDNA3-SEMA3B plasmid, Dr. Edward Greenfield for the assistance with *in vitro* osteoblast and osteoclast assays, and Ms. Patty Lott and the staff at the University of Alabama at Birmingham, Center for Metabolic Bone Disease, Histomorphometry and Molecular Analysis Core Laboratory, for performing the mineralized bone histology and histomorphometry.

Finally, I would like to acknowledge Dr. Bernard Tandler for helping me edit the thesis. I would like to thank my undergraduate teacher, Dr. Zihe Rao, for his continuous care and unconditional support during the past ten years. I would like to thank all the friends in my everyday life. It is their care and encouragement that made me able to accomplish the study abroad. I would like

to thank all my family members, who are so far away, but trying their best to support me to finish my graduate study.

Abbreviations

$1,25(OH)_2D_3$	1,25-dihydroxyvitamin D_3
1α-hydroxylase	25-hydroxyvitamin D-1α-hydroxylase
24-hydroxylase	25-hydroxyvitamin D_3-24-hydroxylase
25-hydroxylase	vitamin D 25-hydroxylase
$25(OH)D_3$	25-hydroxycholecalciferol
9-cis RA	9-cis retinoic acid
AF-2	Activation function-2
ALP	Alkaline phosphatase
AML	Acute myeloid leukemia
ATP	Adenosine triphosphate
ATRA	All trans retinoic acid
BCA	Bicinchoninic acid
BMP	Bone morphogenetic protein
BrdU	5-bromo-2-deoxyuridine
C/EBP	CCAAT/enhancer-binding protein
cAMP	Cyclic adenosine monophosphate
CaSR	Calcium-sensing receptor
Cbfa	Core binding factor
CBP	CREB-binding protein
CBS	Bovine calf serum
CCD	Cleidocranial dysplasia
CDK	Cyclin dependent kinase
CDKI	CDK inhibitor
CM	Conditional media
CT	Computed tomography
CREB	cAMP response element binding protein
CTD	carboxyl terminal domain
DAPI	4',6-diamidino-2-phenylindole
DBD	DNA-binding domain
DEXA	Dual-energy X-ray absorptiometry
Dlx	Distal-less homeobox
DNA	Deoxyribonucleic acid
DR	Direct repeats
DRIP	Vitamin D receptor interacting protein
E2	17β-estradiol
EGFR	Epidermal growth factor receptor
EMSA	Electrophoretic mobility shift assay
ER	Estrogen receptor
FABP4	Fatty acid binding protein 4
FBS	Fetal bovine serum
FGF	Fibroblast growth factor
FRP-4	Fizzled-related protein 4
GAPDH	Glyceraldehyde-3-phosphate dehydrogenase
GDF	Growth/differentiation factor

GR	Glucocorticoid receptor
GRE	Glucocorticoid response element
GRIP	Glucocorticoid receptor interacting protein
HAT	Histone acetyltransferase
HC	Hypertrophic chondrocyte zone
HDAC	Histone deacetylase
Hr	Hairless
IGF	Insulin-like growth factor
IGFBP	IGF binding protein
Ihh	Indian hedgehog
IL	Interleukin
KO	Knockout
LBD	Ligand-binding domain
LOH	Loss of heterozygosity
LPL	Lipoprotein lipase
LRP	Low-density lipoprotein receptor-related protein
MAP	Mitogen-activated protein
MAR	Mineral apposition rate
MARRS	Membrane-associated, rapid response steroid-binding protein
M-CSF	Macrophage colony stimulating factor
MED	Mammalian mediator complex
MEK	Mitogen-activated protein kinase kinase
MEKK	MEK kinase
MEM	Minimal essential media
MEPE	Matrix extracellular phosphoglycoprotein
MGP	Methyl methacrylate
MMA	Matrix Gla protein
MN1	Meningioma 1
mRNA	Messenger RNA
MTT	3-(4,5-dimethylthiazol-2-yl)-2,5-diphenyltetrazolium bromide
NCoA	Nuclear receptor coactivators
NCoR	Nuclear corepressor
NF-κB	Nuclear factor-κB
NR	Nuclear receptor
NTG	Non-transgenic
OPG	Osteoprotegerin
OSE	Osteoblast-specific cis-acting element
PC	Prehypertrophic zone
p/CAF	p300/associated factor
PCR	Polymerase chain reaction
PDGF	Platelet-derived growth factor
PFM	Parietal foramina
PKC	Protein kinase C
PMCA1	Plasma membrane calcium pump isoform 1

PPAR	Peroxisome proliferative activated receptor
pQCT	Peripheral quantitative computerized tomography
PTH	Parathyroid hormone
RAC	Receptor coactivator
RANK	Receptor activator of NF (nuclear factor)-κB
RANKL	RANK ligand
RAR	Retinoic acid receptor
RARE	Retinoic acid response element
Rb	Retinoblastoma
RNA	Ribonucleic acid
Runx	Runt-related transcription factor
RXR	Retinoid X receptor
RT-PCR	Reverse transcription-polymerase chain reaction
SEMA	Semaphorin
SERM	Selective estrogen receptor modulators
Shh	Sonic hedgehog
SKIP	Ski interacting protein
SMRT	Silencing mediator of retinoid and thyroid hormone receptors
SRC	Steroid receptor coactivator
STAT	Signal transducer and activator of transcription
TAZ	Transcriptional activator with PDZ-binding motif
TERT	Telomerase reverse transcriptase
TG	Transgenic
TGF	Tumor growth factor
TIF	Transcriptional intermediary factor
TM	Thrombomodulin
TNF	Tumor necrosis factor
TRAF	TNF receptor associated factors
TRAP	Thyroid receptor interacting protein
TRAP	Tartrate-resistant acid phosphatase
TRPV	Transient receptor potential vanilloid
VDBP	Vitamin D binding protein
VDR	Vitamin D receptor
VDRE	Vitamin D response element
WINAC	WSTF including nucleosome assembly complex
WSTF	Williams syndrome transcription factor
WT	Wild-type

1,25-Dihydroxyvitamin D_3-Induced Genes in Osteoblasts: Uncovering New Functions for Meningioma 1 and Semaphorin 3B in Skeletal Physiology

ABSTRACT

By

Xiaoxue Zhang

The vitamin D endocrine system is essential for calcium and phosphate homeostasis and skeletal mineralization. 1,25-dihydroxyvitamin D_3 ($1,25(OH)_2D_3$) hormone binds to the vitamin D receptor (VDR) to regulate gene expression. In turn, these gene products mediate the actions of $1,25(OH)_2D_3$ in mineral-regulating target cells. $1,25(OH)_2D_3$ impacts bone indirectly by promoting intestinal absorption of calcium and phosphate and directly by acting on osteoblasts and osteoclasts. Despite the direct regulatory roles of $1,25(OH)_2D_3$ in bone, relatively little is known about the mechanisms or $1,25(OH)_2D_3$-target genes in skeletal cells. Here, we identified meningioma 1 (MN1) and semaphorin 3B (SEMA3B) as two novel $1,25(OH)_2D_3$-stimulated genes in osteoblastic cells, and uncovered their new functions in skeletal physiology. We demonstrated that MN1 is a coactivator for VDR-mediated transcription, and calvarial osteoblasts derived from MN1 knockout mice displayed altered morphology, decreased growth rate, impaired motility, attenuated $1,25(OH)_2D_3$/VDR-mediated

transcription, reduced alkaline phosphatase activity, decreased mineralized nodule formation, but enhanced adipogenesis. In addition, MN1 knockout osteoblasts are defective in supporting $1,25(OH)_2D_3$-stimulated osteoclastogenesis, presumably due to marked reduction in the RANKL:OPG ratio. These data indicate an important role for MN1 in maintaining appropriate osteoblast proliferation, maturation and function. This may partially account for the intramembranous ossification defects of cranial bones in MN1 knockout mice. Our data reveal that osteoblast-derived SEMA3B alters the global skeletal homeostasis in intact animals and the bone cell activities in cultures. Transgenic mice with osteoblast-targeted over-expression of SEMA3B develop osteopenia, with decreased body weight, reduced bone mineral density, and aberrant trabecular structure compared to the nontransgenic littermates. Histomorphometry studies indicated that this was likely due to increased osteoclast numbers and activity. Indeed, primary osteoblasts obtained from SEMA3B transgenic mice stimulated osteoclastogenesis to a greater extent than nontransgenic osteoblasts. This study revealed the novel roles of SEMA3B for controlling bone cell activities *in vitro* and bone remodeling *in vivo*. Collectively, we characterized MN1 and SEMA3B as $1,25(OH)_2D_3$-induced genes in osteoblasts and established their significance in regulating osteoblast function, osteoclast formation, and skeletal homeostasis. This provides further insights about the direct actions of $1,25(OH)_2D_3$ in bone remodeling.

Chapter I

Introduction

Discovery of vitamin D

Vitamin D deficiency causes a severe bone deformity called rickets, a softening and weakening of bones (1). Rickets was a rampant disease among poor children during the Industrial Revolution because the dietary vitamin D was inadequate and the environmental pollution blocked sunlight, which is required for synthesizing vitamin D. Rickets was first described scientifically by Daniel Whistler (1645) and Francis Glisson (1650). However, vitamin D was not identified as the cause of rickets until 1910-1930. In the late 1910s, Mellanby found that dogs developed rickets when they were raised indoors in the absence of sunlight under special diets. The phenotype could be prevented by feeding food rich in fat-soluble vitamins, such as cod liver oil, butter, or whole milk, suggesting that there is a fat-soluble trace component with anti-rachitic function. It was called vitamin D because it was the fourth identified vitamin (2).

While scientists were trying to isolate the essential nutrients for curing rickets, a different approach to treat rickets was discovered. In the 1880s, Palm studied the geographical distribution of rickets and found that rickets development was correlated with a shortage of sunlight exposure (2). In 1919, Huldschinsky found that ultraviolet (UV) light exposure was able to cure severe

rickets in children (3). In 1923, Goldblatt and Soames demonstrated that livers from sunlight or UV light irradiated rats could cure rickets when fed to rachitic animals (3). Later, Hess and Weinstock discovered that feeding rachitic rats with UV light irradiated skin or food substances can protect rats against rickets (3). Thus, instead of an essential dietary trace element, the fat-soluble vitamin D can be synthesized by the body in a pathway involving UV irradiation. The chemical structures and the synthetic pathway of vitamin D were established in the 1930s by Windaus and other scientists. Vitamin D_2 (or calciferol) was UV-produced from ergosterol and was chemically characterized in 1932. In 1936, Vitamin D_3 (or cholecalciferol) was synthesized from 7-dehydrocholesterol by UV irradiation. These discoveries showed that the anti-rachitic vitamin D is a secosteroid (3, 4).

Vitamin D metabolism

Vitamin D_3 is obtained directly from diet or synthesized by the epidermis when 7-dehydrocholesterol reacts with sunlight, more specifically, the ultraviolet B portion with the energies between 290-315 nm (5, 6) (Figure I-1). Vitamin D_3 is first hydroxylated to 25-hydroxycholecalciferol [$25(OH)D_3$ or calcidiol] by the catalysis of vitamin D 25-hydroxylase (25-hydroxylase) enzyme in hepatocytes (Figure I-1). $25(OH)D_3$ is the major circulating form of vitamin D. It associates with the carrier protein, vitamin D binding protein (VDBP), and is transported to other organs through the plasma. $25(OH)D_3$ is further hydroxylated in kidney by 25-hydroxyvitamin D-1α-hydroxylase (1α-hydroxylase) to form 1,25-dihydroxyvitamin D_3 [$1,25(OH)_2D_3$ or calcitriol], the bioactive form of vitamin D (7)

(Figure I-1). Mutation of 1α-hydroxylase causes vitamin D-dependent rickets type 1 (8-10), a rachitic syndrome characterized by a lack of detectable $1,25(OH)_2D_3$ in the serum. $25(OH)D_3$ and $1,25(OH)_2D_3$ are inactivated by the ubiquitous cytochrome P450 enzyme, 25-hydroxyvitamin D_3-24-hydroxylase (24-hydroxylase), to generate $24,25(OH)_2D_3$ and $1,24,25(OH)_3D_3$, respectively, which are further oxidized, degraded, and secreted (11) (Figure I-1).

The serum levels of $1,25(OH)_2D_3$ are tightly controlled by calcium and phosphate needs. Regulation of $1,25(OH)_2D_3$ by calcium is mediated primarily through the parathyroid gland. Hypocalcemia induces the secretion of parathyroid hormone (PTH), which targets the kidney proximal tubular cells to promote the synthesis and enzyme activity of 1α-hydroxylase (12, 13). In addition, restriction of dietary phosphate enhances the transcription and activity of 1α-hydroxylase in a calcium- and PTH-independent manner (13, 14). Recent studies suggested that this regulation may be mediated through other systemic hormones, such as phosphatonins, fibroblast growth factor 23 (FGF23), fizzled-related protein 4 (FRP-4), and matrix extracellular phosphoglycoprotein (MEPE) (15, 16). $1,25(OH)_2D_3$ is also regulated by itself through a feedback mechanism. $1,25(OH)_2D_3$ suppresses PTH secretion, stimulates 24-hydroxylase expression, and inhibits 1α-hydroxylase synthesis and activity (17-19).

Vitamin D receptor and cofactors

Vitamin D receptor (VDR)

Most biological activities of $1,25(OH)_2D_3$ are mediated through vitamin D receptor (VDR). VDR is a member of group 1 nuclear receptors (NR), which also include retinoic acid receptors (RARs), thyroid hormone receptors (TRs), peroxisome proliferators-activated receptors (PPARs), RAR-related orphan receptors (RORs), pregnane X receptor (PXR), liver X receptors (LXRs), and constitutive androstane receptor (CAR) (20). Most of them form active heterodimer complexes with retinoid X receptor (RXR) when ligand(s) binds. $1,25(OH)_2D_3$ binding triggers conformational changes in VDR and the formation of VDR-RXR heterodimers, which bind to vitamin D response elements (VDREs) at gene promoter region and recruit various classes of cofactors to regulate the transcription of target genes. These genes mediate the functions of $1,25(OH)_2D_3$ *in vivo.*

The N-terminus of VDR is a DNA-binding domain (DBD) (Figure I-2A). The DBD is the most conserved region among nuclear receptor superfamily members. It is characterized by two zinc-binding modules that direct the sequence-specific association of receptors to DNA. In each module, the zinc atom is coordinated with four conserved cysteine residues that can stabilize the finger structure. Despite their similar structures, the two modules have different functions. The N-terminal module directs the specific binding of VDR to the major DNA groove of the VDRE, and the other module provides an interaction surface for RXR (21, 22). The C-terminus of VDR is a ligand-binding domain (LBD) (Figure I-2A), which includes 12 α-helices. Like the LBDs in other nuclear receptors, the VDR LBD contains a ligand dependent activation function-2 (AF-2)

domain, with the core structure located within helix-12 (23). $1,25(OH)_2D_3$ binding leads to a conformational change of the AF-2 domain, closing the ligand binding pocket of VDR and providing a surface for interaction with other proteins (Figure I-2B) (24). Thus, the LBD is also a multifunctional globular domain that mediates the selective interactions of VDR with RXR as well as with other transcription factors (25). The DBD and LBD are connected by a hinge region (Figure I-2A), which allows the rotational flexibility and facilitates the VDR interaction with DNA and other proteins (26). VDR proteins with mutation(s) on DBD or LBD that are transcriptionally inactive cause vitamin D resistant rickets, a rachitic disorder that is unresponsive to vitamin D treatment (25, 27, 28).

The ligand-activated VDR-RXR heterodimer binds to the VDRE at gene promoter regions to regulate the transcription of primary $1,25(OH)_2D_3$ responding genes (29) (Figure I-3). Classic VDRE are termed DR-3 elements, which contain two conservative hexanucleotide repeats (RGKTSA, R = A or G, K = G or T, S = C or G) separated by a 3-bp spacer (30). Representative DR-3 elements are shown in Figure I-3 (31-34). In addition to the DR-3 type of VDRE, everted repeats, DR-4 and DR-6 (direct repeats with four or six intervening nucleotides) also were discovered (35-39). Their binding affinity and binding pattern to VDR-RXR may be different from the classical DR-3 VDREs (29, 40, 41). Most primary $1,25(OH)_2D_3$ target genes have at least one copy of a VDRE within 1 kb upstream of the transcriptional start site. However, functional VDR binding sites can be distant or downstream from the transcriptional start site. Such VDREs mediate the activation by $1,25(OH)_2D_3$ on LRP5, RANKL, and TRPV6 gene

transcription (42-44). DNA looping or other higher chromatin structures may help bring these distant VDREs close to the basal transcriptional machinery.

VDR cofactors

To regulate gene transcription, VDR interacts with various classes of coactivators and/or corepressors (Figure I-3). Most of the cofactors constitute large multiprotein complexes and act at different molecular levels, such as chromatin remodeling, histone modification, transcriptional machinery formation, and further transcription factor recruitment.

Steroid receptor coactivator (SRC) family members, or nuclear receptor coactivators (NCoA), associate with VDR in a ligand-dependent manner and promote VDR-mediated transcriptional activity. The interaction is mediated through a conserved leucine-rich LXXLL motif (L, leucine; X, any amino acid), or NR box within SRC proteins and a hydrophobic pocket within the LBD of nuclear receptors (45). Structural studies reveal that the carboxylate group of a glutamic acid residue in helix 12 and the amino group of a lysine residue in helix 3 of the LBD are essential for positioning the leucine side chains of LXXLL motif into a hydrophobic cavity of the LBD (Figure I-2B) (46-48). Although the LXXLL motif is required for SRCs to bind VDR and other nuclear receptors, the flanking amino acids of NR box have important roles in selectively recognizing nuclear receptors (49). SRC family proteins include steroid receptor coactivator-1/nuclear receptor coactivator-1 (SRC-1/NCoA-1), steroid receptor coactivator-2/transcriptional

intermediary factor 2/glucocorticoid receptor interacting protein 1/nuclear receptor coactivator-2 (SRC-2/TIF-2/GRIP-1/NCoA-2), and receptor coactivator-3 (RAC-3) (50-52). SRCs contain histone acetyltransferase (HAT) activity (53). HAT acetylates the amino group of lysine in core histone proteins, neutralizes the positive charges on the histone, decreases the binding affinity of histone and DNA, leading to a “loosening” of chromatin structure, and facilitates transcription factor assembly on exposed DNA (54). Partial functional redundancy has been described among SRC coactivators. Ablation of SRC-1 in mice only causes partial resistance to hormonal response, and the mRNA expression of TIF-2 is increased in this model (55).

In addition to binding VDR and promoting transcription, SRCs also directly recruit other transcription factors, such as CREB (cAMP response element binding protein)-binding protein (CBP/p300) (56). CBP/p300 is a co-integrator that associates with a variety of transcription factors (57). CBP/p300 has HAT activity and assists SRCs in remodeling chromatin structure (58, 59). Moreover, CBP/p300 acetylates non-histone proteins, such as TFIIEβ and TFIIF within the basal transcription machinery (60). This potentially facilitates the further “melting” of the promoter, allowing transcription initiation.

Another VDR coactivator complex is the vitamin D receptor interacting protein/thyroid receptor interacting protein (DRIP/TRAP) complex, or MED mammalian mediator complex (MED) (61-63). DRIP contains 22-28 subunits (64). Most hormone receptors and some of their coactivators bind DRIP to

control gene transcription. In *in vitro* transcription assays using a chromatized DNA template, purified DRIP complex strongly activated VDR-mediated transcription in a ligand-dependent manner (62). Knockout of DRIP205 (TRAP220) or DRIP100 (TRAP100) subunit impairs gene activation and causes developmental defects in the mouse (65, 66). Although the DRIP complex does not possess SRC proteins or HAT activity, it communicates with other VDR coactivators to influence the recruitment of RNA polymerase II to gene promoter regions and the formation of transcription pre-initiation complex (67, 68).

Growing numbers of other VDR coactivators have been characterized. p300/associated factor (p/CAF) was discovered as the first mammalian HAT (69). It interacts with p300/CBP and SRCs and stimulates VDR-mediated transcription (70, 71). SWI/SNF complex mediates ATP-dependent nucleosome disruption, which overcomes the repressive effects of chromatin structures and enhances the access of transcription factors to the promoter region (72, 73). Nuclear coactivator-62 kDa /Ski interacting protein (NCoA62/SKIP) associates with the VDR-RXR heterodimer and augments VDR-RXR mediated transcription (74). Furthermore, NCoA62/SKIP regulates RNA processing by interacting with splicing machinery components and nuclear matrix-associated proteins, indicating its role in coupling VDR-mediated transcriptional regulation to RNA splicing (75, 76).

In some cases, VDR-RXR binds VDREs to suppress gene transcription, such as the negative control of PTH expression by $1,25(OH)_2D_3$ (77). Binding of

VDR-RXR to such negative VDREs recruits nuclear corepressor/silencing mediator of retinoid and thyroid hormone receptors (NCoR/SMRT) and histone deacetylases (HDAC) (78-80). HDAC removes the acetyl group from lysine in histone proteins to maintain a higher order, compact chromatin structure that inhibits the formation of transcription pre-initiation complex (54). Some VDR-RXR interacting proteins associate with both coactivators and corepressors. Examples include CBP/p300, NCoA62/SKIP, and WSTF (Williams syndrome transcription factor)-including nucleosome assembly complex (WINAC) (81, 82). Their effects on gene transcription depend on the cellular expression of other cofactors. Therefore, $1,25(OH)_2D_3$ regulation of gene transcription can be both cell and promoter selective.

Non-genomic rapid response

Some cellular responses of $1,25(OH)_2D_3$ are too rapid to involve gene transcription changes. These responses include rapid intestinal absorption of calcium, opening of chloride channels in osteoblasts, insulin secretion by pancreatic cells, and stimulation of protein kinase C (PKC) and mitogen-activated protein (MAP) kinases (81-83). It is proposed that these rapid responses are mediated through functional membrane receptor(s) for $1,25(OH)_2D_3$ (84). One identified receptor is the classical VDR that is located near or within caveolae at plasma membrane. Caveolae-enriched membrane fractions are able to bind $1,25(OH)_2D_3$ with high specificity, and VDR knockout mice are defective in $1,25(OH)_2D_3$-stimulated chloride channel opening (85). Another candidate

receptor is membrane-associated, rapid response steroid-binding protein (MARRS), or ERp57, a thiol-dependent oxidoreductase (86). Knockdown of ERp57 attenuated the $1,25(OH)_2D_3$-induced rapid uptake of phosphate in intestinal cells (87). Nonetheless, knowledge about the non-genomic rapid responses of $1,25(OH)_2D_3$ still is limited, and further investigation is required to elucidate the complex mechanism.

Functions of vitamin D endocrine system in bone development

The classic physiological functions of vitamin D endocrine system are to adjust calcium and phosphate homeostasis and to regulate bone development. In response to low serum calcium, the parathyroid gland produces parathyroid hormone (PTH), which stimulates the expression and activity of renal 1α-hydroxylase to synthesize $1,25(OH)_2D_3$. As a feedback mechanism, $1,25(OH)_2D_3$ inhibits its own expression through suppressing PTH and 1α-hydroxylase, and inducing the inactivating enzyme 24-hydroxylase (19, 77, 88). VDR knockout mice develop hyperparathyroidism, with enlarged parathyroid glands and high serum PTH levels (89). $1,25(OH)_2D_3$ has indispensable roles in active calcium transport by stimulating the expression key components, including TRPV5/6 epithelial calcium channel (ECaC1/2), calbindin-D, and plasma membrane calcium pump isoform 1 (PMCA1) (90-94). Similarly, $1,25(OH)_2D_3$ induces Na-Pi cotransporter type IIB (NPT2b) and promotes transcellular phosphorus movement (95). Calcium and phosphorus absorption defects are observed in rickets patients and in VDR or 1α-hydroxylase knockout mice, and a high

calcium/phosphorus diet is required to reverse the resulting hyperparathyroidism, rickets, and osteomalacia (92, 96, 97). Bone is a major $1,25(OH)_2D_3$ target organ. Although most disorders related to $1,25(OH)_2D_3$/VDR deficiency are secondary to the impaired calcium absorption, certain defects cannot be corrected by mineral normalization (97). In addition, VDR is expressed in osteoblasts and the direct regulation of $1,25(OH)_2D_3$ on bone cell activities has been reported.

Bone structure

The skeletal system is composed of bone and cartilage, both of which support the body structure. They build a platform for muscle attachment, provide mobility, and protect internal organs. While cartilage is characterized by its proteoglycan-rich matrix, bone is distinguished by its mineralized inorganic matrix composed of calcium and phosphate. Cartilage is poorly repaired in adults, but bone is a highly dynamic tissue that continuously undergoes remodeling. Bone remodeling includes removal of mineralized bone and formation of new bone. The remodeling process not only plays significant roles in bone damage repair, but also meets the metabolic needs for minerals. Ninety-nine percent of calcium *in vivo* is kept in the skeleton in the form of highly insoluble calcium phosphate crystals (98). When circulating levels of calcium and phosphate become low, bone contributes to the maintenance of mineral homeostasis by dissolving the calcium phosphate crystals (99).

Bone is formed in two different manners, endochondral ossification and intramembranous ossification. In endochondral ossification, mesenchymal cells differentiate into chondroblasts that produce a hyaline cartilage model around the bone collar. Accompanied by vascular invasion, the chondrocytes proliferate, become hypertrophic, and undergo apoptosis. Then their extracellular matrix becomes a template for osteoblasts, which calcify the remnant cartilage components. Finally the chondrocytes are completely replaced by osteoblasts and calcified bone. Most bones in the skeleton, especially long bones, are developed through endochondral ossification (100, 101). In contrast, intramembranous ossification does not involve a cartilaginous template. Mesenchymal cells migrate to the collagen fibrils, directly differentiate into osteoblasts, and deposit the unmineralized matrix (osteoid), which subsequently is mineralized to form bone. Flat bones that comprise the cranium, medial clavicles, and some other components of craniofacial skeleton are formed through intramembranous ossification (102).

There are two types of mature bones, cortical bone and trabecular bone. They have different morphologies but the same composition. Most of the outer skeleton is cortical bone, which is compact, dense, and has minimal gaps or spaces. Cortical bone has a high resistance to bending, and thus provides mechanical strength and protection. Trabecular bone, also called cancellous bone or spongy bone, is found in all bones. Trabecular bone is less dense and more elastic, with a higher turnover rate. It contributes only twenty percent of

bone mass but eighty percent of bone surface. Therefore, it is the major site for blood vessels and bone marrow and to undergo active remodeling (99).

Bone consists of extracellular matrix and cells (including osteoblasts, osteocytes, and osteoclasts). Seventy percent of bone is inorganic matrix, hydroxyapatite [$Ca_5(PO_4)_3(OH)$], a crystalline mineral. Hydroxyapatite is built on type I collagen fibers, which have a triple-helix structure composed of two identical Iα1 chains and a similar Iα2 chain (103). Collagen constitutes ninety percent of the organic bone matrix. Non-collagenous proteins include proteoglycans, glycoproteins, and γ-carboxylated (Gla) proteins. Decorin and biglycan are two major types of proteoglycans. Decorin co-localizes with type I collagen and regulates fibrillogenesis. Biglycan resides near osteoblasts and modulates their activity. Glycoproteins include osteonectin, osteopontin, bone sialoprotein, tenascin-C, fibronectin, and thrombospondin family members. Glycoproteins regulate bone cell adhesion, migration, proliferation and differentiation. In particular, bone sialoprotein assists the crystallization of hydroxyapatite (104). Gla proteins include MGP (matrix Gla protein) and osteocalcin. Osteocalcin is the major type of non-collagenous protein, which stabilizes hydroxyapatite, regulates bone formation, but inhibits premature or inappropriate mineralization (104, 105).

Bone cells

The continuous remodeling of bone is mediated by osteoblasts and osteoclasts (Figure I-4). Osteoclasts break down calcified bone, and then osteoblasts lay down new matrix. In young adults, bone formation and bone resorption are maintained at a steady state under mechanical and homeostatic controls. An imbalance of bone remodeling causes skeletal disorders. Higher activity of osteoclasts over osteoblasts leads to osteoporosis, a disease with reduced bone mass, decreased structural stability, and increased risk of bone fracture. In contrast, excess bone formation causes osteopetrosis or osteosclerosis, in which bone mineral density is abnormally high and the structural instability enhances spontaneous bone fracture risk (106).

Osteoblasts are derived from mesenchymal stem cells. Osteoblasts have dual activities in bone remodeling, depositing bone matrix and secreting factors to promote osteoclastogenesis. Osteoblasts produce osteoid, which is a protein mixture with type I collagen as the major component. After osteoid becomes mineralized, new osteoblasts line up on the surface of osteoid and secrete collagen and non-collagenous proteins. Osteoblasts produce alkaline phosphatase (ALP). ALP cleaves the phosphate groups from unmineralized osteoid and assists in hydroxyapatite formation. Electron microscopy reveals that the ALP containing vesicles in bone matrix are polarized, with the mineralizing side facing osteoblasts (107). The formation and activities of osteoblasts are under the control of a variety of hormones, including PTH, $1,25(OH)_2D_3$, growth hormone, insulin, thyroid hormone, estrogen and androgen. In addition, osteoblasts produce growth factors, such as insulin-like growth factor

(IGF), bone morphogenetic proteins (BMPs), platelet-derived growth factor (PDGF), fibroblast growth factor (FGF), and tumor growth factor beta (TGF-β) (99). Thus, osteoblasts are actively involved in endocrine, paracrine and autocrine pathways.

Active osteoblasts are not terminally differentiated. They can trans-differentiate into chondroid depositing cells, or become lining cells to cover available bone surfaces. Other osteoblasts are trapped within osteoid to form osteocytes, and the chambers that osteocytes occupy are called lacunae (104). Younger osteocytes still have a Golgi apparatus and synthesize matrix proteins, but they are small. Older osteocytes are smaller and accumulate glycogen. They have reduced endoplasmic reticulum and Golgi apparatus and no longer secrete matrix (108). Osteocytes are strain and stress sensors in bone and assists in the maintenance of bone structure (109).

Osteoclasts are large, multinucleated cells that originate from the monocyte/macrophage lineage of hematopoietic stem cells. Under endocrine and paracrine controls, osteoclast precursors migrate to bone surfaces, and fuse to form giant multinucleated cells, which attach to bone through the anchoring protein, integrin αvβ3. Osteoclasts are polarized cells. The plasma membrane facing the bone surface, or ruffled border, is deeply folded, and forms a sealed bone resorption compartment between osteoclast and bone. Electrogenic protons are pumped out by the H^+-adenosine triphosphatase (H^+-ATPase) from the ruffled border into the resorption compartment, which is acidified to pH~4.5.

The energy-independent Cl^-/HCO_3^- exchanger at the basolateral side and the Cl^- channel at ruffled membrane assist in maintaining the acidity. Osteoclasts are rich in Golgi complex, mitochondria, and transporting vesicles that contain lysosomal enzymes, such as tartrate-resistant acid phosphatase (TRAP) and cathepsin K. Lysosomal proteases are secreted into the resorption microenvironment, and the collagen fibers are digested. Then, the released residues are internalized and transported out of osteoclasts through the basolateral side (110, 111).

Regulation of osteoblast differentiation and activities

Osteoblasts originate from mesenchymal stem cells, which can also differentiate into fibroblasts, adipocytes, chondrocytes, and myoblasts (112). Osteoblast differentiation is controlled by a variety of transcriptional factors, hormones, and growth factors.

Core binding factor 1/runt-related transcription factor 2 (Cbfa1/Runx2) is a pivotal regulator for osteoblast maturation (113). It binds to the osteoblast-specific cis-acting element (OSE) and functions as a transcription factor to stimulate the expression of certain osteoblastic genes, such as osteocalcin, osteopontin, and type I collagen (114). At early embryonic stage, Runx2 is selectively expressed in mesenchymal cells that will become chondrocytes or osteoblasts, and then it becomes more restricted to osteoblasts (113). PPARγ2 signaling inhibits Runx2 expression, and overexpression of PPARγ2 stimulates

adipogenesis and suppresses osteogenesis in bone marrow stromal cells (115). Runx2 heterozygous mice develop hypoplastic clavicles and exhibit delayed ossification in some cranial bones that is similar to cleidocranial dysplasia (CCD) in humans (116). Indeed, loss-of-function mutations of Runx2 gene have been identified in CCD patients (117). Runx2 homozygous knockout mice have normal cartilage development but completely lack osteoblasts, and both endochondral and intramembranous ossification are blocked (118). Transgenic mice with postnatal overexpression of a dominant-negative form of Runx2 develop osteopenia due to the decreased bone formation (119). These animal models support the essential role of Runx2 in osteogenesis. Targeted overexpression of Runx2 in osteoblasts promotes both bone formation and bone resorption, but overall, the high turnover rate leads to reduced bone mineral density (120).

Homeobox family proteins are transcription factors that control organogenesis in embryos. Some homeobox genes that regulate bone formation have been characterized. Distal-less homeobox 5 (Dlx5) is expressed in cells undergoing intramembranous ossification and around cartilage during endochondral ossification (102). Dlx5 knockout mice exhibit craniofacial abnormalities, vestibular organ malfunctions, delayed skull ossification, and impaired osteogenesis (121). Msx2-deficient mice are defective in calvarial structures, endochondral bone ossification, tooth formation, and hair follicle development. The phenotypes are similar to parietal foramina (PFM) in humans, and Msx2 mutations have been observed in PFM patients (122). Msx2 null mice

have reduced expression of Dlx5, suggesting that Msx2 is an upstream regulator for Dlx5 (123).

Bone morphogenetic proteins (BMPs) are important local factors for osteoblast differentiation. There are fifteen identified BMPs and two BMP receptors (BMPRs). Both types of BMPR are required to transmit BMP signals. Osteoblasts express BMPs and BMPRs from their osteoprogenitor lineage to their more mature stages, suggesting a broad involvement of BMP signaling in osteoblast function. Different BMPs exhibit distinctive distribution and activity in osteoblasts. BMP-5 mRNA is found in mesenchymal cells before cartilage development, but BMP-2, BMP-4 and BMP-7 are located around the cartilage anlage (124). In a variety of cell lines, BMP-2, BMP-4, BMP-6, and BMP-7 can stimulate osteoblast differentiation and induce the synthesis of osteoblastic markers, including Cbfa1, ALP, and osteocalcin (125). In myoblasts, BMP-2 suppresses the expression of myoblastic markers and promotes the trans-differentiation of these cells into osteoblasts (126, 127). Mutation of growth/differentiation factor 5 (GDF5), a BMP family member, causes defects in bone and joint development (128). Collectively, both *in vitro* and *in vivo* evidence suggest that BMP signaling plays important roles in osteogenesis and osteoblast functions. Interestingly, interruption of BMP signaling impairs the $1,25(OH)_2D_3$-induced osteoblastic differentiation from human dermal fibroblasts, suggesting that endogenous BMPs mediate $1,25(OH)_2D_3$ functions (129).

$1,25(OH)_2D_3$ has biphasic effects on the osteoblast maturation pathway and can be stimulatory or inhibitory during the proliferation-differentiation process. The exact actions of $1,25(OH)_2D_3$ on osteoblasts *in vitro* depend on the origin, species, differentiation status, and culture condition of the cells (107). In rat calvarial cells, $1,25(OH)_2D_3$ treatment of pre-confluent osteoblasts inhibits their proliferation and differentiation, with decreased expression of ALP and type I collagen and reduced mineralized nodule formation. In contrast, $1,25(OH)_2D_3$ treatment in post-confluent cells promotes the expression of osteoblastic marker genes, such as osteocalcin and osteopontin (130-132). Thus, it is suggested that $1,25(OH)_2D_3$ induces osteoblast differentiation while inhibiting the early mineralization by less mature osteoprogenitors (132). Consistent with this hypothesis, the regulation of Runx2 and osteocalcin by $1,25(OH)_2D_3$ also depends on the maturation stage of osteoblastic cells (133, 134). The biphasic effects of $1,25(OH)_2D_3$ underscore its important roles in determining osteoblast behavior during the differentiation period. Transgenic mice with targeted overexpression of VDR in mature osteoblasts (driven by osteocalcin promoter) exhibit increased trabecular bone volume, enhanced bone strength, and reduced bone resorption (135), indicating that $1,25(OH)_2D_3$/VDR signaling displays anabolic effects in differentiated osteoblasts *in vivo*.

In addition to the direct regulation of osteoblast activity, $1,25(OH)_2D_3$ also modulates the response of osteoblasts to other hormones and growth factors. One example is TGF-β. $1,25(OH)_2D_3$ induces the expression of both TGF-β and its receptor in osteoblasts (136, 137), and a functional VDRE has been identified

in TGF-β promoter (138). Vitamin D deficiency in rat results in reduced TGF-β synthesis selectively in bone (139). Furthermore, the expression of VDR is regulated by TGF-β (140, 141). TGF-β acts synergistically with $1,25(OH)_2D_3$ in stimulating the synthesis of osteoblastic marker genes, such as procollagen type 1 and ALP (142). Smad3, a downstream component of the TGF-β signaling cascade, acts in concert with SRC proteins to augment VDR-mediated transcription (143). In mice, targeted deletion of Smad3 in osteoblasts leads to complete loss of the TGF-β response, and the mice develop osteopenia due to impaired bone formation (144).

Vascular-mediated nutrition is important for the survival of bone cells. Indeed, osteoblast precursor cells are located close to the endothelial cells. Decreased blood vessels in older patients are accompanied by osteoporosis and reduced osteoblast number (142). The angiogenic factor, vascular endothelial growth factor (VEGF), is suggested to connect the functions of endothelial cells to osteoblasts. VEGF has at least six isoforms, which are alternative splicing products of one single gene (145). VEGF isoforms have distinct biological activities, such as differential interaction with VEGF receptors (VEGFRs) and neuropilin co-receptors (146). Impaired angiogenesis and ossification are observed in mice that exclusively express $VEGF_{120}$, indicating the significance of other VEGFs (particularly $VEGF_{164}$ and $VEGF_{188}$) in bone development (147, 148). It is suggested that VEGF stimulates endothelial cells to synthesize osteotropic factors, such as IGF-1 and endothelin-1, which cooperate with $1,25(OH)_2D_3$ to promote osteoblast maturation and matrix deposition (149). In

addition, VEGF signaling directly regulates osteoblast activities. VEGFs, VEGFRs and neuropilins are expressed in osteoblasts, and VEGF stimulates osteoblast proliferation, migration, and differentiation (150, 151). Although canonical VDREs have not been identified, the VEGF promoter is responsive to $1,25(OH)_2D_3$ (152). The stimulation by $1,25(OH)_2D_3$ on VEGF expression has been observed in both osteoblastic culture and osteoblast-endothelial coculture models (142).

The regulation of osteoclast differentiation and activity

Osteoclasts are formed by the fusion of monocyte/macrophage-derived mononuclear progenitor cells. Osteoclast differentiation is influenced by systemic circulating molecules and osteoblast secreted factors.

Osteoclast activity requires the appropriate formation of resorption compartments and acid microenvironments. Genes that regulate osteoclast attachment, survival, ion transport, or matrix degradation directly impact osteoclast activities. Mice lacking c-Src kinase have abundant osteoclasts, but these osteoclasts do not form ruffled borders, and thus fail to absorb bone (153). Similarly, ablation of H^+-ATPase, integrin αvβ3, carbonic anhydrase II, or cathepin K results in malfunction of the resorption compartment and causes osteopetrosis *in vivo* (154-156). The Fas signaling pathway induces apoptosis in osteoclasts, and mutation of Fas or its ligand in mice increases osteoclast number and causes osteoporosis (157). For these reasons, osteoclasts

represent a therapeutic target to treat osteoporosis. Inhibitors of cathepsin K, integrin αvβ3 receptor, or H^+-ATPase can be used to prevent or treat bone loss (158-160). Bisphosphonates inhibit farnesyl diphosphate synthase, which is required for osteoclast survival and activity. Presently, bisphosphonates are one of the most powerful drugs to reduce bone loss in post menopausal women (106).

Although mesenchymal cells and their derivatives do not directly impact osteoclast activity, they produce essential factors that regulate osteoclast formation in an endocrine or paracrine manner. Macrophage colony-stimulating factor (M-CSF) is essential for regulating proliferation, survival, and differentiation of osteoclast precursors. M-CSF is synthesized by a range of mesenchymal-derived cells, including osteoblasts and bone marrow stromal cells (161). M-CSF binds to the monocyte/macrophage surface receptor, c-Fms, and promotes the differentiation of monocyte/macrophage into osteoclasts. Mice with mutated M-CSF or c-Fms develop osteopetrosis due to the osteoclastogenesis defects (162, 163), and administration of soluble M-CSF is able to reverse the osteopetrosis in the toothless rat model (164, 165).

Receptor activator of NF-κB (nuclear factor kappa B) ligand (RANKL) is another essential osteoclastogenic cytokine. RANKL belongs to the tumor necrosis factor (TNF) superfamily and is produced primarily by osteoblasts. In osteoclast precursors, RANKL binds to the surface receptor, RANK, and activates the intracellular signaling pathway by recruiting adaptor molecules, such as TNF receptor associated factors (TRAFs), c-src non-receptor-type

tyrosine kinase, and c-Fos family proteins (166). These adaptor proteins mediate the activation of NF-κB, c-Jun NH_2-terminal kinase (JNK), and mitogen-activated protein kinase (MAPK) (167-169). RANKL-null mice develop osteopetrosis, which is not due to the lack of osteoclast precursors but to the defects in osteoclast differentiation (170). Interruption of the RANKL-RANK signaling pathway, such as by deleting RANK, NF-κB, TRAF6, c-src or c-Fos, also impairs bone resorption (153, 171-175). In certain types of cancer, including T-cell leukemia, multiple myeloma, and breast cancer, the malignant tumor cells produce high level of RANKL. Thus, accelerated bone resorption and hypercalcemia are accompanied with these cancers (176, 177).

Osteoblasts secrete an important osteoclastogenesis inhibiting factor, osteoprotegerin (OPG). OPG is a soluble glycoprotein and a member of TNF receptor family. It binds to RANKL, but functions as a decoy receptor, and blocks the stimulation of RANKL (178). OPG transgenic mice develop profound osteopetrosis, and OPG injection decreases cancer-related hypercalcemia and bone loss (106, 179). In contrast, OPG knockout mice develop severe osteoporosis due to increased osteoclastogenesis, with impaired growth plate structures, reduced trabecular bone, and decreased bone mineral density (180-182).

Because of the roles played by osteoblasts in osteoclast formation, a number of osteoclastogenesis regulating factors target osteoblasts to alter the expression of M-CSF, RANKL and/or OPG. For example, glucocorticoids, PTH,

and prostaglandin E_2 (PGE_2) promote osteoclast differentiation by enhancing the osteoblastic RANKL:OPG ratio (174, 183). Estrogen and selective estrogen receptor modulators (SERMs) exhibit bone protective effects by inducing OPG (184). While stimulating osteoblast differentiation, $1,25(OH)_2D_3$ promotes the osteoblastic expression of M-CSF and RANKL, and inhibits OPG expression (185, 186), stimulating osteoclastogenesis and the subsequent bone resorption.

Transient receptor potential cation channel superfamily V (TRPV5)-deficient mice have normal serum PTH and calcium but higher level of $1,25(OH)_2D_3$, and the thickness of cortical and trabecular bones is reduced (187), indicating that $1,25(OH)_2D_3$ promotes bone resorption more than bone formation in this model. Therefore, $1,25(OH)_2D_3$ exerts dual effects on bone remodeling. It is proposed that the overall effects of $1,25(OH)_2D_3$ on bone are correlated with administration levels (103). At physiological dose, $1,25(OH)_2D_3$ suppresses bone resorption, possibly by inhibiting PTH-induced RANKL expression. At high or pharmacological dose, $1,25(OH)_2D_3$ promotes osteoclast activity and induces hypercalcemia (103).

Similarly, PTH shows dose-dependent effects on bone remodeling regulation. A low level of PTH enhances osteoblast survival by suppressing their apoptosis (188), but a high level of PTH promotes bone resorption by enhancing the osteoblastic RANKL:OPG ratio, especially in response to the serum calcium shortage (188). In addition, it has been suggested that the intermittent treatment of PTH is primarily anabolic, but the continuous PTH administration is more

catabolic (104). Other factors that up-regulate RANKL:OPG ratio and promote osteoclastogenesis include IL-1α, IL-18, IL-11, and TGF-β (189).

Insulin-like growth factor (IGF) is another growth factor whose signaling is correlated with osteoblast and osteoclast functions. IGF-1 and IGF-2 are mediators for growth hormone (GH) and PTH signaling. The activities of IGFs are regulated through their high-affinity binding proteins, IGF binding proteins (IGFBPs). Six types of IGFBP have been identified, and their distribution and functions are cell-specific (190). $1,25(OH)_2D_3$ enhances the expression of IGF-1, IGFBP-2, IGFBP-3, and IGFBP-4 in osteoblastic models (142). Although IGF-1 and IGF-2 stimulate bone matrix synthesis (191), the overall effects of IGF signaling *in vivo* are more catabolic. The circulating level of IGFBP-2 increases with age and can have a deleterious effect on bone density (192), and IGFBP-2 and IGFBP-4 transgenic mice exhibit reduced bone size and density (193, 194).

Bone phenotypes of $VDR^{-/-}$, 1α-hydroxylase$^{-/-}$, and $VDR^{-/-}$/1α-hydroxylase$^{-/-}$ mice

To understand the i*n vivo* functions of VDR and $1,25(OH)_2D_3$, mice with targeted deletion of VDR ($VDR^{-/-}$) gene, 1α-hydroxylase (1α-hydroxylase$^{-/-}$) gene, or both genes ($VDR^{-/-}$/1α-hydroxylase$^{-/-}$) were generated (89, 97, 195). These knockout mice grow normally before three weeks, but after weaning, they exhibit symptoms of rickets, including growth retardation, enlarged epiphyseal growth plate, widened hypertrophic zone, impaired mineralization, hypocalcemia, and hyperparathyroidism. Most phenotypes can be corrected by a special diet

containing high level of calcium, phosphorus, and lactose. Similarly, the bone mineralization defects in rickets patients can be clinically reversed by calcium infusion (196). This evidence suggests that $1,25(OH)_2D_3$/VDR signaling regulates bone development primarily by controlling calcium homeostasis.

However, further comparisons show that $1,25(OH)_2D_3$, VDR, and calcium display distinct activities (97). Under high calcium/phosphorus/lactose rescue diet, all the knockout models have reduced trabecular bone, osteoblast number, mineral apposition rates, and osteoid volume. These defects indicate that calcium cannot entirely replace the functions of $1,25(OH)_2D_3$/VDR in bone. In 1α-hydroxylase$^{-/-}$ mice, neither calcium nor $1,25(OH)_2D_3$ alone is able to completely reverse the distorted cartilaginous growth plate, suggesting that both $1,25(OH)_2D_3$ and calcium are required for appropriate growth plate formation (97). Furthermore, the cartilaginous growth plate defects in VDR$^{-/-}$ mice are less severe than in 1α-hydroxylase$^{-/-}$ or VDR$^{-/-}$/1α-hydroxylase$^{-/-}$ mice, revealing that a VDR-independent, non-genomic signaling of $1,25(OH)_2D_3$ in skeletal development. Therefore, the direct actions of $1,25(OH)_2D_3$ have significant impact in bone cell activities, and the related defects cannot be completely corrected by mineral normalization.

MN1 and SEMA3B are novel target genes of $1,25(OH)_2D_3$ in osteoblasts

As introduced above, $1,25(OH)_2D_3$ promotes osteoblast maturation and matrix protein synthesis. At the same time, $1,25(OH)_2D_3$ induces

osteoclastogenesis by enhancing the osteoblastic RANKL:OPG ratio. Despite these direct actions of $1,25(OH)_2D_3$ in bone, little is known about the molecular mechanism of $1,25(OH)_2D_3$ functions or $1,25(OH)_2D_3$ target genes in the skeletal system. To further understand the physiology of $1,25(OH)_2D_3$ in bone and explore the molecular mechanism, MG-63 human osteoblastic cells were treated with 10 nM $1,25(OH)_2D_3$ for 6 hours, and the gene expression profiles were depicted by microarray analysis. In addition to the established $1,25(OH)_2D_3$ induced genes, such as osteocalcin and 24-hydroxylase, novel targets were identified, including meningioma 1 (MN1) and semaphorin 3B (SEMA3B). Data suggest that MN1 and SEMA3B are involved in skeletal homeostasis. However, their regulation and function in bone cells are largely unknown and need to be further investigated.

MN1 is essential for cranial skeleton development

MN1 is a large protein with 1320 amino acids, but it does not show homology with other proteins. Evolutionary analysis revealed that MN1 is highly conserved among vertebrates (197), implying its potential significance for vertebrate development. MN1 was originally discovered as a gene that is disrupted by a balanced translocation in meningioma (197). Subsequent studies showed that MN1 expression status is correlated with the development and treatment outcome of myeloid disorders. Overexpression of MN1 in bone marrow cells induces myeloid malignancy in mice (198), and high levels of MN1 predict poor treatment outcome in acute myeloid leukemia (AML) patients (199,

200). In addition, a recurrent translocation resulting in mis-expression of an MN1-TEL fusion protein was identified in human myeloid diseases. MN1-TEL has transforming activities in NIH3T3 cells (201), and forced expression of MN1-TEL or MN1 in multipotent progenitor cells causes T-lymphoid tumors and AML in mouse models (202-206).

While most studies suggest that MN1 has important roles in myeloid disorders, targeted deletion of MN1 causes severe abnormalities in cranial skeleton development (Figure I-5) (207). MN1 knockout mice die on birth due to cleft palate, and multiple craniofacial bones are either hypoplastic or agenic. In E18.5 MN1 null embryos, the alisphenoid bone, squamosal bone and vomer are completely absent, the presphenoid, pterygoid and basisphenoid bones are undermineralized, and the formation of supraoccipital bone is delayed. In addition, the frontal, parietal, and interparietal bones that compose the roof of skull are thin and hypoplastic. In MN1 heterozygous mice, these defects are less profound. The alisphenoid and squamosal bones form but are hypoplastic, while the vomer, supraoccipital bone, and the skull roof components are normally mineralized. A minor percentage of MN1 heterozygous mice also have cleft palate and die post-natally. These phenotypes suggest a dose-dependent effect of MN1 on controlling cranial skeleton development. Cumulatively, the MN1 knockout studies reveal that MN1 has essential roles for appropriate cranial skeleton formation. However, the functions of MN1 in bone cells were not analyzed. Therefore, we initiated studies to investigate the roles of MN1 in

$1,25(OH)_2D_3$-mediated cellular responses and to examine the properties of primary calvarial osteoblasts derived from MN1 knockout mouse.

Semaphorin signaling is involved in bone development

Semaphorin family proteins are cell surface or secreted glycoproteins characterized by an N-terminal SEMA domain (208) (Figure I-6A). Semaphorins originally were identified as axonal guidance proteins that affect central nervous system development, but subsequent studies showed that they also regulate cell migration, cell growth, differentiation, and angiogenesis in a variety of tissues (209-212). There are eight classes of semaphorin proteins. Classes 3-7 are found in vertebrates (208). SEMA3 molecules are distinguished by a conserved basic domain at the C-terminal (Figure I-6A). They are secreted proteins that signal through neuropilin receptors and plexin co-receptors (213-216) (Figure I-6B). The SEMA3B gene was first identified based on its position in the chromosomal region 3p21.3, a frequent site of loss-of-heterozygosity (LOH) in lung cancer (217). Later, its LOH was also characterized in kidney, ovarian, and testicular cancers (218-221). Furthermore, re-expression of SEMA3B in either lung or ovarian cancer cells diminishes their proliferative and tumorigenic potential (222, 223). These studies indicate that SEMA3B is a putative tumor suppressor. SEMA3B knockout mice are viable and fertile (224, 225). They are defective in positioning of the anterior commissure, but their skeletal mineralization was not examined.

Accumulating evidence suggests that semaphorin proteins have active roles in bone development. Semaphorin signaling, involving SEMA3A, SEMA3C and their receptors, facilitates cleft formation during early development (226). Deletion of SEMA3A impairs bone and cartilage development, causing vertebral fusions and partial rib duplications (227). SEMA7A polymorphisms are correlated with reduced bone mineral density and increased fracture risk (228). SEMA4D suppresses collagen synthesis in pulp-derived cells and inhibits odontoblast differentiation (229). SEMA3B transcripts are expressed in osteoblastic cell cultures obtained from human oral tissue explants *in vitro* (230). Moreover, neuropilin-1, a receptor for SEMA3B, is expressed in osteoblasts and in osteoclasts *in vitro* and *in vivo*, and is down-regulated as osteoblasts differentiate into more mature osteocytes (231). The involvement of semaphorin proteins in bone development and the expression of SEMA3B signaling components in bone cells suggest the putative roles of SEMA3B in skeletal system. However, the biological effects of SEMA3B in skeletal homeostasis or in osteoblasts/osteoclasts activities are unknown. Therefore, we generated a transgenic mouse model with targeted SEMA3B overexpression in osteoblasts and investigated the impact of osteoblast-derived SEMA3B in global skeleton maintenance and in bone cell functions.

Overall hypothesis

Based on current knowledge, we hypothesized that MN1 and SEMA3B are 1,25$(OH)_2D_3$-induced genes in osteoblasts that regulate bone cell activities and impact global skeletal homeostasis.

Figure I-1

The metabolism of vitamin D.

Vitamin D_3 is obtained directly from the diet, or synthesized from 7-dehydrocholesterol in the epidermis by sunlight catalysis. In liver, vitamin D_3 is hydroxylated by 25-hydroxylase to form $25(OH)D_3$, which is the major circulating type of vitamin D. $25(OH)D_3$ is further hydroxylated by 1α-hydroxylase in kidney to form the bioactive form of vitamin D, 1,25-dihydroxyvitamin D_3 or $1,25(OH)_2D_3$. Both $25(OH)D_3$ and $1,25(OH)_2D_3$ can be inactivated by the ubiquitous enzyme, 24-hydroxylase, to form $24,25(OH)_2D_3$ or $1,24,25(OH)_3D_3$, which are further degraded and excreted.

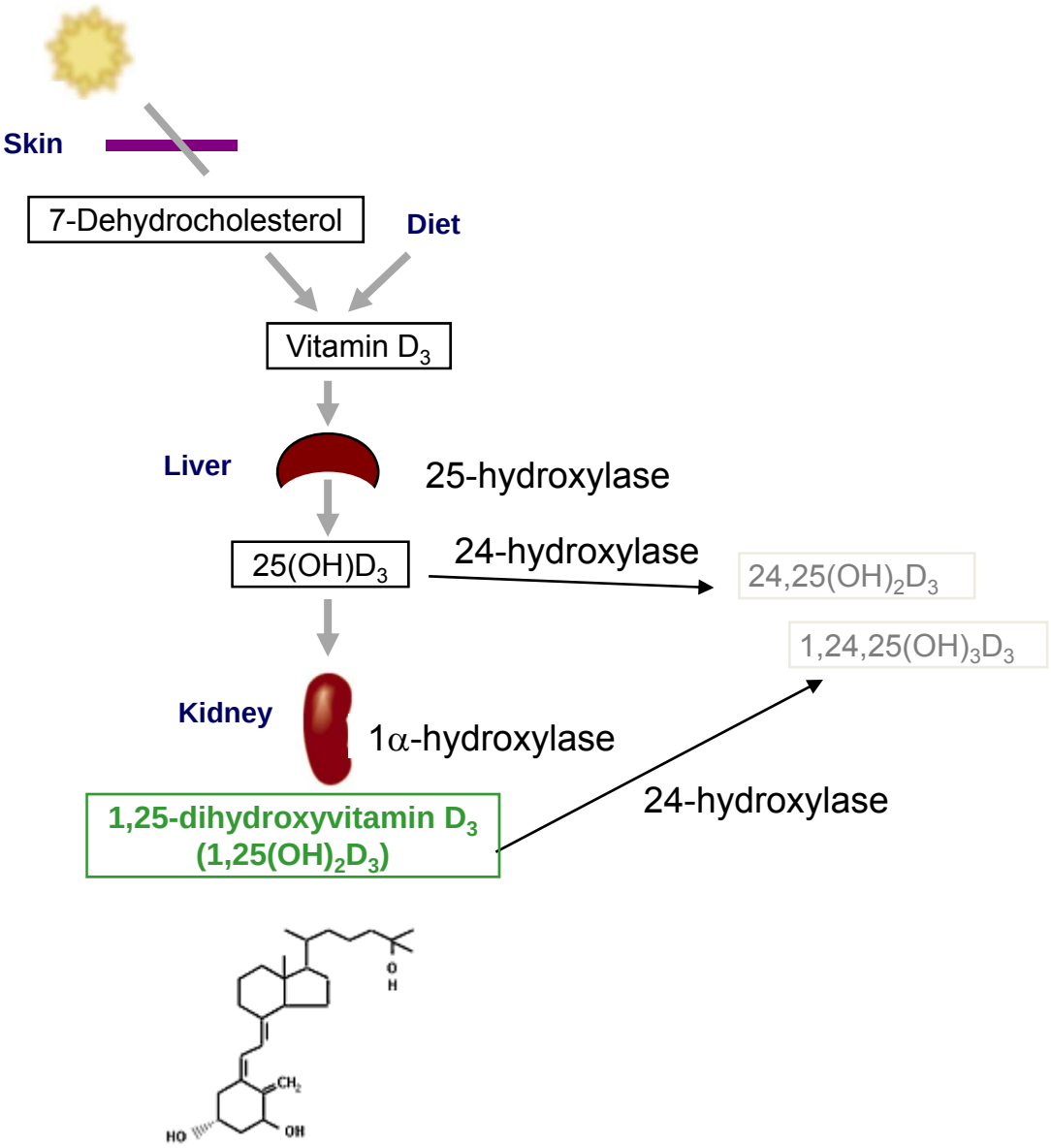
Skin
7-Dehydrocholesterol
Diet
Vitamin D_3
Liver
25-hydroxylase
25(OH)D_3
24-hydroxylase
24,25(OH)$_2D_3$
1,24,25(OH)$_3D_3$
Kidney
1α-hydroxylase
1,25-dihydroxyvitamin D_3
(1,25(OH)$_2D_3$)
24-hydroxylase
HO
OH
OH
CH$_2$

Figure I-2

The structure and activation of VDR.

A, VDR is composed of a DNA-binding domain (DBD) at the N-terminus, a ligand-binding domain (LBD) at the C-terminus, and a hinge region in the middle. The DBD has two zinc-binding modules that direct the sequence-specific association of VDR with DNA. The LBD is a multifunctional globular domain with 12 α-helices that mediate the selective interactions of VDR with RXR and other transcriptional factors. The hinge region allows the rotational flexibility and facilitates the VDR interaction with DNA and other proteins. The numbers above the VDR protein indicate the amino acid residue boundaries of corresponding regions (based on human VDR). B, $1,25(OH)_2D_3$ binding leads to a conformational change of the AF-2 domain, closing the ligand binding hydrophobic pocket and activating VDR. The LXXLL motif (L, leucine; X, any amino acid) of SRC coactivators associates with the hydrophobic groove of VDR through the glutamic acid residue (E) in helix 12 and the lysine residue (K) in helix 3 of the LBD.

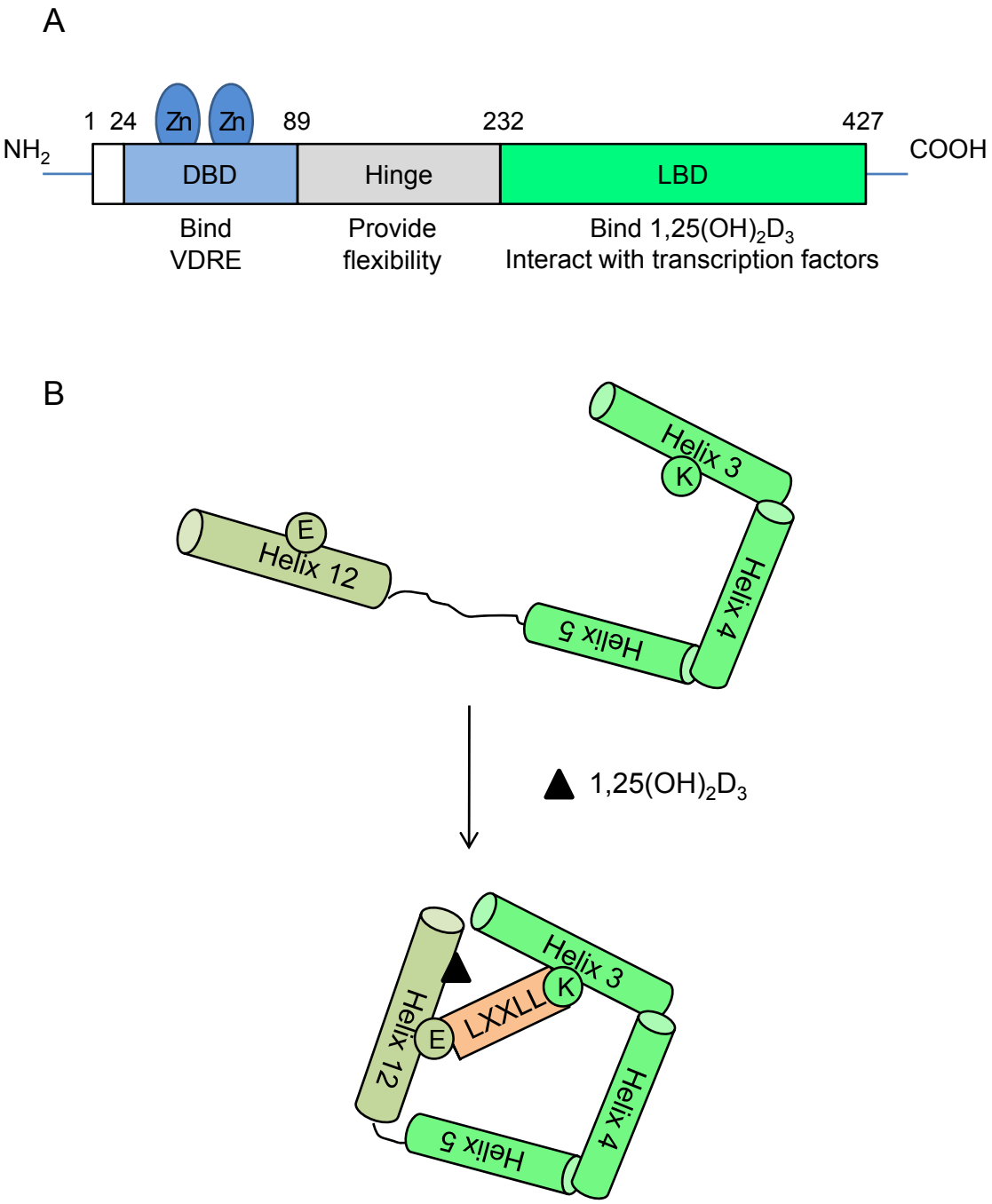
A
1
24
Zn
Zn
89
232
427
NH2
COOH
DBD
Hinge
LBD
Bind
VDRE
Provide
flexibility
Bind 1,25(OH)2D3
Interact with transcription factors
B
Helix 3
K
E
Helix 12
Helix 4
Helix 5
1,25(OH)2D3
Helix 3
K
LXXLL
E
Helix 12
Helix 4
Helix 5

Figure I-3

The model of VDR mediated transcription.

When binding to 1,25$(OH)_2D_3$, VDR forms a heterodimer with retinoid X receptor (RXR). VDR-RXR complex binds to vitamin D response elements (VDREs) at gene promoter regions, and recruits various classes of cofactors to regulate the transcription of target genes. These genes mediate the functions of 1,25$(OH)_2D_3$ *in vivo.* The canonical VDREs are termed DR-3 elements, which contain two conserved hexanucleotide repeats separated by a 3-bp spacer. Representative DR-3 type VDREs from mouse ostepontin (-759 bp)[a], rat 24-hydroxylase (-259 bp)[b], human osteocalcin (-500 bp)[c], and rat PTH related peptide (-1107 bp)[d] are shown (numbers represent the position in relation to the transcriptional start site). The hexameric core binding elements are capitalized, and the deviations from the consensus sequence are underlined.

A

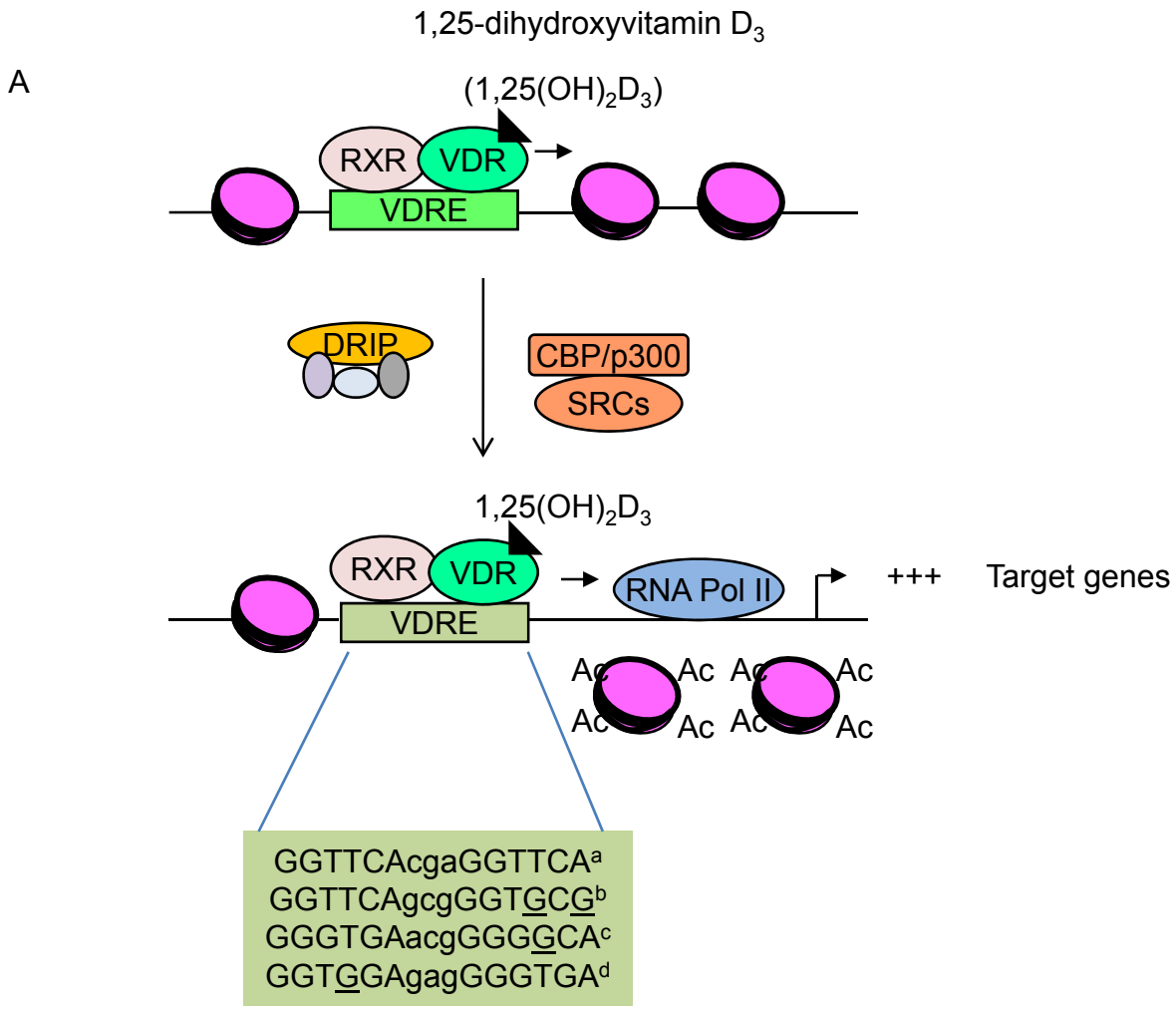
1,25-dihydroxyvitamin D_3
$(1,25(OH)_2D_3)$
RXR
VDR
VDRE
DRIP
CBP/p300
SRCs
$1,25(OH)_2D_3$
RXR
VDR
VDRE
RNA Pol II
+++
Target genes
Ac
GGTTCAcgaGGTTCA[a]
GGTTCAgcgGGTGCG[b]
GGGTGAacgGGGGCA[c]
GGTGGAgagGGGTGA[d]

Figure I-4

The scheme of bone remodeling.

The continuous remodeling of bone is mediated by osteoblasts and osteoclasts. Osteoclasts break down calcified bone, and then osteoblasts lay down new matrix, which they then mineralize. Osteoclasts are large, multinucleated, polarized cells that originate from hematopoietic stem cells. The plasma membrane facing bone surface, or ruffled border, is deeply folded, and forms a sealed bone resorption compartment between osteoclast and bone. Osteoblasts are derived from mesenchymal stem cells and have dual activities in bone remodeling. Osteoblasts build bone by depositing bone matrix. At the same time, osteoblasts produce RANKL and M-CSF, which are essential for osteoclast differentiation. Some factors that control the differentiation of osteoblasts and osteoclasts are listed.

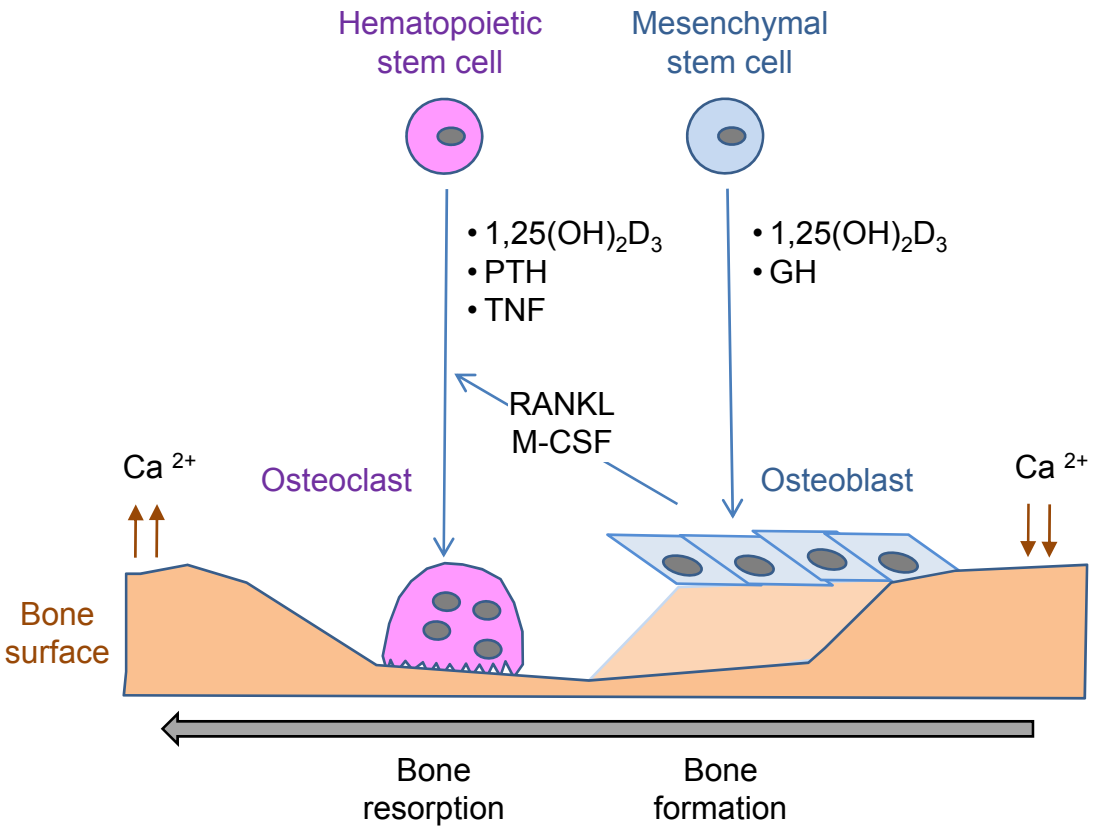
Hematopoietic stem cell
Mesenchymal stem cell
• 1,25(OH)2D3
• PTH
• TNF
• 1,25(OH)2D3
• GH
RANKL
M-CSF
Ca 2+
Osteoclast
Osteoblast
Ca 2+
Bone surface
Bone resorption
Bone formation

Figure I-5

MN1 knockout mice have severe defects in cranial skeletal development.

Skulls from wild-type (WT) and MN1 knockout (MN1 KO) E18.5 (panel A) and E17.5 (panel B) mice are stained with Alizarin Red for bone and Alcian Blue for cartilage. a, alisphenoid bone. b, basioccipital bone. bs, basisphenoid. p, palatine shelf. ps, palatal shelves. pt, pterygoid bone. s, squamosal bone.

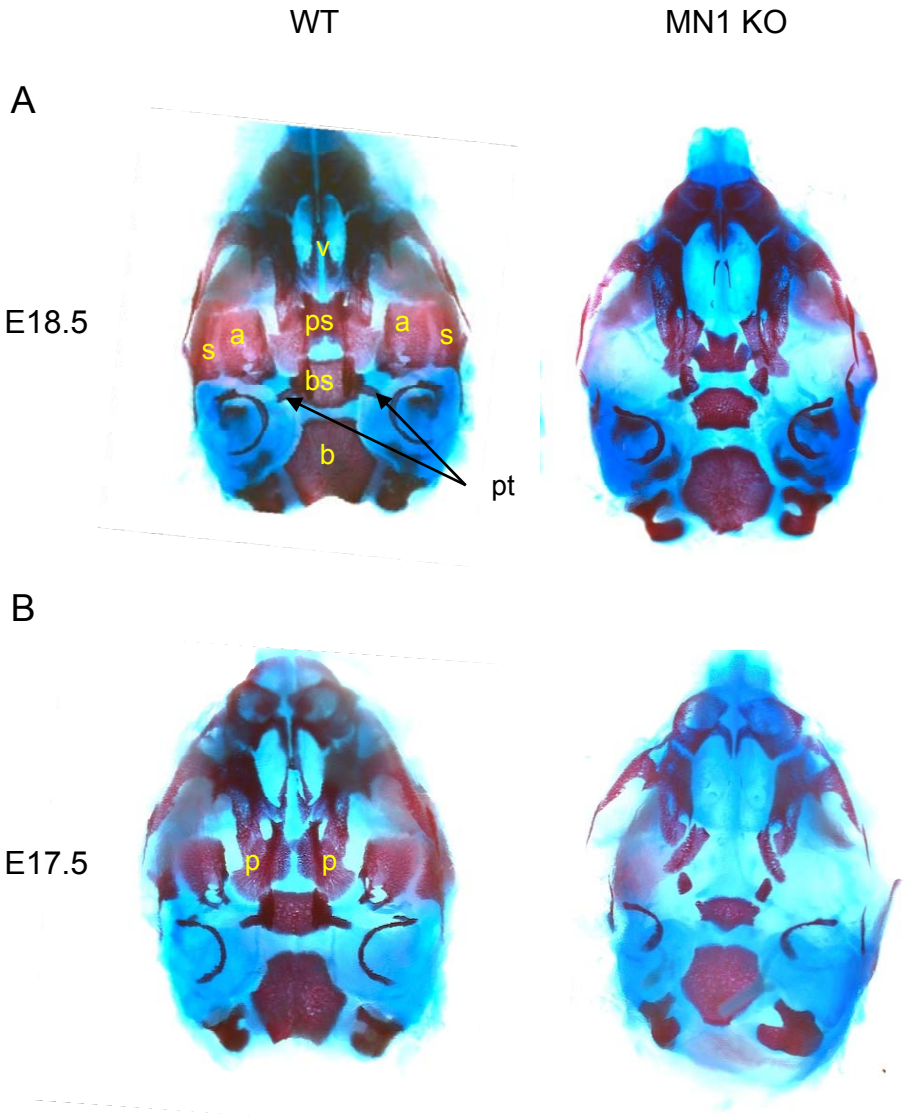
WT
MN1 KO
A
E18.5
v
ps
a
a
s
s
bs
b
pt
B
E17.5
p
p

Figure I-6

The scheme of vertebrate semaphorins and SEMA3B signaling.

A, The structure of vertebrate semaphorins (class 3-7). Semaphorins are cell surface or secreted glycoproteins characterized by an N-terminal SEMA domain, which is essential for signaling. In addition, semaphorins possesses PSI domain, immunoglobin loop, thrombospondin domain, and/or glycophosphatidylinositol (GPI) anchor. SEMA3 molecules are secreted proteins that are distinguished by a conserved basic domain at C-terminal. B, SEMA3B signals through neuropilin receptors and plexin co-receptors. Neuropilins contain two complement binding (CEB) domains, two coagulator-like domains, and a meprin A5 domain. Plexins are characterized by a split cytoplasmic GTPase-activating protein (GAP) domain that transmits signals. The extracellular region contains a SEMA domain, a PSI domain, and glycine-proline (G-P)-rich motifs. Inactive plexins associate with neuropilins on cell surface, with the SEMA domain folding over to auto-inhibit the intracellular signaling. SEMA3B binds to the CEB domains of neuropilin receptors and induces the conformational change of plexin co-receptors. Then the plexin-mediated intracellular signaling is activated.

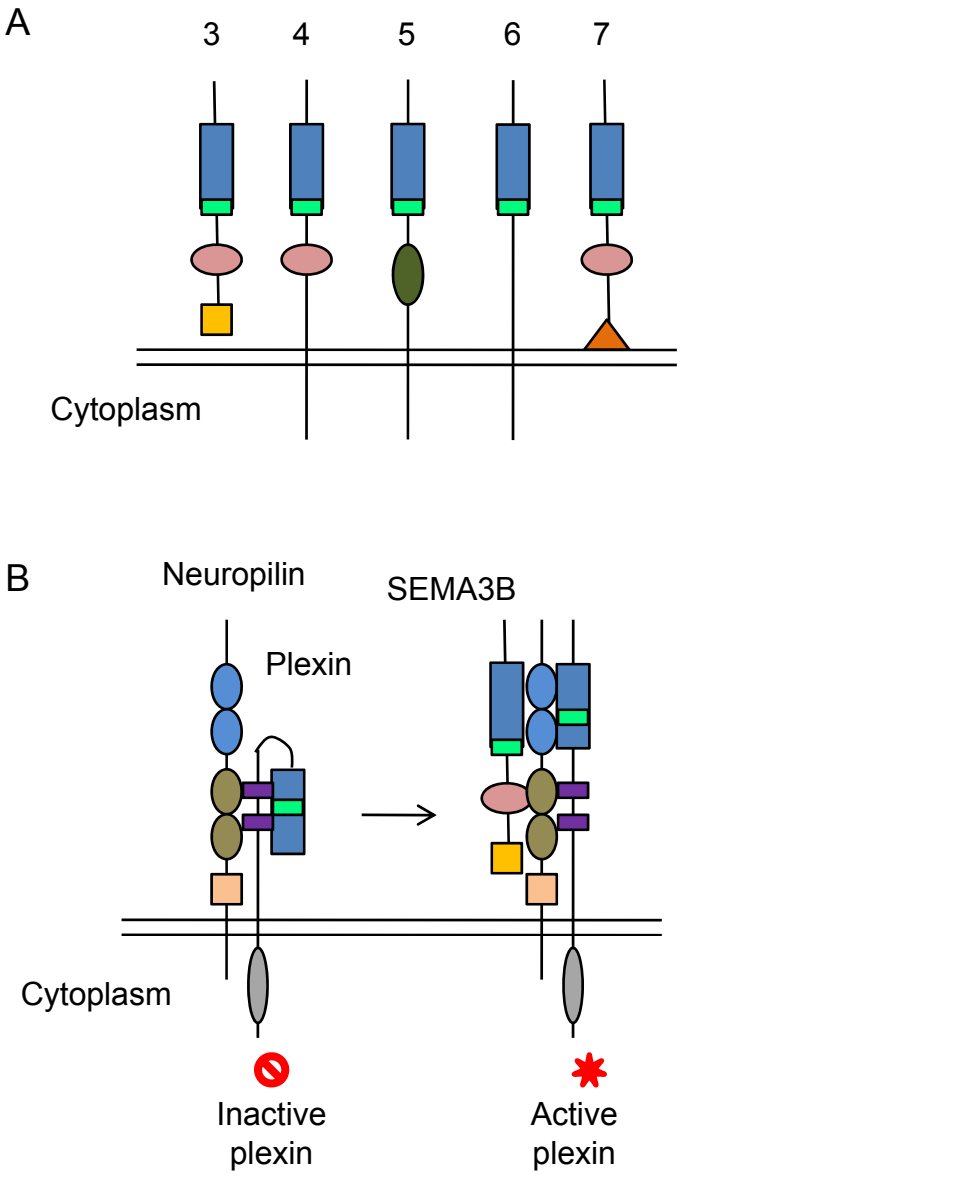
A
3
4
5
6
7
Cytoplasm
B
Neuropilin
SEMA3B
Plexin
Cytoplasm
Inactive plexin
Active plexin
SEMA domain
Immunoglobulin loop
Basic domain
Thrombospondin domain
GPI anchor
GAP domain
PSI anchor
G-P-rich motif
Complement binding domain
Coagulation factor-like domain
Meprin A5 domain

CHAPTER II

MENINGIOMA 1 (MN1) IS A 1,25-DIHYDROXYVITAMIN D_3-INDUCED TRANSCRIPTIONAL COACTIVATOR THAT PROMOTES OSTEOBLAST PROLIFERATION, MOTILITY, DIFFERENTIATION, AND FUNCTION

Introduction

The classic role of vitamin D endocrine system is to regulate proper intestinal calcium and phosphate absorption, which is essential for maintaining appropriate bone mineralization and skeletal development (232). The active form of vitamin D is 1,25-dihydroxyvitamin D_3, or $1,25(OH)_2D_3$. Its physiological functions are mediated through the vitamin D receptor (VDR). Ligand binding induces VDR association with retinoid X receptor (RXR), binding to DNA, and recruitment of coactivators to modulate the transcription of target genes. These gene products mediate the activities of $1,25(OH)_2D_3$ *in vivo.* A variety of coactivators for VDR has been described, including the steroid receptor coactivator (SRC) proteins, the VDR-interacting proteins (DRIP) complex, and the nuclear coactivator 62 kDa/Ski-interacting protein (NCoA62/SKIP) (76). SRCs possess intrinsic histone acetyltransferase (HAT) activity (53), and they also recruit other HATs, such as CBP/p300 (56), thereby allowing the transcriptional machinery better access to gene promoter regions (58, 59). DRIP is a multimeric complex that interacts with RNA polymerase II and may serve as a bridge

between liganded VDR/RXR and basal transcriptional machinery (233-235). NCoA62/SKIP represents a distinct VDR coactivator that may couple transcriptional activation to mRNA splicing (74-76). SRCs and DRIP205, the anchoring subunit of the DRIP complex, interact with liganded VDR through LXXLL motifs, which associate with the hydrophobic cleft in the nuclear receptor ligand binding domain (LBD) (45). Other coactivators interact with the receptor through different mechanisms. Growing numbers of VDR coactivators have been identified, highlighting the complexity of VDR-mediated transcription.

The skeleton is a dynamic organ that undergoes a continuous remodeling process mediated by bone-forming osteoblasts and bone-resorbing osteoclasts. Osteoblast precursors originate from mesenchymal stem cells, which are thought to serve as common progenitors for osteoblasts, adipocytes, and chondrocytes in developing skeletal tissues (112, 236). Osteoblasts promote bone formation by secreting extracellular matrix proteins, such as collagen and non-collagenous proteoglycans, glycoproteins, and gamma-carboxylated proteins (237). Osteoblasts are also required to regulate the formation of mature osteoclasts by producing essential cytokines and regulatory proteins, such as receptor activator of NF-κB ligand (RANKL) which stimulates osteoclastogenesis and osteoprotegerin (OPG) which inhibits it (177). In hematopoietic osteoclast precursors, RANKL binds to the cell surface receptor, RANK, and activates an intracellular signaling pathway by recruiting adaptor molecules, such as TNF receptor associated factors (TRAFs), c-src non-receptor-type tyrosine kinase, and the c-Fos family proteins (166). These adaptor proteins mediate the

activation of NF-κB, c-Jun NH_2-terminal kinase (JNK), and mitogen-activated protein kinase (MAPK) (167-169). In contrast, OPG is an osteoclastogenesis inhibiting factor that functions as a decoy receptor, binding to RANKL and blocking the activation of the RANK signaling cascade (178). The osteoblastic RANKL:OPG expression ratio is a major determinant of osteoclastogenesis. It is enhanced by numerous factors that promote osteoclastogenesis, such as glucocorticoids and parathyroid hormone (PTH) (174, 183), or reduced by factors that inhibit osteoclastogenesis, such as estrogen and growth hormone (GH) (238, 239).

In the skeletal system, both osteoblasts and osteoclasts are responsive to $1,25(OH)_2D_3$. In osteoblasts, $1,25(OH)_2D_3$ promotes the synthesis of bone matrix proteins and regulates the expression of osteoclastogenic factors. For example, $1,25(OH)_2D_3$ enhances RANKL synthesis and inhibits OPG secretion, generating a RANKL:OPG ratio that favors osteoclastogenesis (240). In osteoclasts, $1,25(OH)_2D_3$ enhances bone resorption activity and promotes calcium release. This is critical for maintaining mineral homeostasis when serum calcium and phosphate levels are low. The lack of active hormone or functional receptor results in undermineralized skeletal disorders, including rickets in children and osteomalacia in adults (232).

To better understand the role of $1,25(OH)_2D_3$ in bone, we used gene expression array analysis to identify $1,25(OH)_2D_3$-regulated genes. Meningioma 1 (MN1) was identified as a novel $1,25(OH)_2D_3$ target gene in the MG-63

osteoblastic cell system (241). MN1 originally was discovered as a gene that is disrupted by a balanced translocation in meningioma (197). However, subsequent studies showed that overexpression of MN1 in bone marrow cells induces myeloid malignancy in mice and predicts poor treatment outcome in acute myeloid leukemia (AML) patients (198-200). In addition, a recurrent translocation resulting in mis-expression of an MN1-TEL fusion protein was identified in human myeloid diseases. Forced expression of MN1-TEL or MN1 in multipotent progenitor cells causes T-lymphoid tumors as well as AML (202-206). While MN1 overexpression is highly correlated with myeloid disorders, studies with the MN1 knockout mouse point to other fundamental physiology. Targeted deletion of MN1 is lethal post-natally due to severe cleft palate (207). Moreover, multiple craniofacial bones that form by intramembranous ossification are either undermineralized or absent in MN1-null mice. The mechanisms underlying these defects in MN1 null mice are unknown.

The ossification defects in the cranial skeleton of MN1 knockout mice combined with the regulation of MN1 in osteoblasts suggest a potential role for MN1 in osteoblast functions. Here, we characterized that MN1 is a $1,25(OH)_2D_3$ target gene in multiple osteoblast models and is a transcriptional coactivator for VDR. Using primary osteoblasts derived from the MN1 knockout mouse, we showed that MN1 knockout osteoblasts display various proliferation and differentiation defects, including attenuated motility, decreased growth rate, reduced VDR-mediated transcription, impaired ability to support osteoclastogenesis, reduced differentiation and mineralization, but enhanced

adipogenesis. Collectively, our studies indicate that MN1 is an important regulator for 1,25$(OH)_2D_3$-activated gene transcription, osteoblast and osteoclast differentiation, and the balance of osteogenesis/adipogenesis from mesenchymal precursors.

Materials and Methods

Cell culture

MG-63 human osteoblastic cells were maintained in growth media consisting of modified essential media (MEM) supplemented with 10% fetal bovine serum (FBS). COS-7 green monkey kidney cells were maintained in DMEM supplemented with 10% bovine calf serum (CBS). MC3T3-E1 mouse fetal calvarial cells were grown in α-MEM (Invitrogen, Calsbad, CA) with 10% FBS. For differentiation studies, MC3T3-E1 cells were grown to confluence and then the growth media were supplemented for 2 weeks with 50 μg/ml L-ascorbic acid and 10 mM β-glycerophosphate to promote osteoblast differentiation. Media were replenished twice per week during the differentiation period. All the culture media were supplemented with 100 units/ml penicillin and 100 μg/ml streptomycin.

Northern blot

mRNA was isolated from MG-63 cells with the FastTrack system (Invitrogen) according to the manufacturer's instructions. Total cellular RNA was extracted from osteoblastic cell cultures with RNA-Bee isolation reagent according to the manufacturer's recommendations (Tel-Test, Friendswood, TX). For Northern blot analysis, 15-20 μg of total RNA was separated on a formaldehyde/agarose gel and transferred to Magna nylon membrane (GE Osmanics, Minnetonka, MN) by capillary action. The blots were hybridized with [α^{32}-P]-labeled probes synthesized using a Prime-A-Gene kit (Promega, Madison, WI). Mouse probes were generated by RT-PCR from mouse osteoblast RNA with the amplification primers listed in Table 1. Autoradiograms were quantitated using scanning densitometry and normalized using 18S RNA.

Plasmids and reporter gene analysis

The reporter plasmids $(VDRE)^4$-TATA-luciferase (luc), $(VDRE)^4$-TK-luc, $(GRE)^2$-TK-luc, $(RARE)^4$-TK-luc, and $(GAL4)^5$-TK-luc were generated by subcloning the promoter regions from $(VDRE)^4$-TATA-GH (74), $(VDRE)^4$-TK-GH (242), $(GRE)^2$-TK-GH (243), $(RARE)^4$-TK-GH (244), and $(GAL4)^5$-TK-GH (245), respectively, into pGL3 basic vector (Promega). To create the hRANKL(-1 kb)-luc reporter vector, the human RANKL promoter (-922 - +23 relative to the transcriptional start site) was amplified by PCR and subcloned into pGL3 vector. The $1,25(OH)_2D_3$-responsive construct cyp24(-1200)-luc was generated by amplifying the human 24-hydroxylase promoter (-1.2 kb - +120 bp) and ligating the product into the pGL3 vector. pSG5-VDR (242), pSG5-GAL4-VDR (25),

pSG5-RARα (25), pSG5-GR (246), pCR-SRC-1 (247), and pSG5-SRC-2/GRIP1 (248) have been previously described. Plasmids encoding GAL4 DBD fusions with all other nuclear receptor LBDs were constructed by PCR amplification of the LBDs from either a human fetal brain or a human placental cDNA library (BD Biosciences Clontech, Palo Alto, CA) and ligating them in frame with the GAL4 DBD. CMVTAG2B-MN1 was constructed by subcloning the MN1 cDNA from pSCTOP-MN1 (201) in frame with the FLAG epitope tag in the CMVTAG2B vector (Stratagene, La Jolla, CA).

The firefly luciferase reporter construct together with the CMV-Renilla plasmid (and appropriate other factors) were transiently transfected into COS-7 cells using standard calcium phosphate transfection (242) or into primary osteoblasts using Fugene 6 regent (Roche Applied Science, Indianapolis, IN) following the manufacturer's instructions. Cells were treated as indicated, lysed with passive lysis buffer (Promega), and assayed for the firefly and renilla luciferase activities with the Dual Luciferase Reporter Assay System (Promega) using an LMax microplate luminometer (Molecular Devices, Sunnyvale, CA). All values are presented as the normalized firefly:renilla luciferase activity.

In siRNA knockdown experiments, On-Target plus SMARTpool (Dharmacon Inc., Chicago, IL) siRNAs specific for mouse MN1 or non-specific controls (siCONTROL) (Dharmacon Inc.) were transfected in triplicate into MC3T3-E1 cells with lipofectamine 2000 reagent (Invitrogen) following the manufacturer's instructions. Twenty-four hours later, the hRANKL(-1 kb)-luc or

pGL3 control reporter constructs were transfected, and the reporter gene expression was analyzed after 48 hours.

MTT assay

Primary osteoblasts were seeded at a density of $1x10^3$ cells/cm^2 in 24-well culture plates and treated as indicated. At various times, 0.1 ml of 3-(4,5-dimethylthiazol-2-yl)-2,5-diphenyltetrazolium bromide, or MTT (5 mg/ml) was added to 0.4 ml culture media for each well, and cells were incubated for another 3 hours. Then the media were removed and the purple formazan product was dissolved in isopropanol containing 0.04 M HCl for 10 min at 37˚C. The absorbance at 570 nm of each sample was determined with a scanning multi-well spectrophotometer. Experiments were performed in quadruplicate.

BrdU labeling assay

BrdU labeling and analysis of primary osteoblast cultures was similar to previous studies (241). Briefly, primary osteoblasts were seeded in 4-well lab-Tak chamber slides and treated as described. Cells were pulse-labeled for 4 hours with media containing 10 μM BrdU, fixed with 4% paraformaldehyde for 10 min, and permeablized by 0.1% Triton X-100 in PBS for 5 min. The BrdU incorporation sites were exposed by treating the monolayers with 100 U/ml DNase I (Amersham Biosciences, Piscataway, NJ) for 30 min. The monolayers were then blocked with 1.5% normal goat serum and incubated with anti-BrdU

mouse monoclonal antibody (BD Biosciences, San Jose, CA) followed by Alexa Fluorophore 594 conjugated goat anti-mouse secondary antibody (Molecular Probes, Invitrogen). ProLong Antifade reagent with DAPI (Vector Laboratories, Burlingame, CA) was used to mount glass coverslips and the samples were visualized using fluorescence microscopy. Cells from three different areas (80-120 cells each) were counted and the ratio of BrdU-positive cells versus total cell number was determined.

To measure BrdU incorporation in embryonic calvaria, BrdU (0.1 mg/g body weight) was injected into pregnant (18.5 day post conception) MN1 heterozygous mice and then the E18.5 calvaria were isolated 3 hours later. These calvaria were fixed overnight in 10% neutral phosphate-buffered formalin and decalcified overnight in Immunocal formic acid solution (American Mastertech Scientific, Lodi, CA). Following an overnight equilibration in PBS-buffered 30% sucrose, the calvaria were embedded in Tissue-Tek O.C.T. frozen tissue matrix (Sakura Finetek, USA, Torrance, CA). Replicate five micron cryostat sections were cut from three different areas of each calvaria separated by 200-250 microns. The sections were immersed in 2N HCl for 15 min at room temperature to expose the BrdU incorporation sites, and then blocked and stained as described above except that Alexa Fluorophore 488 conjugated goat anti-mouse secondary antibody (Molecular Probes) was used. The sections were then counterstained with 0.5 μg/ml DAPI and mounted with ProLong Antifade reagent (Vector Laboratories). Overlapping images were taken to cover the entire calvarial slice, cells from the 3 different areas of each calvarium were

counted and the ratio of BrdU positive cells versus total cell number was determined. Five animals from each genotype were analyzed.

In vitro wound repair assay

In vitro wound repair assays was performed as described (249). Briefly, confluent primary osteoblast monolayers were wounded by creating a linear scratch using a sterile pipette tip. The cells were washed with PBS to remove debris and then fresh media were replaced. Images were taken 0 and 16 hours after injury, and the percentage of wound closure was determined.

Primary osteoblast culture

MN1 heterozygous breeding pairs of mice were kindly provided by Gerard C. Grosveld (St. Jude Children's Research Hospital) and Ellen C. Zwarthoff (Erasmus Medical Center, Rotterdam, The Netherlands). All animals were maintained on a 12-h light, 12-h dark cycle following the rules of Institutional Animal Care and Use Committee at Case Western Reserve University. Primary osteoblasts were isolated from E18.5 calvaria as described (250). Briefly, connective tissue was removed from the isolated calvaria and the osteoblasts were released through sequential 15 min digestions in 60% α-MEM supplemented with 0.024 mg/ml type 1 collagenase (Worthington Biochemical Corporation, Lakewood, NJ), 0.072 mg/ml type 2 collagenase (Worthington), 0.1 mM $CaCl_2$, 0.06% BSA, and 15 mM Hepes (pH 7.4) at 37°C. The first two

digestions were discarded, and the next four digestions were collected and combined. Collagenase was removed with sequential media washes, and the osteoblasts were maintained in α-MEM supplemented with 15% FBS. Osteoblasts from different animals with the same genotype were combined for experiments. Individual embryos were genotyped by PCR of tail digests as described (207). For differentiation experiments, the osteoblasts were seeded at a density of $6x10^3$ cells/cm^2, grown to confluence within 48 hours, and replaced with growth media supplemented with 10 mM β-glycerophosphate and 50 μg/ml L-ascorbic acid. Media were changed every 3-4 days and differentiating osteoblasts were collected at the indicated time for individual analysis.

Osteoclast differentiation and TRAP activity staining

Primary osteoblasts were isolated and allowed to differentiate for 15 days as described above. Spleen cells were isolated from 7-10 week old female wild-type mice as described previously (251), and were plated overnight in phenol red-free α-MEM (Invitrogen) supplemented with 10% heat-inactivated FBS (Atlanta Biologicals, Lawrenceville, GA) and 10 ng/ml macrophage colony-stimulating factor (M-CSF) (R & D Systems, Inc., Minneapolis, MN). Non-adherent cells containing osteoclast precursors were added to differentiated osteoblasts at a density of 500,000 cells per cm^2 in phenol red-free α-MEM containing 10% heat-inactivated FBS, 100 nM dexamethasone, and the indicated concentrations of $1,25(OH)_2D_3$. The cocultures were incubated for 8 days and the media were changed twice during this time. Mature osteoclasts were

analyzed for enzymatic activity of TRAP (tartrate-resistant phosphatase) using the leukocyte acid phosphatase kit (Sigma Aldrich, Saint Louis, MO). TRAP-positive multinucleated cells with 3 or more nuclei were counted in triplicate wells.

Alkaline phosphatase activity analysis

Primary osteoblast cultures were isolated and differentiated as described above. To stain for alkaline phosphatase activity, the cultures were fixed with 4% paraformaldehyde and then incubated for 20 min at room temperature with freshly prepared 0.4 mg/ml Fast Red TR in 0.2 mg/ml naphthol AS-MX phosphate alkaline solution (Sigma-Aldrich). Quantitative analysis of soluble alkaline phosphatase activity in cell extracts was performed using a colorimetric kit (Sigma-Aldrich) that measures the conversion of p-nitrophenyl phosphate to p-nitrophenol according to the manufacturer's instructions. Alkaline phosphatase activity was normalized to protein concentration of the lysate as measured by the bicinchoninic acid (BCA) assay (Pierce Biotechnology, Inc., Rockford, IL).

Mineralization and adipogenesis assay

Primary osteoblasts were isolated and allowed to differentiate as described above. For mineralization assays, cells were fixed with 70% ethanol for 10 min at room temperature and then stained with freshly prepared 1% Alizarin Red S solution for 10 min. For adipogenesis assays, 3 mg/ml Oil Red O stock solution in isopropanol was diluted with water at a 60:40 ratio and filtered

by Whatman paper before use. The cultures were fixed with 10% formalin for 30 min at room temperature and pre-incubated with 60% isopropanol for 5 min. Then cells were stained with freshly diluted Oil Red O solution for 5 min and counterstained with hematoxylin for 1 min. All experiments were performed in triplicate.

RESULTS

MN1 mRNA transcripts are induced by 1,25(OH)$_2$D$_3$ and by osteoblastic cell differentiation

Microarray analysis was used as an initial screen to identify 1,25(OH)$_2$D$_3$-regulated genes in MG-63 cells, a human osteoblastic cell line. In this analysis, there was an approximately 8-fold induction of MN1 in response to a 6-hour treatment with 10 nM 1,25(OH)$_2$D$_3$ (data not shown). Northern blot analysis was performed to validate the microarray results in MG-63 cells. As shown in Figure II-1, 1,25(OH)$_2$D$_3$ increased MN1 mRNA levels in a time- and dose-dependent manner. This increase was apparent as early as 3 hours and is maximal at 12 hours (Figure II-1A). As little as 0.1 nM 1,25(OH)$_2$D$_3$ stimulated MN1 expression, and mRNA levels continued to rise up to 100 nM 1,25(OH)$_2$D$_3$ (Figure II-1B). This effect was specific for 1,25(OH)$_2$D$_3$ because cholicalciferol (vitamin D$_3$), an inactive precursor molecule of 1,25(OH)$_2$D$_3$, and 24,25(OH)$_2$D$_3$, a metabolite of vitamin D$_3$, had little effect on MN1 mRNA levels (Figure II-1A and data not shown). Finally, using an affinity purified polyclonal antibody raised against the

N-terminal region of human MN1, Western blot analysis detected doublelet bands that were induced by 24-hour treatment of 10 nM $1,25(OH)_2D_3$ in MG-63 nuclear extracts (Figure II-1C). These data establish MN1 as a novel $1,25(OH)_2D_3$ target gene in MG-63 osteoblastic cells.

To enhance the mRNA expression of MN1, $1,25(OH)_2D_3$ may promote its transcription or inhibit its degradation. To examine whether $1,25(OH)_2D_3$ modulates MN1 mRNA stability, MG-63 cells were treated with ethanol or 10 nM $1,25(OH)_2D_3$ for 6 hours, and then the mRNA synthesis was blocked by actinomycin D. The MN1 transcripts level during the next 6 hours was examined by Northern blot analysis. As shown in Figure II-2A and -2B, 6-hour treatment of $1,25(OH)_2D_3$ induced MN1 as expected, but MN1 mRNA has a short half-life (~1 hour) and $1,25(OH)_2D_3$ had little effect on the degradation rate. Thus, $1,25(OH)_2D_3$ induces MN1 mRNA expression primarily by stimulating mRNA synthesis instead of suppressing its degradation. Further analysis revealed that active RNA synthesis is required for this response. Pretreatment of actinomycin D abolished the basal expression and $1,25(OH)_2D_3$-mediated induction of MN1 (Figure II-2C). When *de novo* protein synthesis was blocked with cycloheximide pretreatment, $1,25(OH)_2D_3$-mediated induction of MN1 mRNA was preserved (Figure II-2D). However, the basal expression of MN1 was enhanced, diminishing the extent of $1,25(OH)_2D_3$ stimulation. Taken together, these data suggest that $1,25(OH)_2D_3$ increases the steady-state levels of MN1 mRNA by a process that involves active transcription.

The MG-63 osteosarcoma cell line is an immortalized, transformed cell line representing a limited window of the osteoblast life cycle, namely that of the immature osteoblast (241). To more firmly establish the relevance of MN1 in osteoblastic cell biology, we examined more native osteoblastic cell systems, including the MC3T3-E1 mouse fetal calvarial cell line and primary osteoblasts obtained from embryonic mouse calvaria. Both models undergo a well-defined differentiation program that progresses from immature proliferating cells to post-confluence mature, mineralized-matrix secreting cells *in vitro*. Thus, we could monitor $1,25(OH)_2D_3$-activated expression of MN1 in immature proliferating osteoblasts as well as more fully differentiated, mature osteoblasts. Moreover, we could address whether MN1 expression is impacted by the process of osteoblastic cell differentiation. MC3T3-E1 cells or primary murine calvarial osteoblasts were treated with $1,25(OH)_2D_3$ during proliferation or differentiation and the steady-state levels of MN1 were examined. As shown in Figure II-3A, $1,25(OH)_2D_3$ enhanced MN1 transcript levels in proliferating MC3T3-E1 cells in a time-dependent manner with increases evident as early as 1 hour and maximal induction of 4.2-fold at 24 hours. This induction preceded the induction of 24-hydroxylase, a well-established primary VDR target gene, and paralleled the induction of the VDR transcript. The induction of MN1 was not as profound in differentiating MC3T3-E1 cells, possibly due to the dramatic down-regulation of VDR in this system (Figure II-3A). Indeed, $1,25(OH)_2D_3$-induced expression of 24-hydroxylase also was dramatically reduced in differentiating MC3T3-E1 cells.

Similar to MC3T3-E1 cells, steady-state levels of MN1 mRNA in proliferating primary calvarial osteoblasts were increased by 1,25$(OH)_2D_3$ in a time-dependent manner with a maximal induction of 7-fold at 24 hours (Figure II-3B). We also observed modest induction (1.4-fold) of MN1 transcripts by 1,25$(OH)_2D_3$ in more differentiated osteoblasts (Figure II-3B). In addition, differentiating primary osteoblasts expressed a higher basal level of MN1 than did their proliferating counterparts (Figure II-3B). Elevated MN1 mRNA levels were apparent after 7 days of differentiation and continued to increase modestly throughout the 28-day differentiation regimen (Figure II-3C). Finally, endogenous MN1 transcripts were readily detected in extracts of bone obtained from mouse tibia (Figure II-3D), which, in addition to brain and cardiac muscle, represented one of the richest tissue sources of MN1 transcripts. Overall, these expression studies provide support for a potential role of MN1 in skeletal biology and in osteoblast cell differentiation and/or function.

MN1 augments VDR-mediated transcription

Given the evidence indicating that MN1 stimulates RAR-mediated transcription of MSV-LTR (252), we tested whether MN1 modulates VDR-mediated transcription. COS-7 cells were transfected with a VDR expression vector and a 1,25$(OH)_2D_3$-responsive reporter gene composed of four copies of a VDRE and a minimal TATA promoter fused upstream of firefly luciferase [$(VDRE)^4$-TATA-luc]. As shown in Figure II-4A, transfection of an MN1 expression plasmid augmented 1,25$(OH)_2D_3$-induced reporter gene activity 6-7

fold. MN1 also stimulated 1,25$(OH)_2D_3$-mediated induction of a reporter gene driven by 24-hydroxylase promoter, a native 1,25$(OH)_2D_3$-responsive regulatory sequence (data not shown). The effect of MN1 was both VDR- and 1,25$(OH)_2D_3$-dependent because MN1 expression had minimal effects on basal reporter gene activity in the absence of VDR or in the absence of 1,25$(OH)_2D_3$ (Figure II-4B). MN1 also enhanced the ligand-dependent transcriptional activity of a fusion protein composed of the GAL4 DNA binding domain (DBD) and the ligand-binding domain (LBD) of VDR (Figure II-4C). Therefore, it is likely that MN1 acts through the VDR LBD to stimulate VDR-mediated transcription.

To test the putative role of MN1 in other nuclear receptor pathways, GAL4 DBD was fused with the LBDs of different receptors, and the activity of these fusion proteins was measured by activation of a GAL4-responsive reporter gene. MN1 stimulated the VDR LBD as expected, but MN1 did not alter the transcription mediated by LBD of RAR, PXR, TR and PPAR, which all form heterodimer with RXR upon ligand binding (Figure II-5A). In addition to the ligand-activated nuclear receptors, we also tested whether MN1 impacts the transcriptional activity of the ROR orphan nuclear receptors. As shown in Figure II-5B, MN1 modestly stimulated the activity of RORγ, but not RORα or RORβ. Although MN1 failed to activate the LBD of RARα (Figure II-5A), it augmented the transcriptional activity of full-length RARα with respect to a synthetic RARE-driven reporter gene (Figure II-5C). In contrast, MN1 inhibited the GR-mediated transcription (Figure II-5C). Collectively, these data indicate that MN1 selectively stimulates the transcriptional activity of VDR, RAR, and RORγ, while the

mechanisms underlying MN1 transactivation are distinct among these nuclear receptors.

The SRC proteins are well-characterized coactivators of VDR and other nuclear receptors. To test whether MN1 cooperates with SRCs to stimulate VDR-mediated transcription, COS-7 cells were transfected with VDR and $(VDRE)^4$-TATA-luc. MN1 alone or in combination with SRC-1 or SRC-2 were cotransfected. As shown in Figure II-6A and -6B, SRC-1 and SRC-2 both stimulated the VDR-mediated transcription 3-4 fold, MN1 alone similarly stimulated VDR activity 2-3 fold. However, MN1 and SRC-1 together augmented VDR-mediated transcription 20-fold, and MN1 and SRC-2 stimulated VDR transactivation 16-fold. These data suggest that MN1 acts with SRCs to synergistically stimulate VDR-mediated transcription.

MN1 knockout osteoblasts have diminished VDR-mediated transcriptional responses

We characterized MN1 as a coactivator for VDR-mediated transcription using ectopic expression approaches in heterologous cell lines. To evaluate the significance of endogenous MN1 in VDR/1,25$(OH)_2D_3$-mediated transcription in the osteoblasts, we examined the consequence of MN1 ablation on VDR/1,25$(OH)_2D_3$-activated reporter gene activity in primary osteoblastic cell cultures derived from MN1 knockout mice. As shown in Figure II-7A, 1,25$(OH)_2D_3$-activated expression of the cyp24(-1200)-luc reporter containing the

native promoter of the human 24-hydroxylase gene was dramatically reduced in MN1 knockout osteoblasts compared to the wild-type cells. Similar results were obtained with $(VDRE)^4$-TATA-luc (Figure II-7B). We also consistently observed impaired $1,25(OH)_2D_3$ activation of the native 24-hydroxylase gene expression in the MN1 knockout cells compared to wild-type controls (Figure II-7C). These data strongly support a significance for MN1 in $1,25(OH)_2D_3$/VDR-mediated transactivation in osteoblasts.

MN1 knockout osteoblasts have reduced growth rate

MN1 knockout mice display severe abnormalities in cranial skeletal development (207), but the cellular basis for these defects is unresolved. To explore the potential significance of MN1 in bone cell function, we examined a variety of osteoblastic cell parameters using calvarial osteoblasts derived from E18.5 MN1 knockout and wild-type embryos. Cell proliferation, as determined by counting trypan blue-excluding cells, indicated that MN1-null primary osteoblasts grew at a much reduced rate compared to wild-type cells (Figure II-8A). Moreover, BrdU labeling analysis consistently showed that MN1 knockout osteoblasts exhibited lower BrdU incorporation, indicating reduced S-phase entry in MN1 knockout cells (Figure II-8B). Cell cycle analysis revealed that MN1 null osteoblasts have a higher percentage of G_0/G_1 cells (66%) compared to the wild-type cells (56%) (data not shown). The antiproliferative effects of $1,25(OH)_2D_3$ were modest in these primary osteoblasts, but there was no statistically significant difference in the response of wild-type cells or MN1 null cells to

1,25$(OH)_2D_3$ as measured by multiple MTT analysis (Figure II-8C), indicating that MN1 may not be required for the antiproliferative effects of 1,25$(OH)_2D_3$ in this cell system. To explore the *in vivo* significance of MN1 in controlling osteoblast proliferation, BrdU incorporation was determined in embryonic calvaria. Consistent with *in vitro* observations, MN1 knockout calvaria had 40% less BrdU labeled cells compared to the wild-type controls (Figure II-9). These studies indicate that MN1 is required for appropriate osteoblast proliferation *in vitro* and *in vivo*.

MN1 knockout osteoblasts show altered morphology and reduced motility

In proliferating osteoblast cultures, we observed a dramatic difference in cell morphology between MN1 knockout and wild-type cells (Figure II-10A). In general, subconfluent MN1 knockout calvarial osteoblasts appeared abnormal, displaying a large, flattened morphology. When observed using phase contrast microscopy, the MN1 knockout cells were much less refractile along their edges compared to the wild-type cells. This morphological difference suggested a possible role for MN1 in cell migration. Thus, the motility of wild-type and MN1 knockout osteoblasts was analyzed. Confluent osteoblast monolayers were "wounded" with a pipette tip to create a linear scratch, and the movement of cells into the wound area was determined. Compared to the wild-type controls, the wound closure in MN1 knockout cells was markedly impaired (Figure II-10B, -10C). Delayed wound closure in this model may result from impaired cell migration or proliferation. However, the 16-hour time frame in which these

migration studies were conducted was significantly less than the 40- and 60-hour doubling times of the wild-type and knockout cells, respectively (Figure II-8A). Thus, contributions of cell proliferation were minimized under these conditions.

MN1 knockout calvarial cells show reduced differentiation and mineralization

Mature primary calvarial osteoblasts express alkaline phosphatase and produce a mineralized matrix *in vitro*. To investigate the functional roles of MN1 in osteoblast maturation, MN1 wild-type or knockout osteoblasts were differentiated and analyzed for alkaline phosphatase expression as well as calcium deposition. To minimize the effects of proliferation differences on this analysis, MN1 wild-type or knockout osteoblasts were seeded at a high initial density ($6x10^3$ cells/cm^2). Under these conditions, proliferative differences were minimal and both cultures reached a state of confluence within 48 hours. As shown in Figure II-11, both mRNA expression and enzymatic activity of alkaline phosphatase were reduced in MN1 knockout osteoblasts. In addition, MN1 knockout osteoblasts formed fewer and smaller Alizarin Red S-stained mineralized nodules (Figure II-12A, -12B). These data indicate that MN1 is required for appropriate differentiation and mineralized matrix production in this *in vitro* osteoblast culture system. To evaluate the significance of MN1 in osteoblastic maturation *in vivo*, the expression of osteoblast marker genes was examined in extracts obtained from MN1 wild-type and knockout calvaria (Figure II-12C). MN1 transcripts were readily detected in WT calvaria and calvarial MN1 expression levels showed a gene dosage effect in the $MN1^{+/-}$ and $MN1^{-/-}$ mice.

The expression levels of alkaline phosphatase and osteocalcin, markers of mature osteoblasts, were markedly reduced in MN1 knockout calvaria compared with the wild-type controls. The expression of bone sialoprotein 2 (BSP2) was not dramatically altered. Cumulatively, these data strongly suggest that intact E18.5 calvaria from the MN1 knockout mice have fewer or less differentiated osteoblasts *in vivo* and that MN1 is an important gene that controls osteoblast differentiation and mineralization *in vitro* and *in vivo.*

MN1 knockout calvarial osteoblast cultures exhibit enhanced adipogenesis

Surprisingly, MN1 knockout cells cultured under osteogenic conditions had copious amounts of highly refractive, intracellular vesicles indicative of lipid vesicles (data not shown). Oil Red O staining confirmed that the MN1 knockout osteoblasts had more lipid droplets than the wild-type cells (Figure II-13A, -13B). Gene expression analysis showed that differentiating MN1 knockout osteoblasts expressed high amounts of adipocyte marker genes, such as adipocyte fatty acid binding protein 4 (FAPB4), lipoprotein lipase (LPL), adiponectin, and peroxisome proliferator activated receptor gamma (PPARγ) (Figure II-13C). Elevated expression of these adipocyte markers was evident as early as 7 days of differentiation and continued throughout differentiation period. This was not observed in subconfluent MN1 knockout cells or in wild-type cells under these conditions (Figure II-13C). These data indicate that MN1 deletion suppresses osteogenesis and promotes adipogenesis. It is shown that cadherin-11 (OB-cadherin)-mediated cell-cell interaction plays a key role in linage decision of

mesenchymal stem cells (253, 254). Cadherin-11 promotes osteogenesis (255), and cadherin-11 knockout osteoblasts have reduced mineralization (256). The impaired motility in MN1-null osteoblasts (Figure II-10) implies a change in cell adhesion/migration signaling. Therefore, we examined the expression of cadherin-11 in wild-type and MN1 knockout osteoblasts. As shown in Figure II-13C, the mRNA transcripts of cadherin-11 were stimulated by osteoblast differentiation, while this induction was compromised in MN1 knockout osteoblasts. These data suggest that MN1 promotes osteogenesis and inhibits adipogenesis from the mesenchymal precursors possibly through regulating cadherin-11 signaling pathway.

MN1 knockout osteoblasts have reduced ability to support 1,25(OH)$_2$D$_3$-induced osteoclastogenesis

Osteoblasts secrete essential factors to regulate osteoclastogenesis and a key function of 1,25(OH)$_2$D$_3$ in osteoblasts is to stimulate the expression of genes that support osteoclast differentiation. To determine the significance of osteoblastic MN1 in 1,25(OH)$_2$D$_3$-stimulated osteoclastogenesis, wild-type or MN1 knockout osteoblasts were used in spleenocyte coculture studies as described in “Materials and Methods”. As expected, no TRAP-positive multinucleated cells were detected in the absence of 1,25(OH)$_2$D$_3$ (Figure II-14B). However, in the presence of 10 nM or 100 nM 1,25(OH)$_2$D$_3$, the numbers of TRAP positive multinucleated osteoclasts in the coculture with MN1 knockout osteoblasts were dramatically lower than in the coculture with wild-type controls

(Figure II-14A and -14B). These data suggest that osteoblast-derived MN1 plays an important role in supporting $1,25(OH)_2D_3$-stimulated osteoclast differentiation.

To investigate the mechanism underlying the reduced ability of MN1 knockout osteoblasts to support $1,25(OH)_2D_3$-induced osteoclastogenesis, osteoblast expression of key osteoclastogenic factors was compared in wild-type and MN1 knockout cells. $1,25(OH)_2D_3$ suppressed the expression of OPG, a factor that inhibits osteoclast differentiation (Figure II-14C). However, compared to wild-type controls, MN1 knockout osteoblasts produced much higher levels of OPG in both the absence and presence of $1,25(OH)_2D_3$ (Figure II-14C). In contrast, MN1 knockout cells had lower basal and $1,25(OH)_2D_3$-induced expression of RANKL and M-CSF, which are both osteoclastogenesis stimulating factors (Figure II-14C). These data indicate that MN1 is essential for maintaining an appropriate RANKL:OPG ratio to support optimal osteoblast-mediated osteoclastogenesis.

MN1 stimulates RANKL promoter activity

The previous data (Figure II-14C) suggest that MN1 may stimulate RANKL promoter activity and enhance the synthesis of RANKL mRNA. To test this hypothesis, the activity of a -1 kb human RANKL promoter was examined under MN1 overexpression or MN1 depletion conditions. As shown in Figure II-15A, the RANKL promoter was stimulated by ectopic expression of MN1 in primary osteoblasts. Furthermore, decreased RANKL promoter activity was observed

when MN1 was knocked down by siRNA (Figure II-15B) in MC3T3-E1 osteoblasts. Moreover, RANKL promoter activity was significantly lower in MN1 knockout osteoblasts compared to the wild-type cells (Figure II-15D). Importantly, expression of the promoter-less pGL3 control reporter gene was unaffected by MN1 overexpression or MN1 ablation (Figure II-15). The stimulation of RANKL promoter activity by MN1 supports a potential mechanism in which MN1 promotes osteoclastogenesis via increased transcription of the RANKL gene in osteoblasts.

DISCUSSION

Here, we identified MN1 as a novel osteoblastic gene that is up-regulated by $1,25(OH)_2D_3$ and that has a previously unrecognized significance in osteoblasts. The present study shows that MN1 positively influences VDR-activated transcription, and primary osteoblasts derived from the MN1 knockout mouse are defective in VDR-mediated gene expression, in osteoblast proliferation, migration and mineralization, and in osteoblast-mediated osteoclastogenesis. We further provide a mechanistic basis for the involvement of MN1 in osteoblast-directed osteoclastogenesis that likely involves transcriptional regulation of the RANKL promoter resulting in enhanced RANKL:OPG ratios that favor osteoclast formation. These new findings provide strong support for a role of MN1 in maintaining appropriate osteoblast function.

MN1 was revealed as a 1,25$(OH)_2D_3$-induced gene in multiple osteoblastic models in our studies. Another microarray study also showed that MN1 mRNA expression was increased by a synthetic 1,25$(OH)_2D_3$ analog, EB1089, in squamous cell carcinoma cells (257). These data clearly point to MN1 as a 1,25$(OH)_2D_3$-induced gene in multiple 1,25$(OH)_2D_3$ target cells. 1,25$(OH)_2D_3$ likely induces MN1 expression through a transcriptional mechanism because 1,25$(OH)_2D_3$ does not affect its mRNA stability (Figure II-2A and -2B). The 1,25$(OH)_2D_3$ response of MN1 promoter (up to -6 kb relative to transcriptional starting site) was examined using reporter gene analysis. However, no 1,25$(OH)_2D_3$ stimulation was detected (data not shown). A potential VDRE was identified at +1.9 kb (relative to translational start site) of human MN1 gene (258), but functional assays did not detect its response to 1,25$(OH)_2D_3$ (data not shown). Our data indicate that pretreatment of transcription inhibitor, actinomycin D, completely abolished 1,25$(OH)_2D_3$ induction of MN1 mRNA (Figure II-2C), and pretreatment of protein synthesis inhibitor, cycloheximide, diminished that (Figure II-2D). Therefore, 1,25$(OH)_2D_3$ can target other protein(s) and these protein(s), in turn, promotes MN1 expression. Further studies are required to dissect the molecular details of the 1,25$(OH)_2D_3$-mediated induction of MN1 expression.

MN1 is a transcription factor that functions, in part, as a nuclear receptor coactivator protein. Heterologous expression studies in Hep3B and COS-7 cells show that MN1 selectively augments VDR- and RAR-activated transcription, perhaps through direct interactions with the receptor and/or with p160 and p300 coactivator proteins (252). It is not surprising that MN1 augments the activity of

both VDR and RAR because these two nuclear receptors are structurally related and both utilize RXR as their heterodimeric partner (259). However, MN1 likely enhances the transcriptional activity of these two nuclear receptors through distinct mechanisms. Whereas MN1 stimulates VDR through its LBD, RARα activation requires an intact receptor. Furthermore, our data show that MN1 is not a general nuclear receptor coactivator, instead, it selectively stimulates VDR, RAR, and, to a lesser extent, RORγ activity, inhibits GR activity, and does not affect the transactivation potential of the other nuclear receptors analyzed in this study. Although the exact mechanism underlying the transcriptional stimulation of nuclear receptors is not known, current study suggests that MN1 cooperates with both SRC-1 and SRC-2 in a synergistic manner (Figure II-6). Coupled with the previous report showing that MN1 cooperates with RAC-3 in RAR-dependent transcription (252), these data provide further evidence of a functional link between MN1 and the SRC family of coactivators. However, no physical interactions of MN1 with VDR or SRC-1/2 were identified in our studies.

Limitations of these studies on nuclear receptor pathways include a reliance on overexpression of MN1 and a lack of approaches addressing a functional role for MN1 in appropriate target cells. Thus, the observations that MN1 ablation reduces both VDR-activated reporter gene expression as well as $1,25(OH)_2D_3$-activated expression of the native 24-hydroxylase gene (a direct VDR target gene) in primary osteoblastic cells (Figure II-7) provides important support for the significance of MN1 in the mechanism of VDR-mediated gene expression in osteoblasts. MN1 ablation also dramatically reduces $1,25(OH)_2D_3$-

stimulated, osteoblast-mediated osteoclastogenesis (Figure II-14), thus showing a requirement for MN1 in critical VDR/1,25$(OH)_2D_3$-mediated biological activities in the osteoblast. While these *in vitro* studies provide a solid foundation for the significance of MN1 in VDR-mediated transcription, it will be important to explore the *in vivo* requirement of MN1 in the vitamin D endocrine system and the maintenance of global mineral homeostasis or hair follicle cycling. Currently, this cannot be addressed because the MN1 knockout mice do not survive postnatally when disruptions in the vitamin D endocrine system become evident. Tissue-directed MN1 null models that survive postnatally, perhaps targeting intestine or bone, need to be developed to tackle this important issue.

In addition to interacting with nuclear receptors and coactivator proteins to influence their transcriptional activities, MN1 also binds DNA directly via a CACCCAC promoter sequence to increase transcription of the IGFBP5 gene as well as a variety of other genes (260, 261). Our studies indicate that ectopic expression of MN1 stimulates RANKL promoter activity in osteoblastic cells and knockdown or ablation of MN1 attenuates it. Thus, these observations support a transcriptional role for MN1 in the regulation of RANKL gene expression in osteoblast. Indeed, several CACCCAC-like elements exist in the approximately 1 kb of the 5'-flanking region of the human RANKL gene that was used here. Clearly, additional studies are needed to test whether this transcriptional role for MN1 is direct and mediated through binding of MN1 to the RANKL promoter or whether alternative mechanisms exist. It is unlikely that these effects are mediated through the VDR since the vitamin D responsive elements of the

RANKL gene reside at extreme upstream distal regions (at 16-76 kb upstream from the transcriptional start site) (43), far outside the immediate promoter regions tested here. However, based on the established role of MN1 in VDR-activated transcription, it would be intriguing to test the interplays between MN1 and these distal regulatory regions since $1,25(OH)_2D_3$-mediated expression of RANKL is also impacted in MN1 knockout osteoblasts.

The combination of defective osteoblast differentiation, mineralization, and impaired osteoblast-directed, RANKL-stimulated, osteoclastogenesis has the potential to produce a global bone cell imbalance in the cranial vault that may explain, in part, the undermineralized phenotype in the MN1 knockout mice. The craniofacial phenotype of the MN1 knockout embryo highlights the additional concept that MN1 also functions in critical developmental pathways that are independent of the VDR/$1,25(OH)_2D_3$ endocrine system. This is perhaps best illustrated by the lack of overt defects in cranial skeletal development or palatal defects in the 1α-hydroxylase or VDR knockout mice, which lack $1,25(OH)_2D_3$ or its receptor, respectively (89, 195), or in humans with inactivating mutations in these genes (262, 263). Thus, VDR is unlikely to play a major role in the function that MN1 exerts during mouse development at embryonic stage. Interestingly, the MN1 knockout skeletal defects are restricted to cranial skeletal elements, many of which form by intramembranous ossification processes (207). Long bones of the appendicular skeleton that form by endochondral ossification appear to develop normally in the MN1 knockout embryos when analyzed for gross mineralization using Alcian Blue and Alizarin Red whole skeletal stains

(207). Indeed, we observed no differences in bone mineral densities and morphological parameters of tibia from E18.5 $MN1^{+/+}$ and $MN1^{-/-}$ embryos using more refined quantitative μCT imaging (data not shown). Meester-Smoor et al. suggested that MN1 was selectively involved in intramembranous bone formation (207). However, there are several important exceptions to this selectivity issue. Not all bones that form by intramembranous ossification are affected in the MN1 null embryos. The mandible and clavicle develop mainly through intramembranous ossification and their development is intact in the MN1 knockout embryo. Moreover, MN1 knockout embryos display anomalies in numerous skeletal elements that form by endochondral ossification processes including the agenic, delayed, deformed, and/or undermineralized development of the pterygoid, basisphenoid, alisphenoid, supraoccipital, exoccipital, and sternum (ref. 207 and data not shown). This indicates that the selectivity of the skeletal elements that require MN1 for normal development may not be related to the processes through which they form (e.g., intramembranous versus endochondral), but instead, may arise through other, as yet unknown, mechanisms.

The vertebrate skeleton is derived from three distinct sources. In general, the craniofacial skeleton originates from cranial neural crest cells, the axial skeleton is formed by paraxial mesoderm (somites), and the appendicular skeleton is derived from lateral plate mesodermal cells (264). The restricted craniofacial defects of the MN1 knockout mice indicate the potential involvement of MN1 in neural crest cell migration and/or differentiation. Indeed, a recent

study revealed that MN1 acts upstream of Tbx22, a gene that is mutated in X-linked cleft palate in humans (265). This supports an important role for MN1 in regulating the expression of genes involved in neural crest-initiated, palatal shelf development. This, combined with the defects in osteoblast function in MN1 knockout calvarial cells, point to more global roles for MN1 in early development of neural crest-derived skeletal structures, in the subsequent differentiation and mineralization of osteoblasts during embryonic development of the skull, and perhaps in postnatal skeletal homeostasis. Similarly, multi-faceted roles in embryonic development and in embryonic and/or postnatal osteoblast dynamics exist for a variety of other genes including several of the Distal-less (Dlx) homeobox transcription factors (266), several of the hox family of transcription factors including hoxA10 (267), SATB2 (268), Connexin43 (269), Odd-skipped related 2 (270), TGFβ and BMP family members (271), and numerous others. The significance of osteoblastic MN1 in postnatal skeletal dynamics can only be revealed with the development of an osteoblast-targeted MN1 gene knockout that survives postnatally. The profound osteoblastic defects uncovered here provide strong justification for the development of such a model.

Our data reveal that MN1 knockout osteoblasts exhibit reduced mineralization and enhanced adipogenesis compared to wild-type cells. MN1 expression is increased during osteoblast differentiation. Interestingly, the time course of increased MN1 expression in wild-type cells is similar to the induction of adipocyte marker gene expression in the differentiating MN1 knockout cells (compare Figures II-3C and -13C). Furthermore, MN1 is down regulated during

adipogenesis in a 3T3-L1 adipocyte model (data not shown). Thus, the elevated expression of MN1 in differentiated osteoblasts may be important for maintaining the osteoblast phenotype and suppressing adipocyte formation. Osteoblasts and adipocytes may originate from common mesenchymal stem cells, and the differentiation of these two lineages is believed to be inversely correlated (272, 273). Indeed, increased adipogenesis in bone marrow is associated with osteoporosis, age-related osteopenia, and other conditions of low bone mass or density. Consequently, the adipogenesis pathway has emerged as a new therapeutic target to prevent or treat osteopenic bone disorders (274, 275). Some of the proteins and pathways that modulate mesenchymal cell differentiation into osteoblasts and adipocytes have been characterized (276-279). Runx2 knockout calvarial cells are defective in osteoblast differentiation but display enhanced adipogenesis and adipocyte marker gene expression (279). TAZ (transcriptional coactivator with PDZ-binding motif), a coactivator for Runx2-mediated transcription, blocks adipogenesis of mesenchymal cells (276). Cadherin-11 regulates cell-cell interaction and the linage decision of mesenchymal stem cells (253, 254). Importantly, MN1 knockout osteoblasts have impaired motility as well as decreased cadherin-11 expression, suggesting that MN1 may impact the fate of mesenchymal cells by regulating cadherin-11 signaling. $1,25(OH)_2D_3$ inhibits adipocyte differentiation (280, 281). In 3T3-L1 pre-adipocytes, $1,25(OH)_2D_3$ treatment reduces the expression of PPARγ, C/EBPα, LPL and FABP4 in a dose-dependent manner (280), but no further mechanism has been suggested. Our data reveal that $1,25(OH)_2D_3$ induces

MN1 in both osteoblasts and 3T3-L1 adipocytes (Figure II-1, -3, and data not shown). Thus, MN1 may be another important molecular switch that regulates the osteoblast/adipocyte balance from their mesenchymal precursors.

In summary, our studies provide key evidence for a significance of MN1 in vitamin D-mediated transcription and in numerous other critical aspects of osteoblast biology. Our findings help to establish MN1 as a critical protein that is needed for appropriate osteoblast growth, differentiation, and function. Understanding detailed molecular and cellular mechanisms underlying these functional aspects of osteoblastic MN1 is an important area of future research efforts.

Table 1. Amplification primers used to generate cDNA probes for Northern blot analysis.

Gene	Primers
MN1	F: CTTTAACGAAGCCGGACTGA
	R: GCCAAACCTCTCGAAGAACA
24-hydroxylase	F: CAAGGTCCGTGACATCCAAG
	R: GATGCAGGGCTTGACTGATT
VDR	F: CTGGTGACTTTGACCGGAAT
	R: TTATGAGGGGTTCGATCAGC
OPG	F: ATTGAATGGACAACCCAGGA
	R: ACGCTGCTTTCACAGAGGTC
RANKL	F: TATACACAACCTGTACAGGCTC
	R: CCATGAGCCTTCCATCATAGCTGG
ALP	F: GGGACGAATCTCAGGGTACA
	R: CTGGCCTTCTCATCCAGTTC
Osteocalcin	F: GAACAGACTCCGGCGCTA
	R: AGGGAGGATCAAGTCCCG
BSP2	F: AGTACCGGCCACGCTACTTT
	R: ACGGTGCTGCTTTTTCTGAT
PPARγ	F: GTTGACACAGAGATGCCATTCTGG
	R: ACAAATGGTGATTTGTCCGTTG
LPL	F: TTCAACCACAGCAGCAAGAC
	R: CCATCCTCAGTCCCAGAAAAG
Adiponectin	F: GTTGCAAGCTCTCCTGTTCC
	R: GGGCTATGGGTAGTTGCAGTC
M-CSF	F: CTGCTGCTGGTCTGTCTCCT
	R: GTGAGTCTGTCCCCATGGTT
Cadherin-11	F:GACAGGGACACCAACAGACC
	R:AGGCTCATCGGCATCTTCTA
FABP4	F: CACCTGGAAGACAGCTCCTC
	R: AATTTCCATCCAGGCCTCTTCC
Cyclophilin B	F: AGCGCAATATGAAGGTGCTC
	R: GCACAGAACCTTGTGACTGG
18S RNA	F: CGGGTCATAAGCTTCGTT
	R: CCGCAGGTTCACCTACGG

Figure II-1

$1,25(OH)_2D_3$ induces MN1 expression in MG-63 osteoblastic cells.

A, MG-63 cells were treated for the indicated times with 10 nM $1,25(OH)_2D_3$ or 10 nM cholecalciferol (chol). B, MG-63 cells were treated with ethanol vehicle control (0) or 0.1-100 nM $1,25(OH)_2D_3$ for 6 hours. The mRNA expression of MN1 and β-actin was analyzed by Northern blots. C, MG-63 cells were treated with ethanol vehicle control (–) or 10 nM $1,25(OH)_2D_3$ (+) for 24 hours. The protein expression of MN1 and β-actin was determined by Western blot analysis.

A

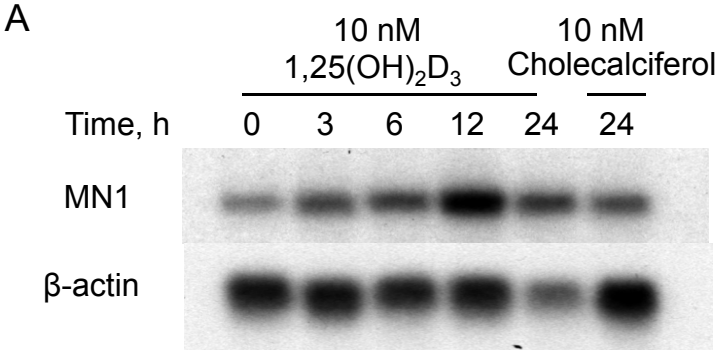
10 nM
1,25(OH)2D3
10 nM
Cholecalciferol
Time, h
0
3
6
12
24
24
MN1
β-actin

B

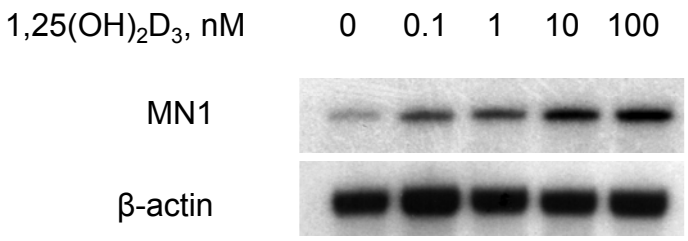
1,25(OH)2D3, nM
0
0.1
1
10
100
MN1
β-actin

C

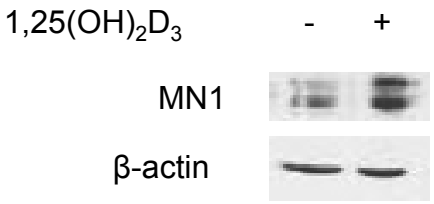
1,25(OH)2D3
-
+
MN1
β-actin

Figure II-2

The mechanism of MN1 regulation in MG-63 cells.

A, MG-63 cells were treated with ethanol vehicle control or 10 nM $1,25(OH)_2D_3$ for 6 hours, and further incubated with 1 μg/ml actinomycin D for the indicated times. The mRNA expression of MN1 and GAPDH was analyzed by Northern blots. B, The quantitation of MN1 mRNA levels normalized by GAPDH. C, MG-63 cells were pretreated with ethanol vehicle control (- ACTD) or 1 μg/ml actinomycin D (+ ACTD) for 1 hour. D, MG-63 cells were pretreated with ethanol control (- CHX) or 10 μg/ml cycloheximide (+ CHX) for 1 hour. Cells were then treated with ethanol control (Et) or 10 nM $1,25(OH)_2D_3$ (1,25) for 6 hours. The mRNA expression of MN1 and β-actin was analyzed by Northern blots.

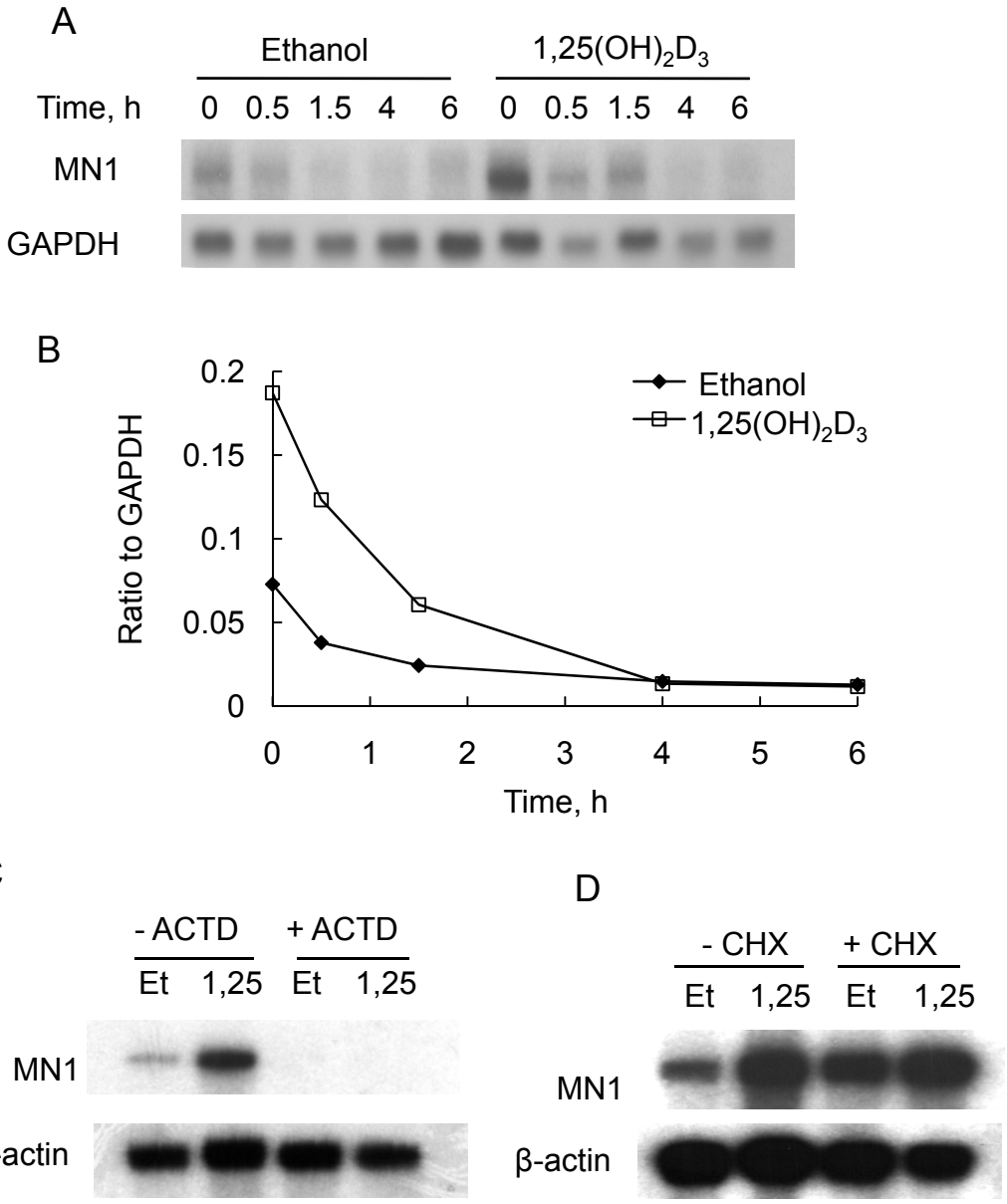
A
Ethanol
1,25(OH)2D3
Time, h
0 0.5 1.5 4 6 0 0.5 1.5 4 6
MN1
GAPDH
B
Ethanol
1,25(OH)2D3
Ratio to GAPDH
0.2
0.15
0.1
0.05
0
0 1 2 3 4 5 6
Time, h
C
- ACTD
+ ACTD
Et 1,25 Et 1,25
MN1
β-actin
D
- CHX
+ CHX
Et 1,25 Et 1,25
MN1
β-actin

Figure II-3

MN1 mRNA transcripts are induced by 1,25(OH)$_2$D$_3$ and by osteoblastic cell differentiation.

MC3T3-E1 cells (panel A) or primary calvarial osteoblasts (panel B) were maintained at proliferating stage or differentiated for 2 weeks as described in "Materials and Methods". Proliferating or differentiating cells were treated with 10 nM 1,25(OH)$_2$D$_3$ for the indicated times and the expression of MN1, 24-hydroxylase, VDR, or 18S RNA were examined by Northern blot analysis. C, Primary osteoblasts were differentiated for the indicated times and the expression of MN1 or 18S RNA was examined by Northern blot analysis. D, Total RNA was extracted from the indicated tissues of 6-week-old wild-type mice, and the expression of MN1 was determined by Northern Blot analysis. Ethidium bromide staining of 18S/28S ribosomal RNA was used to normalize loading differences.

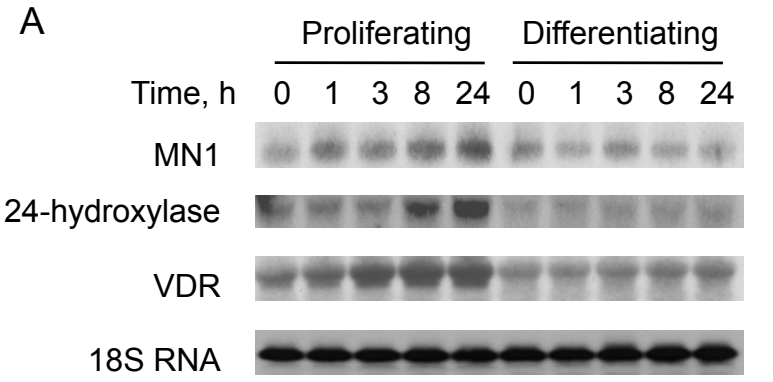
A
Proliferating
Differentiating
Time, h
0 1 3 8 24 0 1 3 8 24
MN1
24-hydroxylase
VDR
18S RNA

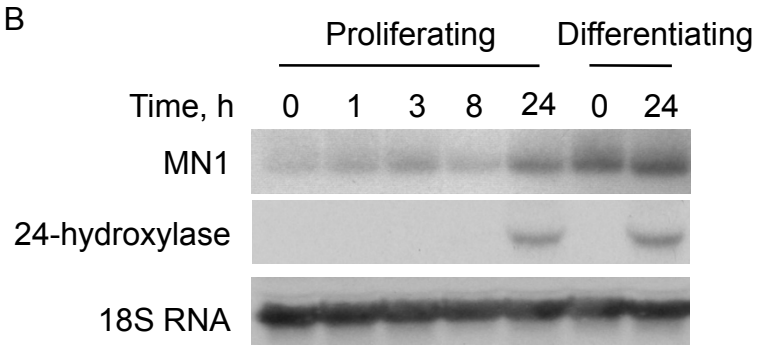
B
Proliferating
Differentiating
Time, h
0 1 3 8 24 0 24
MN1
24-hydroxylase
18S RNA

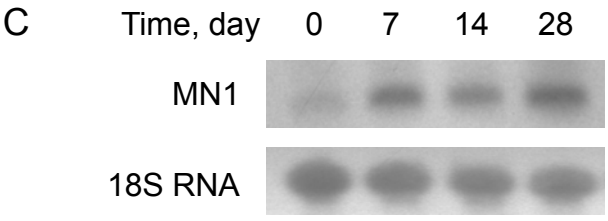
C
Time, day
0 7 14 28
MN1
18S RNA

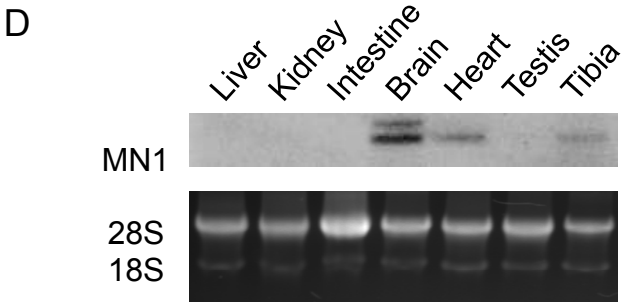
D
Liver
Kidney
Intestine
Brain
Heart
Testis
Tibia
MN1
28S
18S

Figure II-4

MN1 augments $1,25(OH)_2D_3$/VDR mediated transcription.

A, COS-7 cells were transiently transfected with $(VDRE)^4$-TATA-luc, SG5-VDR (VDR), and CMVTAG2B (Vector) or CMVTAG2B-MN1 (MN1). Cells were treated with ethanol vehicle control (-D) or 10 nM $1,25(OH)_2D_3$ (+D) for 24 hours. B, COS-7 cells were transiently transfected with $(VDRE)^4$-TATA-luc, SG5 (Vector) or SG5-VDR, and CMVTAG2B (Vector) or CMVTAG2B-MN1 (MN1). Cells were treated with ethanol vehicle control (-D) or 10 nM $1,25(OH)_2D_3$ (+D) for 24 h. C, COS-7 cells were transiently transfected with $(GAL4)^5$-TK-luc, GAL4 DBD (GAL4) or fusion of GAL4 DBD with VDR LBD (GAL4-VDR LBD), and CMVTAG2B (Vector) or CMVTAG2B-MN1 (MN1). Cells were treated with indicated doses of $1,25(OH)_2D_3$ for 24 hours. The firefly:renilla ratio (normalized luciferase activity) was measured as described in “Materials and Methods”. Data represent the mean ± SD (n = 3 in each group).

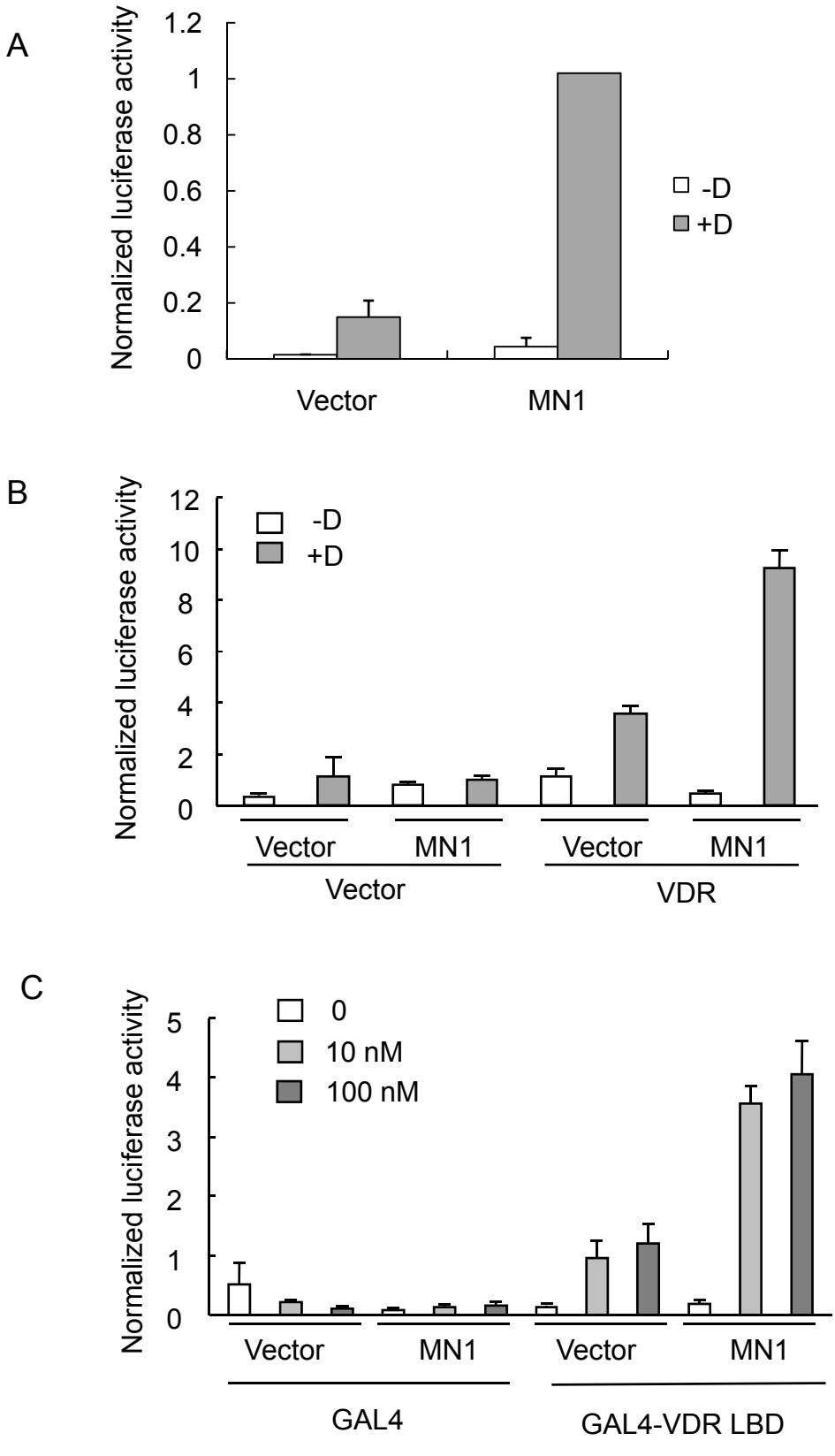
A
Normalized luciferase activity
1.2
1
0.8
0.6
0.4
0.2
0
-D
+D
Vector
MN1
B
Normalized luciferase activity
12
10
8
6
4
2
0
-D
+D
Vector
MN1
Vector
MN1
Vector
VDR
C
Normalized luciferase activity
5
4
3
2
1
0
0
10 nM
100 nM
Vector
MN1
Vector
MN1
GAL4
GAL4-VDR LBD

Figure II-5

MN1 shows selectivity on coactivating nuclear receptors.

A, COS-7 cells were transiently transfected with $(GAL4)^5$-TK-luc, fusions of GAL4 DBD with LBD of indicated nuclear receptors, and either CMVTAG2B (-) or CMVTAG2B-MN1 (+). Cells were treated with vehicle control (- ligand) or appropriate ligand (+ Ligand) for 24 hours. The ligands used in the assay are: 10 nM $1,25(OH)_2D_3$ for VDR, 10 nM thyroid hormone for TRβ, or 100 nM all-trans-retinoic acid for RAR, 1 μM traglitozone for PPARγ, and 10 μM rifampicin for PXR. B, COS-7 cells were transiently transfected with $(GAL4)^5$-TK-luc, fusions of GAL4 DBD with LBD of indicated ROR receptors, and either CMVTAG2B (Vector) or CMVTAG2B-MN1 (MN1). C, COS-7 cells were transiently transfected with indicated intact receptors and their responsive reporters. CMVTAG2B (Vector) or CMVTAG2B-MN1 (MN1) was cotransfected. Cells were treated with ethanol vehicle control or appropriate ligand (10 nM $1,25(OH)_2D_3$ for VDR, 1 μM dexamethasone for GR, or 100 nM all-trans-retinoic acid for RAR) for 24 hours. The firefly:renilla ratio (normalized luciferase activity) was measured as described in “Materials and Methods”. Data represent the mean ± SD (n = 3 in each group).

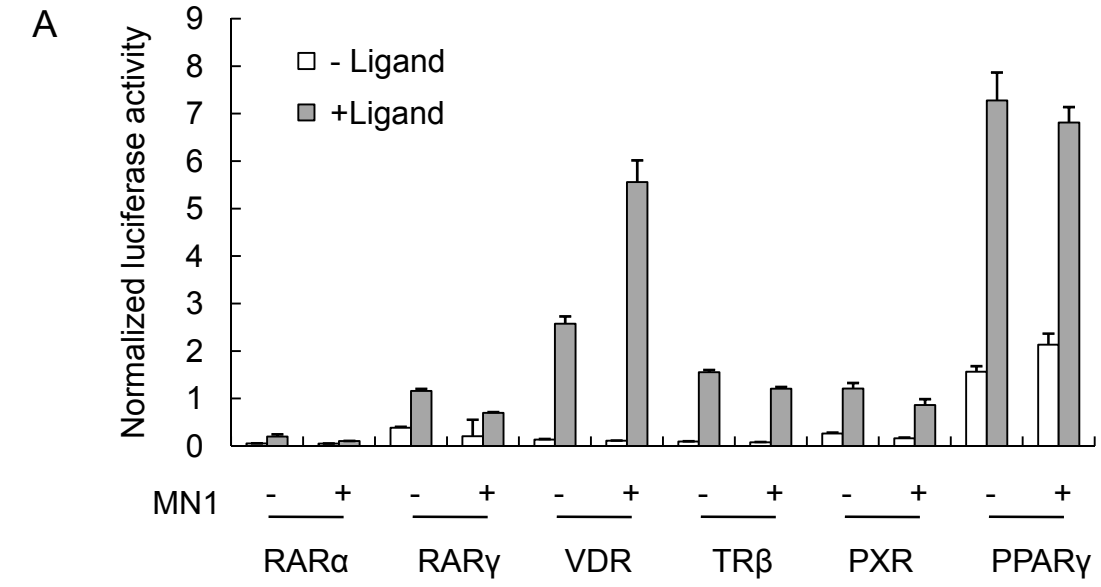
A
Normalized luciferase activity
9
8
7
6
5
4
3
2
1
0
- Ligand
+Ligand
MN1
- + - + - + - + - + - +
RARα
RARγ
VDR
TRβ
PXR
PPARγ

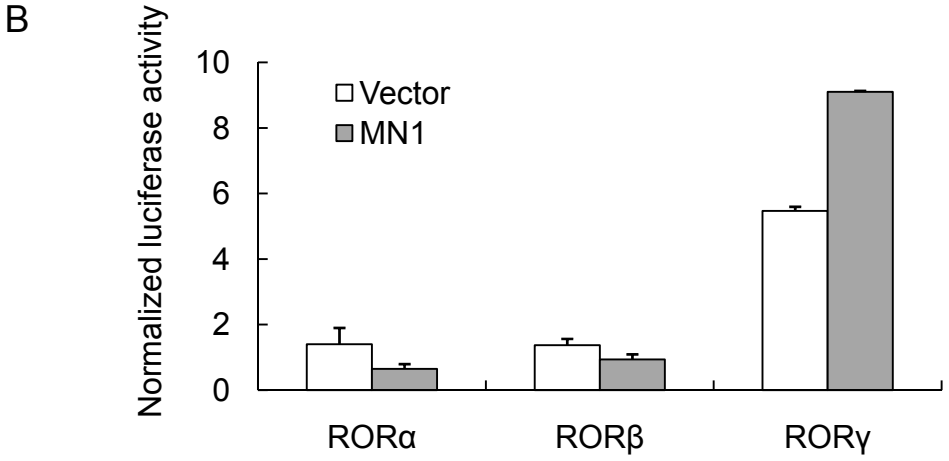
B
Normalized luciferase activity
10
8
6
4
2
0
Vector
MN1
RORα
RORβ
RORγ

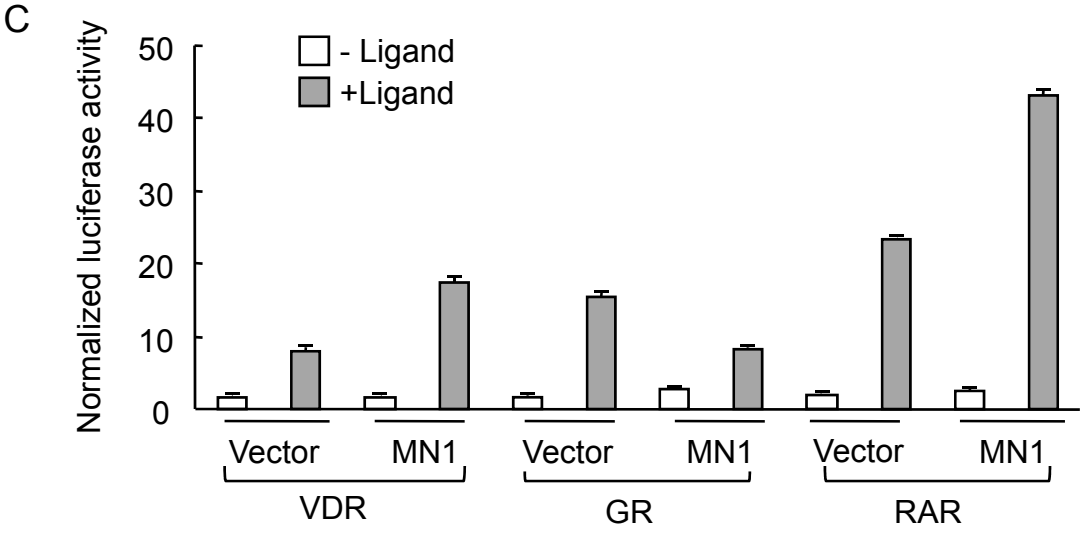
C
Normalized luciferase activity
50
40
30
20
10
0
- Ligand
+Ligand
Vector
MN1
Vector
MN1
Vector
MN1
VDR
GR
RAR

Figure II-6

MN1 cooperates with SRC coactivators to stimulate VDR-mediated transcription.

COS-7 cells were transiently transfected with $(VDRE)^4$-TATA-luc, SG5-VDR, and either CMV-TAG2B vector (Vector) or CMV-MN1 (MN1). SRC-1 (panel A) or SRC-2 (panel B) was co-transfected as indicated. Cells were treated with ethanol vehicle control (-D) or 100 nM $1,25(OH)_2D_3$ (+D) for 24 hours. The firefly:renilla ratio (normalized luciferase activity) was measured as described in “Materials and Methods”. Data represent the mean ± SD (n = 3 in each group).

A

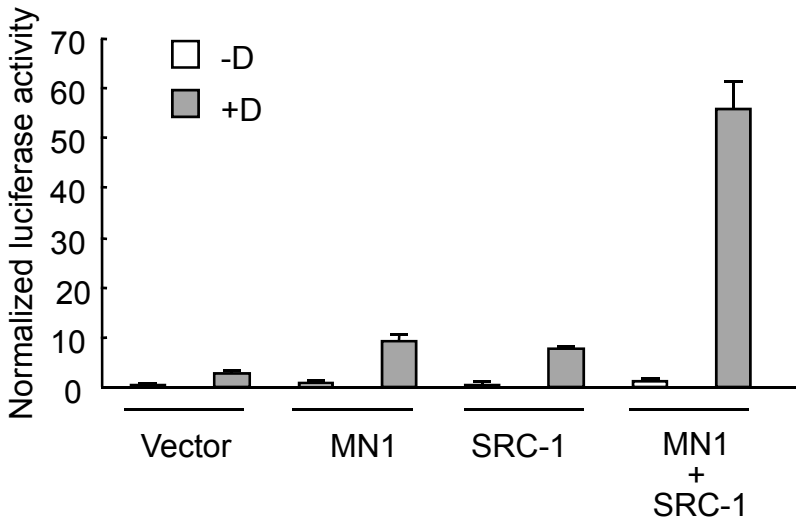
Normalized luciferase activity
70
60
50
40
30
20
10
0
-D
+D
Vector
MN1
SRC-1
MN1
+
SRC-1

B

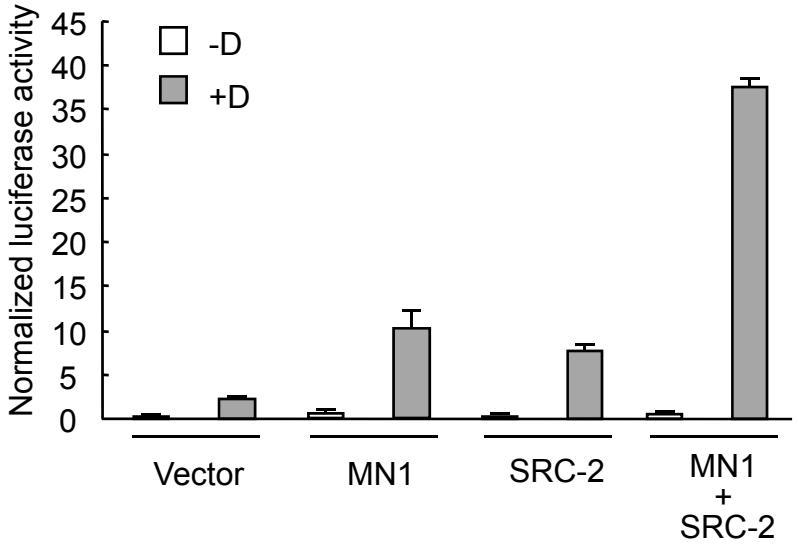
Normalized luciferase activity
45
40
35
30
25
20
15
10
5
0
-D
+D
Vector
MN1
SRC-2
MN1
+
SRC-2

Figure II-7

MN1 knockout osteoblasts have diminished VDR-mediated transcriptional responses.

Sub-confluent wild-type (WT) and MN1 knockout (KO) primary osteoblasts were transiently transfected with a 1.2 kb human 24-hydroxylase promoter reporter [cyp24(-1200)-luc in panel A] or a multi-copy VDRE driven reporter [$(VDRE)^4$-TATA-luc in panel B]. Cells were treated with the indicated concentration of $1,25(OH)_2D_3$ for 24 hours and the firefly:renilla ratio (normalized luciferase activity) was measured as described in "Materials and Methods". Data represent the mean ± SD (n = 4 in each group). C, RNA was isolated from MN1 WT or KO cells that were treated ethanol vehicle (-) or 10 nM $1,25(OH)_2D_3$ (+) for 24 hours. The expression of 24-hydroxylase and GAPDH was examined by Northern blot analysis.

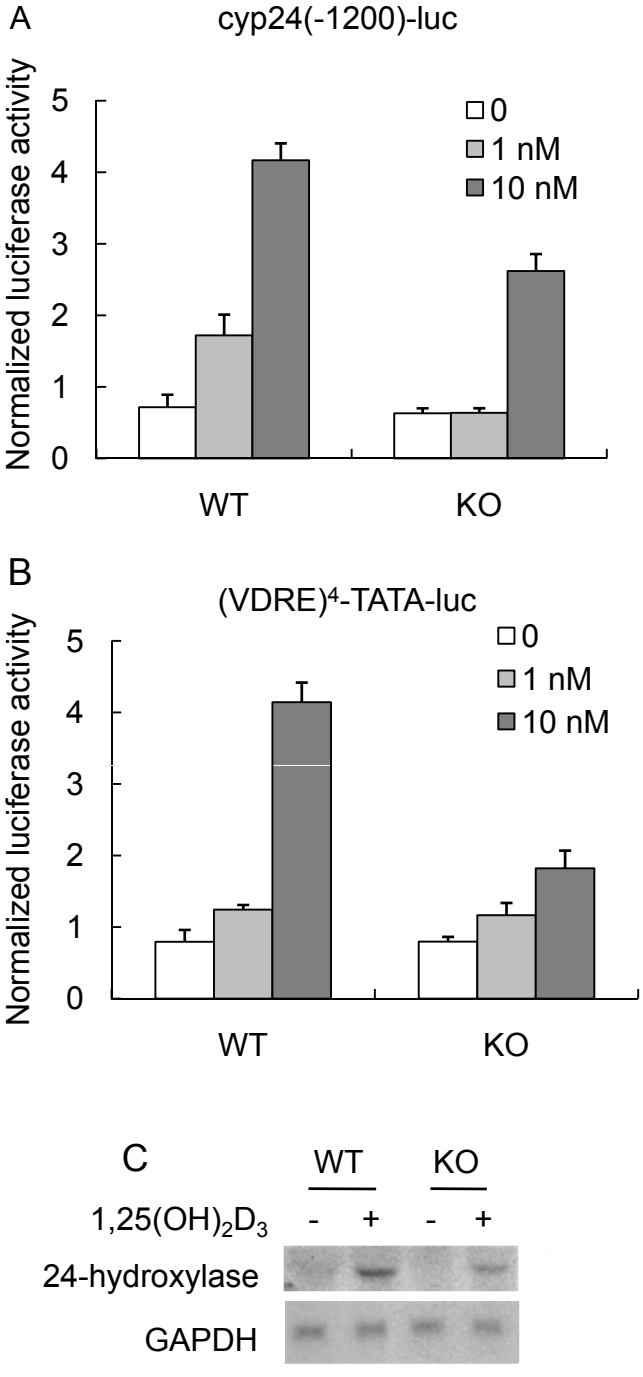
A
cyp24(-1200)-luc
Normalized luciferase activity
0
1 nM
10 nM
WT
KO
B
(VDRE)4-TATA-luc
Normalized luciferase activity
0
1 nM
10 nM
WT
KO
C
WT
KO
1,25(OH)2D3
- + - +
24-hydroxylase
GAPDH

Figure II-8

MN1 knockout osteoblasts have reduced growth rate *in vitro*.

A, Wild-type (WT) and MN1 knockout (KO) primary osteoblasts were plated at equal densities and treated with ethanol vehicle (-D) or 10 nM 1,25$(OH)_2D_3$ (+D) at day 0. Trypan blue-excluding cells were counted at the indicated time points. Data represent the mean ± SD (n = 3 in each group). B, MN1 WT and KO primary osteoblasts were plated at equal densities and treated with ethanol vehicle (-D) or 10 nM 1,25$(OH)_2D_3$ (+D) for 72 hours. Cells were labeled with BrdU and the BrdU-positive cells were quantitated. Data represent the mean ± SD (n = 3 in each group). C, The percentage of growth inhibition by 4-day treatment of 10 nM 1,25$(OH)_2D_3$ from three independent MTT assays. Data represent the mean ± SD (n = 3 in each group).

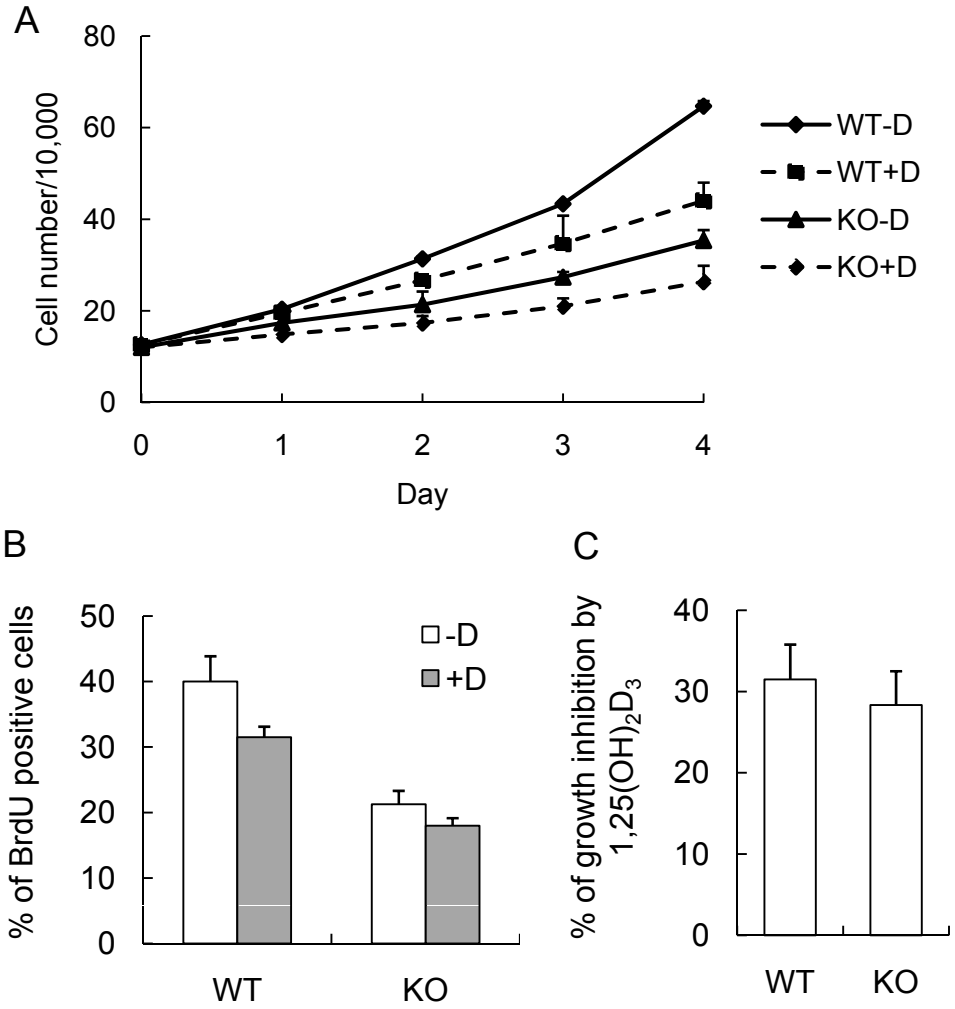
A
Cell number/10,000
80
60
40
20
0
0
1
2
3
4
Day
WT-D
WT+D
KO-D
KO+D
B
% of BrdU positive cells
50
40
30
20
10
0
-D
+D
WT
KO
C
% of growth inhibition by 1,25(OH)2D3
40
30
20
10
0
WT
KO

Figure II-9

MN1 knockout calvarial cells have reduced proliferation *in vivo*.

The BrdU labeled calvaria from wild-type (WT) or MN1 knockout (KO) E18.5 embryos were prepared as described in “Materials and Methods”. Three distinct sections from different areas of each calvarium were stained with BrdU and counterstained with DAPI. A, Representative images of BrdU and DAPI stained sections. B, The ratio of BrdU positive cells was quantitated. Five embryos from each genotype were analyzed. Data represent the mean ± SD (n = 15 individual sections in each group).

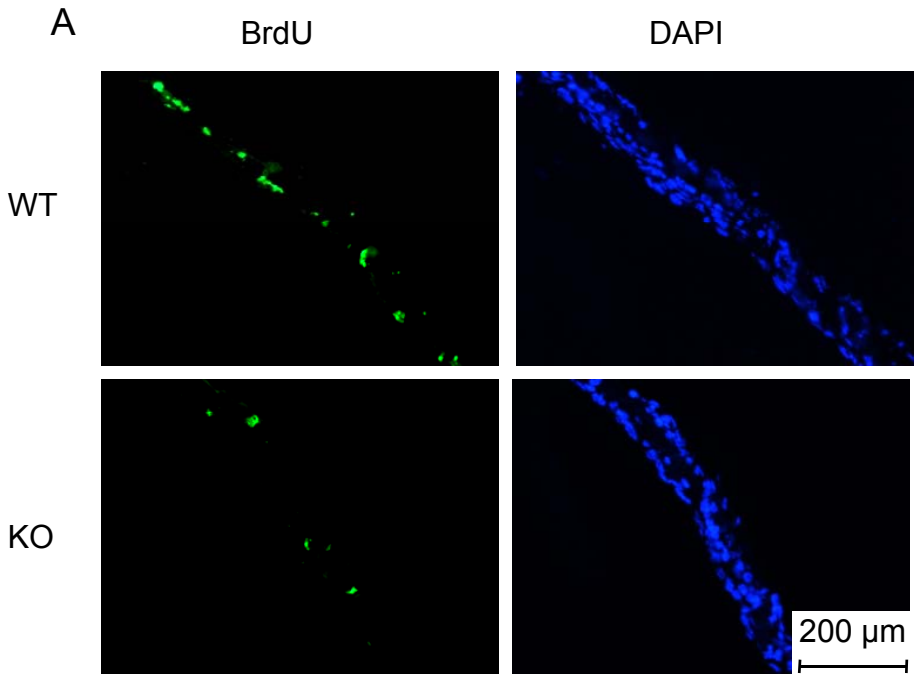
A
BrdU
DAPI
WT
KO
200 μm

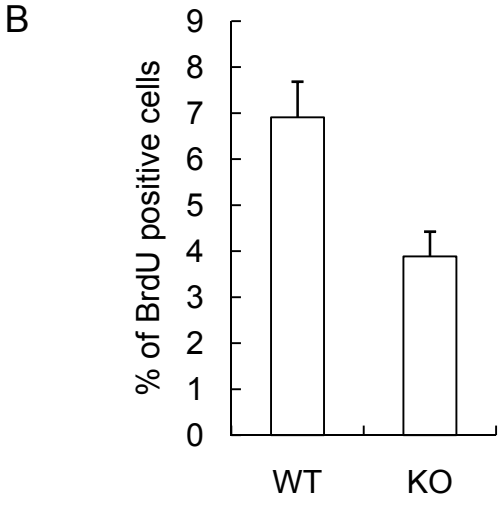
B
% of BrdU positive cells
0
1
2
3
4
5
6
7
8
9
WT
KO

Figure II-10

MN1 knockout osteoblasts have altered morphology and reduced motility.

A, Representative phase contrast images of sub-confluent wild-type (WT) and MN1 knockout (KO) primary osteoblasts. B, MN1 WT or KO cells were grown to confluence and linear scratches were created. Pictures were taken 0 and 16 hours after injury. The black dash lines mark the wound edges. C, The percentage of wound closure was quantitated and presented as the mean ± SD (n = 9 in each group).

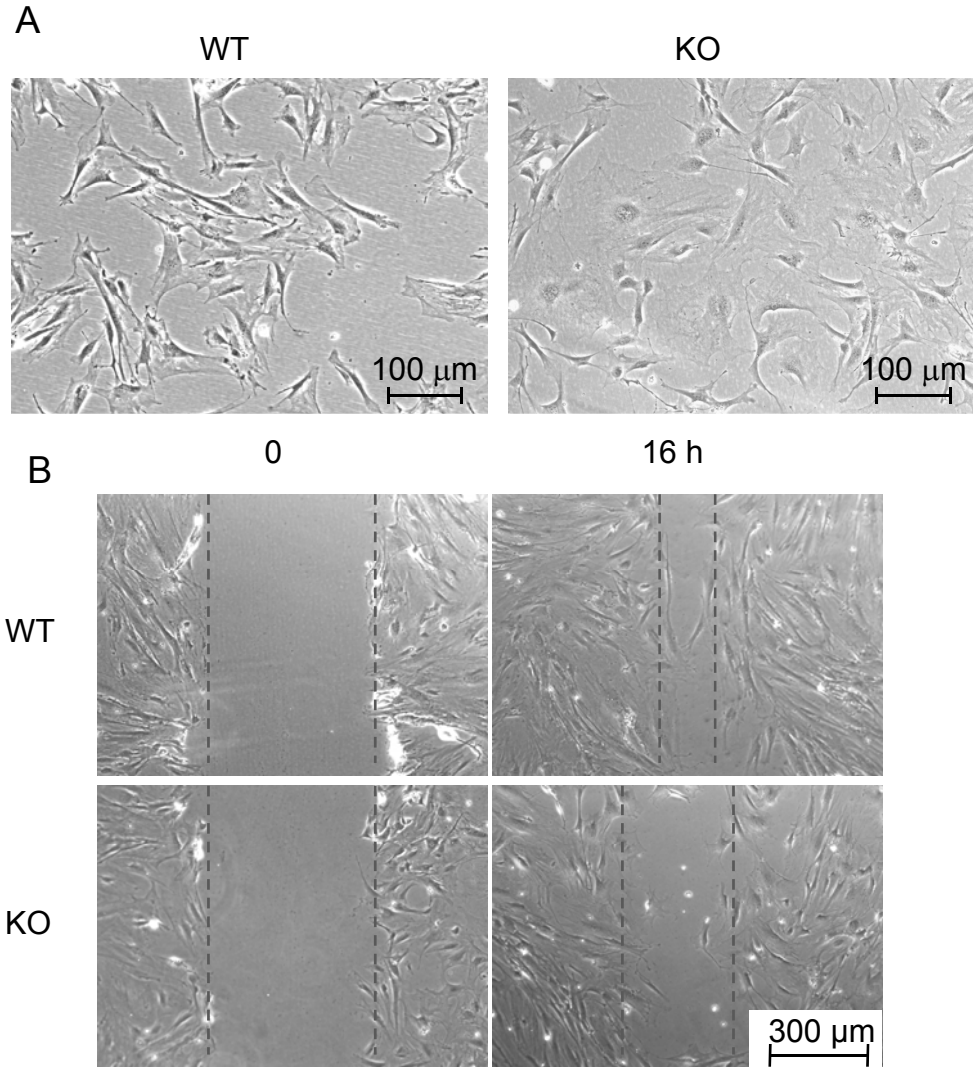
A
WT
KO
100 μm
100 μm
B
0
16 h
WT
KO
300 μm
C
% of closure
80
70
60
50
40
30
20
10
0
WT
KO

Figure II-11

MN1 knockout osteoblasts have reduced alkaline phosphatase activity.

A, Wild-type (WT) and MN1 knockout (KO) osteoblasts were cultured for 28 days in differentiation media and stained for the enzymatic activity of ALP. Shown are the representative images of ALP stained cultures. B and C, MN1 WT or KO osteoblasts were cultured under osteogenic conditions for the indicated times. The ALP activity was measured by a colorimetric assay as described in “Materials and Methods” (panel B), and the expression of ALP and 18S RNA was determined by Northern blot analysis (panel C).

A

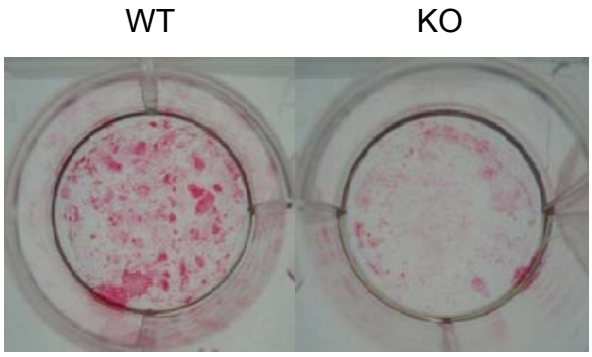
WT
KO

B

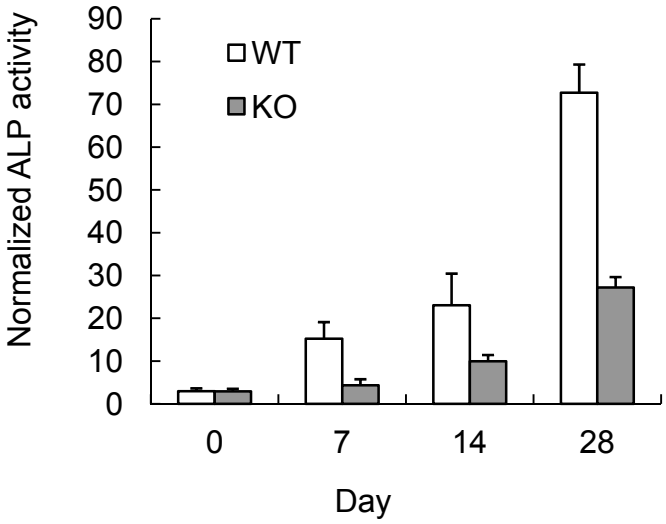
Normalized ALP activity
90
80
70
60
50
40
30
20
10
0
WT
KO
0
7
14
28
Day

C

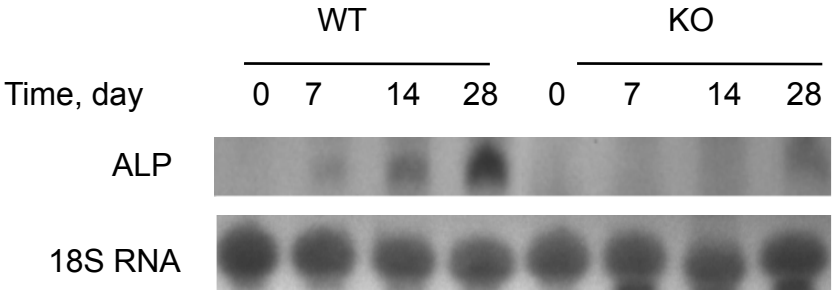
WT
KO
Time, day
0
7
14
28
0
7
14
28
ALP
18S RNA

Figure II-12

MN1 knockout osteoblasts show decreased mineralization.

Wild-type (WT) and MN1 knockout (KO) osteoblasts were cultured for 31 days in differentiation media and stained for mineralized nodules with Alizarin Red S. A, Representative images of Alizarin Red S stained cultures. Darkened areas are mineralized nodules. B, Mineralized nodules were quantitated and compared (unfilled bars). The Alizarin Red S stain was extracted with 100 mM cetylpyridinium chloride and the optical density at 500 nm (OD_{500nm}) was measured (filled bars). Data represent the mean ± SD (n = 3 in each group). C, Total RNA was extracted from wild-type (WT), MN1 heterozygous (HET), and MN1 knockout (KO) E18.5 calvaria. The expression of MN1, BSP2, ALP, osteocalcin, and cyclophilin B was examined by Northern blot analysis.

A

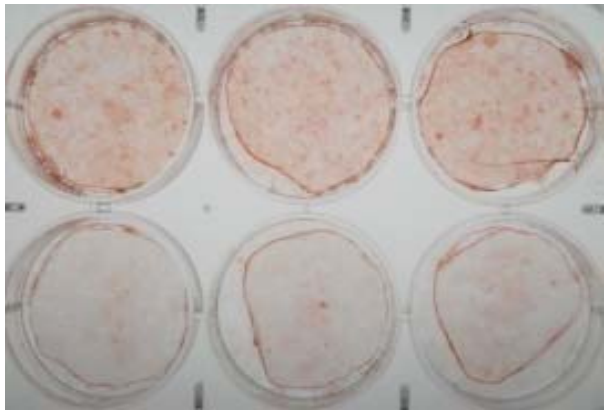
WT
KO

B

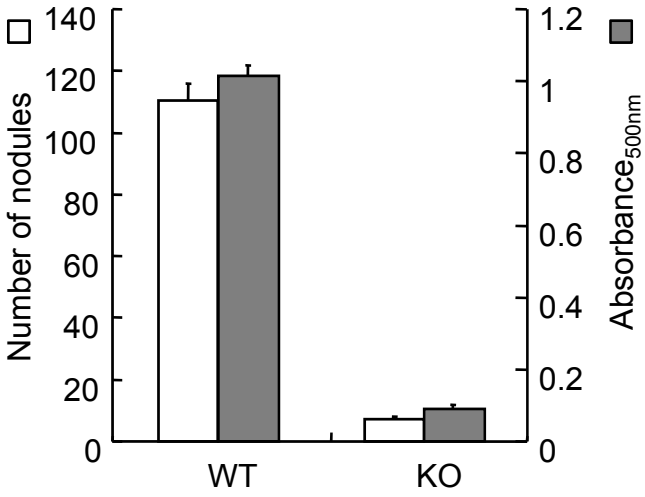
Number of nodules
140
120
100
80
60
40
20
0
1.2
1
0.8
0.6
0.4
0.2
0
Absorbance500nm
WT
KO

C

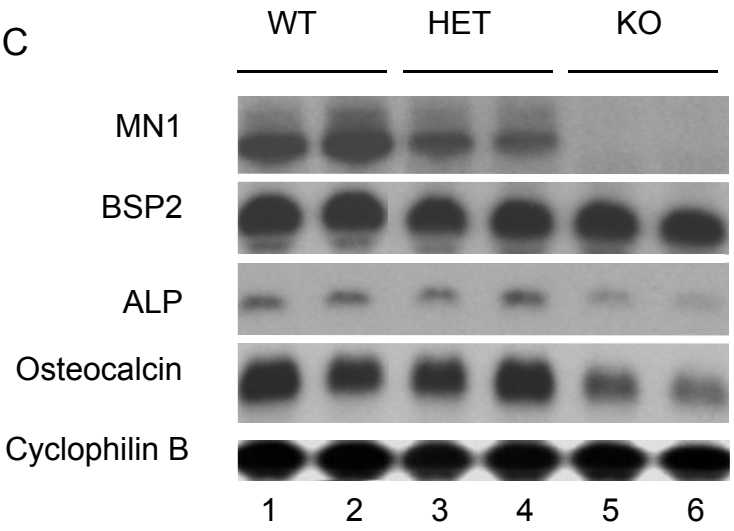
WT
HET
KO
MN1
BSP2
ALP
Osteocalcin
Cyclophilin B
1
2
3
4
5
6

Figure II-13

MN1 knockout osteoblasts show enhanced adipogenesis.

Wild-type (WT) and MN1 knockout (KO) osteoblasts were incubated for 2 weeks in differentiation media. The cultures were stained with Oil Red O for lipid droplets and counterstained with hematoxylin. A, Representative fields of Oil Red O and hematoxylin stained cultures. A high magnification image from an MN1 KO culture is shown in the inset. The bar represents 50 μm. B, The Oil Red O stain was extracted with isopropanol and the optical density at 500 nm (OD_{500nm}) was measured. Data represent the mean ± SD (n = 3 in each group). C, MN1 WT or KO osteoblasts were cultured under osteogenic conditions for the indicated times. The expression of FABP4, LPL, adiponectin, PPARγ, cadherin-11, and 18S RNA was determined by Northern blot analysis.

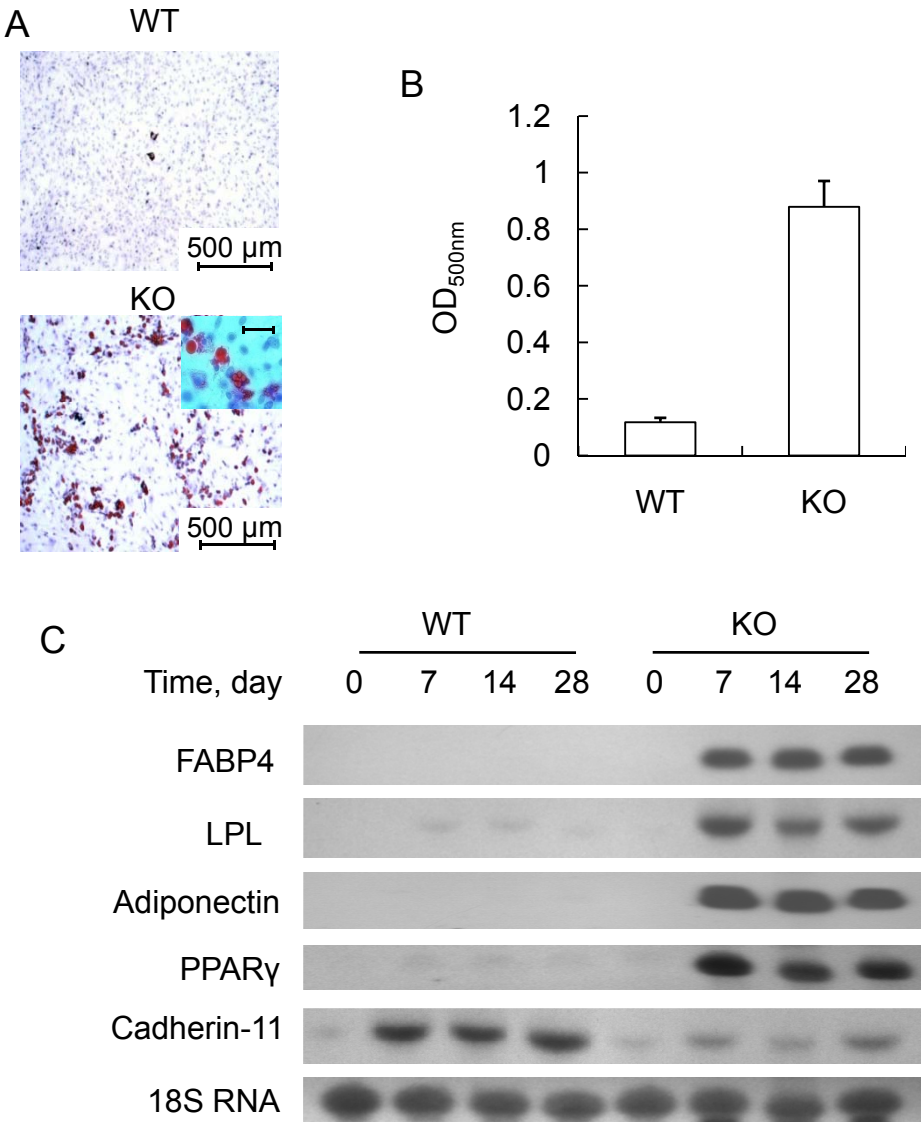
A
WT
500 μm
KO
500 μm
B
1.2
1
0.8
0.6
0.4
0.2
0
OD500nm
WT
KO
C
WT
KO
Time, day
0
7
14
28
0
7
14
28
FABP4
LPL
Adiponectin
PPARγ
Cadherin-11
18S RNA

Figure II-14

MN1 knockout osteoblasts have reduced ability to support 1,25(OH)$_2$D$_3$-stimulated osteoclastogenesis.

A, Osteoclastogenic co-culture analysis was performed as described in “Materials and Methods” using wild-type (WT) and MN1 knockout (KO) osteoblasts. Co-cultures were stained for TRAP. Representative images of TRAP-stained co-cultures are shown. B, TRAP positive multinucleated cells (≥3 nuclei) were counted and compared. Data represent the mean ± SD (n = 3 in each group). The inset shows a high magnification image of TRAP positive, multinucleated osteoclasts. The scale bar represents 60 μm. C, MN1 WT and KO osteoblasts were differentiated for 15 days and treated with ethanol (-) or 10 nM 1,25(OH)$_2$D$_3$ (+) for 24 h. Northern blot analysis was performed to examine mRNA expression levels of OPG, RANKL, M-CSF, or 18S RNA.

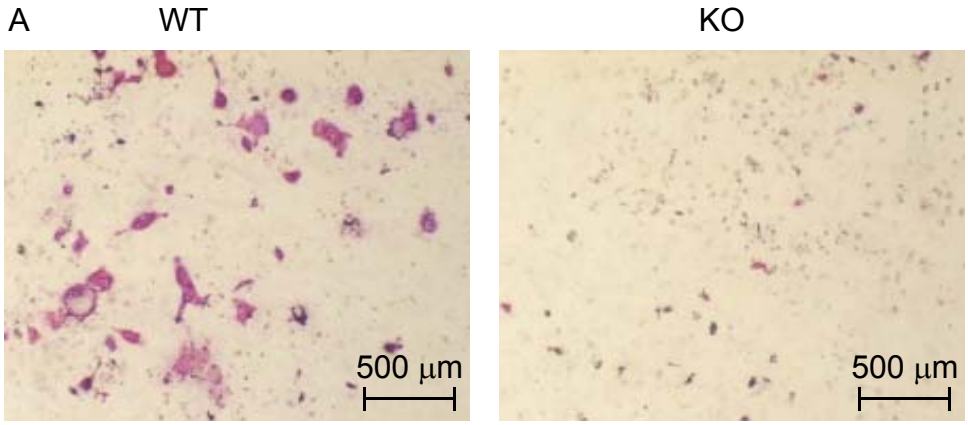
A
WT
KO
500 μm
500 μm

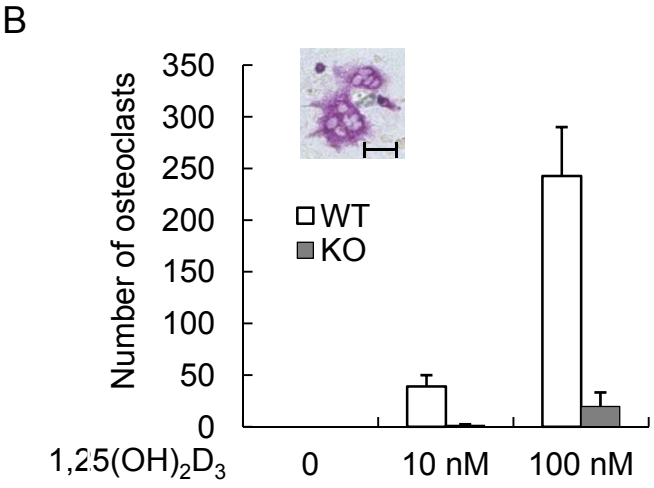
B
Number of osteoclasts
350
300
250
200
150
100
50
0
WT
KO
1,25(OH)2D3
0
10 nM
100 nM

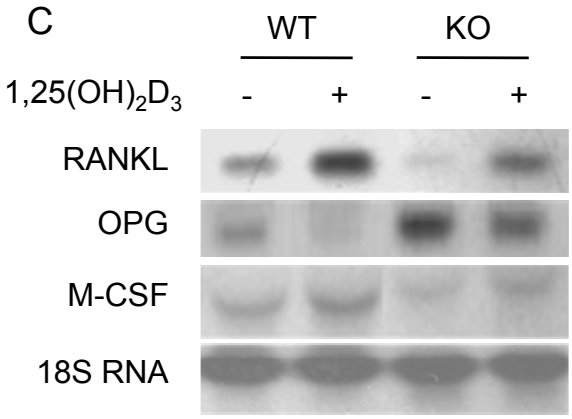
C
WT
KO
1,25(OH)2D3
-
+
-
+
RANKL
OPG
M-CSF
18S RNA

Figure II-15

MN1 stimulates RANKL promoter activity.

A, MC3T3-E1 cells were transiently transfected with a 1 kb human RANKL promoter reporter gene [hRANKL(-1kb)-luc] or pGL3 control reporter gene. The indicated amounts of the pcDNA-MN1 expression plasmid were co-transfected with the total molar amount of expression plasmid DNA kept constant by the addition of pcDNA empty vector. The normalized luciferase activity was measured after 48 hours. Data represent the mean ± SD (n = 3 in each group). B, Control siRNA (-) or MN1 siRNA (+) was transfected into MC3T3-E1 cells 24 h before pGL3 or hRANKL(-1kb)-luc was transfected. The normalized luciferase activity was measured 48 hours later. Data represent the mean ± SD (n = 3 in each group). C, Control siRNA (-) or MN1 siRNA (+) was transfected into MC3T3-E1 cells, and the expression of MN1 mRNA and 18S RNA was examined 24 hours later by Northern blot analysis. D, Wild-type (WT) or MN1 knockout (KO) primary osteoblasts were transfected with pGL3 or hRANKL(-1kb)-luc. The normalized luciferase activity was measured after 48 h. Data represent the mean ± SD (n = 3 in each group).

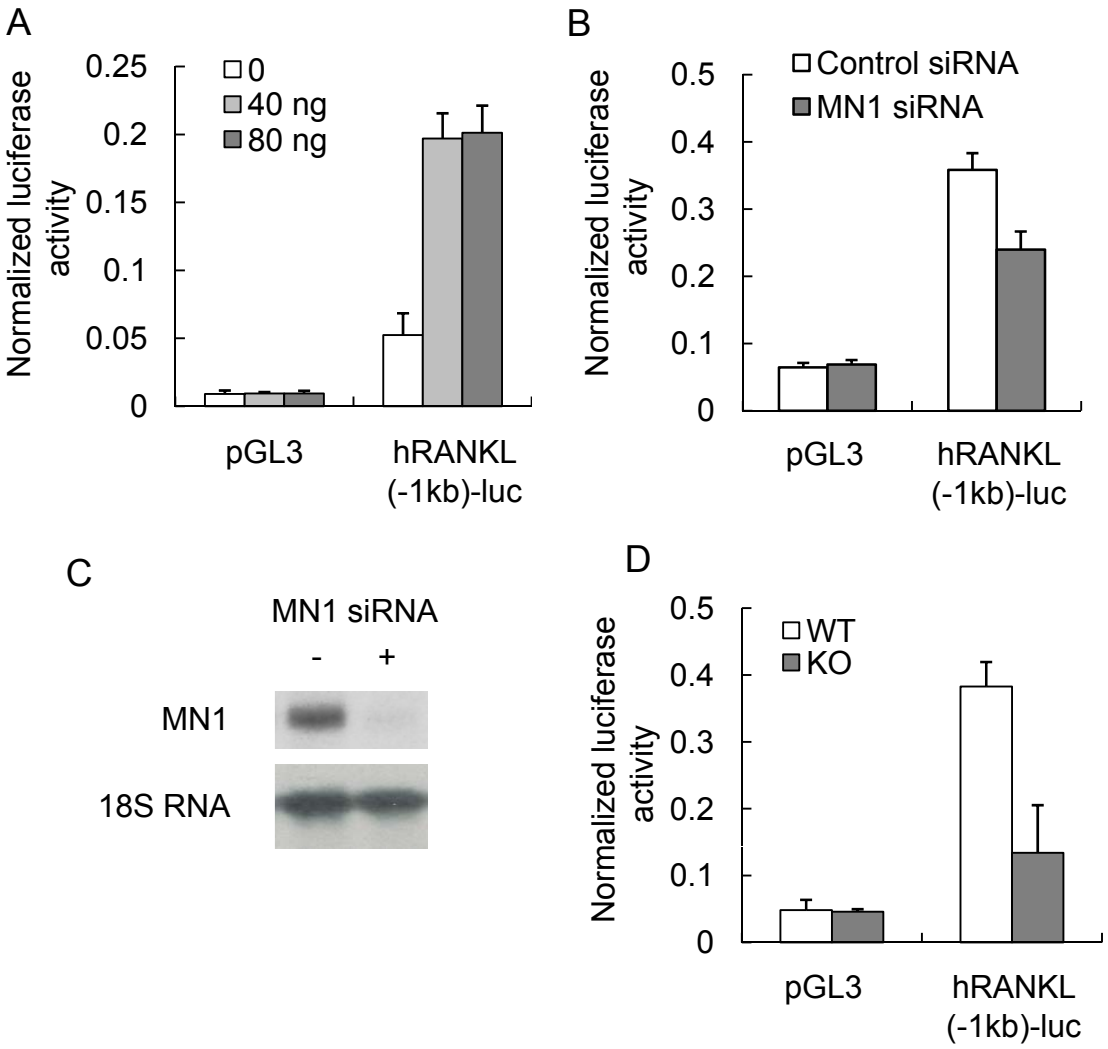
A
Normalized luciferase activity
0.25
0.2
0.15
0.1
0.05
0
0
40 ng
80 ng
pGL3
hRANKL (-1kb)-luc
B
Normalized luciferase activity
0.5
0.4
0.3
0.2
0.1
0
Control siRNA
MN1 siRNA
pGL3
hRANKL (-1kb)-luc
C
MN1 siRNA
-
+
MN1
18S RNA
D
Normalized luciferase activity
0.5
0.4
0.3
0.2
0.1
0
WT
KO
pGL3
hRANKL (-1kb)-luc

CHAPTER III

SEMAPHORIN 3B (SEMA3B) IS A 1,25-DIHYDROXYVITAMIN D_3-INDUCED GENE IN OSTEOBLASTS THAT PROMOTES OSTEOCLASTOGENESIS AND INDUCES OSTEOPENIA IN MICE

Introduction

1,25-dihydroxyvitamin D_3 ($1,25(OH)_2D_3$) is the bioactive metabolite of vitamin D. This hormone functions through the vitamin D receptor (VDR), a member of the nuclear hormone receptor superfamily, to regulate the transcription of target genes in a number of tissues including the intestine, bone, parathyroid gland, skin, and a variety of other systems (80, 282). The $1,25(OH)_2D_3$/VDR endocrine system functions in diverse biological processes, such as hair follicle cycling, mammary gland development, and immune cell function (282). One of the most profound actions of $1,25(OH)_2D_3$ is to protect skeletal integrity because deficiencies in either the hormone or the receptor result in undermineralized bones (232, 283).

Acting in concert with parathyroid hormone, $1,25(OH)_2D_3$ preserves bone mineralization primarily by maintaining calcium and phosphate homeostasis. $1,25(OH)_2D_3$ controls serum levels of these minerals by stimulating calcium and

phosphate absorption by the intestine, by increasing reabsorption of calcium and phosphate in the kidney, and by liberating calcium and phosphate from skeletal stores (232). When dietary sources of calcium are inadequate, $1,25(OH)_2D_3$ promotes osteoclastogenesis and bone resorption, in part, by stimulating osteoblasts to express receptor activator of NF-κB ligand (RANKL) (240), a molecule essential for osteoclast formation and function (170, 178). Under conditions of normocalcemia, the $1,25(OH)_2D_3$/VDR endocrine system also modulates osteoblast differentiation and mineralization (107, 284-286). Thus, $1,25(OH)_2D_3$ functions both systemically to regulate serum concentrations of calcium and phosphate and locally to fine-tune the balance between bone formation and bone resorption. However, with the exception of RANKL and a few bone matrix proteins (240, 287-289), the network of target genes that mediate the effects of $1,25(OH)_2D_3$ on osteoblast function remain largely unknown.

In this study, we characterize the regulation and actions of semaphorin 3B (SEMA3B), a $1,25(OH)_2D_3$-induced gene, in osteoblasts. Semaphorins are a family of cell surface and secreted glycoproteins that originally were identified as axonal guidance proteins, but subsequently have been found to regulate cell migration, cell growth, differentiation, and angiogenesis in a variety of tissues (290). SEMA3 molecules are secreted proteins that signal through neuropilin receptors (213, 214) and plexin co-receptors (215, 216). The SEMA3B gene was first identified based on its position in the chromosomal region 3p21.3, a frequent site of loss-of-heterozygosity (LOH) in lung, kidney, ovarian, and testicular

cancers (217). Re-expression of SEMA3B in either lung or ovarian cancer cells diminishes their proliferative and tumorigenic potential (222, 223), indicating that SEMA3B is also a putative tumor suppressor. SEMA3B transcripts have been detected in osteoblastic cell cultures obtained from human oral tissue explants *in vitro* (230). Moreover, neuropilin-1 expression has been detected in osteoclasts and in osteoblasts *in vitro* and *in vivo* and appears to be down-regulated as osteoblasts differentiate into more mature osteocytes (291). However, biological effects of SEMA3B in the skeletal system or in osteoblast/osteoclast function currently are unknown.

The present study characterizes SEMA3B as a novel $1,25(OH)_2D_3$-activated gene in multiple osteoblastic cell lines as well as in primary mouse osteoblasts. The SEMA3B gene expression also is dramatically increased during osteoblastic cell differentiation, suggesting that SEMA3B may play an important role in osteoblast function. To probe the potential role(s) of osteoblast-derived SEMA3B, transgenic mice were created that express SEMA3B under the control of an osteoblast-selective 2.3 kb promoter of the mouse pro-α1 (I) collagen gene. Mice that express the SEMA3B transgene exhibited decreased body weight, shorter tibias, and displayed a deficit in trabecular and cortical bone mineralization. Although osteoblast number and function appeared normal in SEMA3B transgenic mice *in vivo*, osteoclast number was dramatically increased. *In vitro* studies indicated that transgenic osteoblasts supported increased osteoclastogenesis. Thus, this study identifies osteoblast-derived SEMA3B as a

novel regulator of bone mass that might function by stimulating osteoclastogenesis and osteoclast activity.

Materials and Methods

Cell culture

MG-63 human osteoblastic cells were maintained in growth media consisting of MEM supplemented with 10% FBS, 100 units/ml penicillin, and 100 µg/ml streptomycin. MC3T3-E1 and ST-2 cells were maintained in α-MEM (Invitrogen, Calsbad, CA) supplemented with 10% FBS, 100 units/ml penicillin and 100 µg/ml streptomycin. For differentiation experiments, MC3T3-E1, ST-2, and primary osteoblasts were grown to confluence and then the media were changed to growth media supplemented with 50 µg/ml L-ascorbic acid and 10 mM β-glycerophosphate to promote osteoblastic differentiation. Media were replenished twice per week during the 3-week differentiation period.

RNA extraction and Northern blot analysis

mRNA was isolated from MG-63 cells with the FastTrack system (Invitrogen) according to the manufacturer's instructions. For bone RNA isolation, humeruses were ground to a fine powder using a mortar and pestle over liquid nitrogen. Total RNA was extracted from the powder by homogenization in Trizol Reagent (Invitrogen) according to the manufacturer's instructions. Total RNA

was extracted from osteoblastic cell cultures using RNA-Bee (Teltest, Friendswood, TX). RNA was separated on a formaldehyde/agarose gel and transferred to a Duralon membrane (Stratagene, La Jolla, CA) by capillary action. [α^{32}P]-labeled probes were synthesized using a Prime-A-Gene kit (Promega, Madison, WI) and hybridized to the blots using standard methods. The human SEMA3B probe, consisting of the entire human coding sequence, was obtained from pcDNA3-SEMA3B (provided by J. Minna, University of Texas Southwestern Medical Center). Other mouse gene probes were generated using RT-PCR from murine osteoblasts RNA. Random hexamers (Invitrogen) were used for first strand synthesis and the PCR amplification primers were listed as following: SEMA3B: 5'-GCTCTGCTTTCAAGAATTACA-3' and 5'-GTCTTGCTGGGGCAGAT-3'; RANKL: 5'-AGAACGATCGCGGAGCAG-3' and 5'-TGCTAATGTTCCACGAAATGA-3'; 24-hydroxylase: 5'-CCAGCGGCTAGAGATCAAAC-3' and 5'-CACGGGCTTCATGAGTTTCT-3'. Autoradiograms were quantitated using scanning densitometry and normalized using either β-actin or GAPDH.

Western blot and immunohistochemical detection of SEMA3B

An affinity purified rabbit polyclonal antibody directed against human SEMA3B (residues T732-W749) was generated by Bio-synthesis Incorporated (Lewisville, TX). This peptide sequence is 100% conserved between the human and mouse proteins. This same epitope was used to generate an anti-SEMA3B antibody in a previous study (222). Tibias from 8-week male C57BL/6J mice

were fixed overnight in 10% neutral buffered formalin at room temperature, decalcified in Immunocal formic acid solution (American Mastertech Scientific, Lodi, CA) for 4 days at room temperature, embedded in paraffin, and sectioned. Following blocking in goat serum, sections were incubated with 2.5 μg/ml affinity-purified anti-SEMA3B antibody. The rabbit IgG Vectastain ABC kit and the DAB peroxidase substrate kit (Vector Laboratories, Burlingame, CA) were used for detection of the primary antibody according to the manufacturer's recommendations.

Generation of SEMA3B transgenic mouse

All animal studies were approved by the Institutional Animal Care and Use Committee at Case Western Reserve University. The human SEMA3B (hSEMA3B) transgene was obtained from pcDNA3-SEMA3B. The osteoblast-targeted transgene was constructed by replacing the *lacZ* cassette to hSEMA3B coding sequence in the 2300/*acZ* plasmid (292). The expression was driven by a 2.3-kb osteoblast-specific promoter derived from mouse pro-α1 (I) collagen gene. Transgenic mice were generated by the Case Western Reserve University Transgenic Core Facility. Briefly, the transgene was linearized, purified, and injected into the pronuclei of fertilized C57B6/SJL hybrid oocytes. Oocytes were then transferred into the uteri of pseudopregnant females**.** Transgenic mice of the resulting progeny were identified by PCR amplification of tail genomic DNA using the following transgene-specific primers: 5'-GATTCAGCCGGAGGGAAG-3' (located in the 3' region of the SEMA3B cDNA) and 5'-

GGCATCTGCTCCTGCTTT-3' (located in the MP1 poly-adenylation signal sequence). All transgenic animals and non-transgenic littermates used in these studies were greater than 95% C57BL/6J. All adult mice were sacrificed by asphyxiation with CO_2.

Bone imaging analysis and histomorphometry

Tibias from non-transgenic and transgenic mice were dissected, fixed in formalin overnight, and transferred to 70% ethanol. Volumetric bone mineral density (mg/cm^3) measurements of the tibiae were performed using an XCT Research peripheral quantitative computer tomography (pQCT) densitometer (Stratec Medizintechnik, Pforzheim, Germany) as previously described (293, 294). Trabecular bone volume fraction and microarchitecture were evaluated on the proximal tibia 12 mm distal to the end of growth plate using a μCT 40 (Scanco Medical, Southeastern, PA). One hundred 12 μm slices of each bone were analyzed.

For histomorphometric analysis, mice were injected intraperitoneally with calcein (10 mg/kg) at 5 days before sacrifice and with tetracycline (25 mg/kg) at 1 day before sacrifice at 31 days of age (295). Tibiae were dissected, fixed in formalin overnight under a vacuum, and dehydrated sequentially in 70% ethanol and 95% ethanol to preserve the fluorescent labels. Longitudinal 5 μm sections were cut from methyl methacrylate (MMA) embedded blocks of frontal sections of each tibia. Sections were stained with Goldner's Trichrome stain for the static

measurements, and unstained sections were used to visualize the fluorescent labels and perform the dynamic measurements. Standard bone histomorphometry was performed as described using Bioquant Image Analysis software (R & M Biometrics, Nashville, TN) (296).

Primary osteoblast isolation and differentiation

Individual calvaria were dissected from 1-3 day old newborn mice and the adherent tissue was removed. Primary osteoblasts were liberated from the bone by serial collagenase digestions (250). Cultures were established in α-MEM (Invitrogen, Calsbad, CA) supplemented with 15% fetal bovine serum, and combined based on genotype. For differentiation studies, cells were seeded at a density of 50,000 cells per well of a six-well dish, grown to confluence, then switched to differentiation media containing β-glycerophosphate and L-ascorbic acid as described above. Alkaline phosphatase (ALP) activity was determined by using a colorimetric kit that measures the conversion of p-nitrophenyl phosphate to p-nitrophenol according to the manufacturer's instructions (Sigma Aldrich, St. Louis, MO). ALP activity was normalized to protein concentration of the lysate as measured by the bicinchoninic acid (BCA) assay (Pierce Biotechnology, Rockford, IL). Mineralized nodules were visualized by staining fixed cells with 1% alizarin red S for 10 minutes and destaining in distilled water.

Osteoclast differentiation and TRAP staining

Primary osteoblasts were differentiated for 15 days as described above before overlaying osteoclast precursor cells. Osteoclast precursor cells were derived from the spleens of 7-10 week old female C57BL/6J mice. Spleen cells were plated overnight in phenol red-free α-MEM supplemented with 10% heat-inactivated FBS and 10 ng/ml M-SCF (R & D Systems, Minneapolis, MN). Non-adherent cells were added to the osteoblast cultures at a density of 500,000 cells per cm^2 in phenol red-free α-MEM containing 10% heat-inactivated FBS, 100 nM dexamethasone, and the indicated concentrations of $1,25(OH)_2D_3$. The cocultures were grown for an additional 8 days, and media were replenished twice. Cells were stained for tartrate-resistant phosphatase (TRAP) expression using the leukocyte acid phosphatase kit (Sigma Aldrich) according to the manufacturer's instructions (297). TRAP-positive cells with ≥3 nuclei were counted in triplicate wells.

RAW 264.7 differentiation assay

To prepare conditioned media (CM), COS-7 cells were transfected overnight with pcDNA-SEMA3B (for CM-SEMA3B) or pcDNA empty vector (for CM-control) by standard calcium phosphate precipitation. Transfected cells were washed with PBS, and DMEM supplemented with 10% FBS was added. Conditioned media were collected 24 hours later, filtered and used in the RAW 264.7 assay. The presence of SEMA3B in conditioned media was verified by Western blot analysis. Murine macrophage-like RAW 264.7 cells were cultured in DMEM with 10% FBS. For osteoclastogenesis experiments, RAW 264.7 cells

were seeded in 48-well plates at $2x10^3$ cells/well and supplemented with 50% of CM-SEMA3B or CM-control conditioned media with or without 20 ng/ml RANKL (R & D Systems). After 3 days, cells were stained for TRAP as described above. TRAP-positive multinucleated (≥3 nuclei) cells were counted.

Results

SEMA3B is induced by 1,25(OH)$_2$D$_3$ and by differentiation in osteoblasts

SEMA3B was identified as a 1,25(OH)$_2$D$_3$-induced gene in MG-63 human osteoblastic cells by microarray analysis. In this microarray screen, a 6 hour treatment of MG-63 cells with 10 nM 1,25(OH)$_2$D$_3$ resulted in a 10-fold induction of the SEMA3B transcript (data not shown). Northern blot analysis confirmed that 1,25(OH)$_2$D$_3$ increased SEMA3B mRNA levels in a time- and dose-dependent manner. This increase was evident as early as 3 hours following 1,25(OH)$_2$D$_3$ addition, and maximal induction (25-fold) was observed at 12 hours (Figure III-1A). As little as 1 nM 1,25(OH)$_2$D$_3$ induced SEMA3B, and transcript levels continued to increase up to 10 nM 1,25(OH)$_2$D$_3$ (Figure III-1B). This increase in SEMA3B mRNA was specific for 1,25(OH)$_2$D$_3$ since neither cholecalciferol, an inactive 1,25(OH)$_2$D$_3$ precursor molecule, nor 24,25(OH)$_2$D$_3$, a vitamin D metabolite, altered SEMA3B mRNA levels (Figure III-1A and data not shown). Finally, Western blot analysis showed that the SEMA3B protein also is induced by 10 nM 1,25(OH)$_2$D$_3$ treatment, and the induction is higher at 48 hours than at 24 hours (Figure III-1C). Collectively, these data indicate that

$1,25(OH)_2D_3$ increases SEMA3B mRNA and protein expression in MG-63 osteoblastic cells.

To examine whether $1,25(OH)_2D_3$ regulates the mRNA stability of SEMA3B, MG-63 cells were treated with ethanol or 10 nM $1,25(OH)_2D_3$ for 6 hours, and then mRNA synthesis was blocked by actinomycin D. The SEMA3B transcripts level during the next 6 hours was determined by Northern blot analysis. As shown in Figure III-2A and -2B, 6-hour treatment of $1,25(OH)_2D_3$ induced SEMA3B expression as expected, while SEMA3B mRNA is relatively stable and little degradation was observed within the next 6 hours. Thus, $1,25(OH)_2D_3$ primarily stimulates SEMA3B transcription instead of inhibiting its mRNA stability. Further analysis revealed that active RNA and protein synthesis was required for this response. $1,25(OH)_2D_3$ failed to increase SEMA3B mRNA levels when cells were pre-treated with actinomycin D (Figure III-2C), and $1,25(OH)_2D_3$-mediated induction of SEMA3B was compromised by pre-treatment of cycloheximide, a protein synthesis inhibitor, suggesting that the *de novo* synthesis of a protein factor(s) is required for optimal response (Figure III-2C). Collectively, these data indicate that $1,25(OH)_2D_3$ increases SEMA3B mRNA levels in MG-63 cells through an active transcriptional process that requires expression of one or more additional proteins.

To further establish the relevance of the vitamin D endocrine system in controlling osteoblastic expression of the SEMA3B gene, we expanded our studies to other osteoblastic model systems that undergo a well-defined

differentiation program from immature proliferating cells to mature, mineralized-matrix secreting cells *in vitro*. ST-2 mouse bone marrow stromal cells, MC3T3-E1 mouse fetal calvarial cells, and mouse primary calvarial osteoblasts were examined in the proliferative stage or following differentiation for 2 weeks post confluence in media containing L-ascorbic acid and β-glycerophosphate. The proliferating or differentiating osteoblasts were treated with $1,25(OH)_2D_3$ and SEMA3B expression was measured by Northern blot analysis. Similar to the MG-63 cells, 10 nM $1,25(OH)_2D_3$ treatment induced steady-state SEMA3B mRNA levels in a time-dependent manner in proliferating ST-2 cells, with a maximal induction of approximately 9-fold at 24 hours (Figure III-3A). Treatment with $1,25(OH)_2D_3$ also induced SEMA3B expression in proliferating MC3T3-E1 cells (Figure III-4A) and in primary osteoblasts (Figure III-4B). RANKL and 24-hydroxylase, established $1,25(OH)_2D_3$-responsive genes in osteoblastic cells, were induced as expected.

Of importance, we also observed increases in SEMA3B gene expression as these three model systems differentiated into more mature osteoblasts. Differentiating ST-2 cells expressed dramatically higher levels of SEMA3B compared to the proliferative counterpart (Figure III-3B). In addition, basal SEMA3B expression was 3-fold higher in differentiating MC3T3-E1 cells compared to proliferating MC3T3-E1 cells (Figure III-4A). As shown in Figure III-3B and -4A, $1,25(OH)_2D_3$ stimulated the expression of 24-hydroxlase, but the fold increase in differentiating ST-2 and MC3T3-E1 cells was lower than in proliferating cells. Similar results were obtained with SEMA3B, namely

$1,25(OH)_2D_3$ stimulated its expression in both proliferating and differentiating cells, but the stronger induction was apparent in proliferating MC3T3-E1 and ST-2 cells. $1,25(OH)_2D_3$ showed obvious stimulation on SEMA3B expression in proliferating primary osteoblasts, and SEMA3B transcripts increased dramatically as primary osteoblasts differentiated into more mature osteoblasts (Figure III-4B). In summary, these observations show that SEMA3B is a $1,25(OH)_2D_3$ target gene in numerous osteoblastic cell systems, and that differentiating osteoblasts express higher levels of SEMA3B than do proliferating osteoblasts. These data suggest that SEMA3B is an important factor in $1,25(OH)_2D_3$-related bone physiology and perhaps in osteoblast differentiation and function.

SEMA3B is expressed in osteoblasts in vivo

To determine the *in vivo* expression of the murine SEMA3B gene, total RNA from various organs was isolated from mice, and SEMA3B transcripts were visualized by Northern blot analysis. As indicated in Figure III-5A, endogenous SEMA3B transcripts were detected in kidney, intestine, and bone. All of these are well established $1,25(OH)_2D_3$-target organs. Although previous reports indicate that semaphorins are involved in axonal guidance and neural development, we detected comparatively low levels of SEMA3B expression in whole brain extracts.

Having shown SEMA3B transcripts in skeletal tissue extracts and in various osteoblast cell lines, we employed immunohistochemistry using an

antibody against SEMA3B to determine the cellular distribution of the SEMA3B protein in demineralized sections of mouse tibia. As shown in Figure III-5D, SEMA3B staining was detected in several types of chondrocytes in the growth plate. SEMA3B was selectively expressed in proliferating chondrocytes within the prehypertrophic zone (PC in Figure III-5D). Its expression was not detected in cells within the hypertrophic chondrocyte zone (HC in Figure III-5D). Both osteoblasts and osteocytes expressed SEMA3B throughout the growth plate as well as in cortical bone (Figure III-5D and -5F). Additionally, staining was observed in the bone marrow (M in Figure III-5D and -5F), indicating that SEMA3B also is expressed in cells giving rise to the hematopoietic system. This is not surprising based on the known expression of other semaphorins in B-cells, monocytes, hematopoietic cells, and bone marrow stromal cells.

SEMA3B transgenic mice develop osteopenia

Although SEMA3B is expressed in bone, the biological or cellular effects of SEMA3B on skeleton maintenance or in osteoblasts have previously not been addressed. Therefore, we used a transgenic mouse approach to determine whether osteoblast-derived, secreted SEMA3B alters skeletal homeostasis *in vivo* and whether it impacts bone cell function *in vitro*. Similar approaches have been useful in uncovering the biological activity of other signaling proteins in the skeleton (120, 294, 298). Thus, to understand the role of osteoblast-derived SEMA3B in bone, transgenic mice were created in which human SEMA3B (hSEMA3B) expression was driven by the osteoblast-selective mouse 2.3 kb pro-

α1 (I) collagen promoter. To confirm that the hSEMA3B transgene is selectively expressed in bone of transgenic mice, a tissue distribution Northern blot analysis was performed. As shown in Figure III-6A, strong expression of hSEMA3B transgene was detected only in bone RNA from transgenic mice. A weak signal was present in intestinal RNA in both NTG and TG littermates, suggesting cross hybridization of the human cDNA probe with the abundant murine SEMA3B transcript in the intestine. Using a murine cDNA probe, we confirmed that the endogenous SEMA3B transcript levels were similar in all tested tissues of transgenic mice compared to those of non-transgenic littermate controls (data not shown).

Compared to non-transgenic littermates, transgenic mice were smaller, displaying a 34% reduction in body weight and a 6% reduction in tibia length (Figure III-6B and -6C). Peripheral quantitative computerized tomography (pQCT) analysis revealed that tibias from the transgenic mice displayed dramatic reductions in trabecular, cortical, and total bone mineral density (Figure III-7A). The microarchitecture of the trabecular bone also was dramatically altered as determined by high-resolution μCT (Figure III-7B). Consistent with the pQCT analysis, μCT measurements indicated that transgenic bones had decreased trabecular bone volume, number, thickness and connectivity density, but increased exposed surface and spacing of trabeculae (data now shown). To explore potential cellular mechanisms underlying the trabecular bone defects in the transgenic mice, histomorphometric analysis was performed to examine osteoblastic and osteoclastic parameters (Figure III-8). While there were no

alterations in osteoblast cell number and bone formation rate in SEMA3B transgenic tibias as compared to non-transgenic mice (Figure III-8A and -8B), tibias obtained from transgenic animals displayed a significant increase in the number of osteoclasts per unit bone surface area (Figure III-8C). This increase in osteoclast number was reflected in a more than 2-fold enhancement of bone resorption as measured by the percentage of bone surface undergoing erosion (Figure III-8D). Collectively, the imaging and histomorphometry data clearly indicate that in SEMA3B transgenic mice, there is a reduction in bone mineral density and trabecular architecture that is not the result of impaired osteoblastic activity but rather increased osteoclastogenesis and bone resorption.

SEMA3B transgenic osteoblasts display increased differentiation and mineralization in vitro

To determine the cellular basis for the low bone density in the SEMA3B-expressing transgenic mice, we examined the differentiation and mineralization *in vitro* using osteoblasts derived from nontransgenic and SEMA3B-expressing transgenic mice. SEMA3B-expressing osteoblasts showed appropriate transgene expression in differentiated osteoblast cultures after two weeks in culture with L-ascorbic acid and β-glycerophosphate. Minimal SEMA3B transgene expression was detected in proliferating osteoblast cultures obtained from either nontransgenic or transgenic mice. In contrast, significant SEMA3B expression was observed in differentiating osteoblasts obtained from the transgenic mice, but not from the non-transgenic controls (Figure III-9A). Thus,

appropriate expression of the transgene driven by the 2.3 kb promoter region of the mouse pro-α1 (I) collagen gene was observed in this *in vitro* primary cell culture. Coincident with the enhanced expression of the SEMA3B transgene, differentiating cultures from transgenic mice also expressed higher levels of alkaline phosphatase, a marker of osteoblast differentiation, as compared to osteoblasts derived from non-transgenic littermates (Figure III-9B). This was particularly evident in the late stage mineralizing osteoblast cultures. Enhanced mineralized nodule formation was also observed in SEMA3B transgenic osteoblasts as measured by calcium staining (Figure III-9C). These data collectively indicate that overexpression of SEMA3B does not impair, but rather promotes, osteoblastic differentiation *in vitro.*

Osteoblast-derived SEMA3B promotes osteoclastogenesis in vitro

$1,25(OH)_2D_3$ stimulates osteoblasts to secrete essential factors to promote osteoclastogenesis. Because histomorphometric analysis suggests that osteoclastogenesis was increased in transgenic mice, we also compared the ability of transgenic and nontransgenic osteoblasts to support *in vitro* osteoclast formation from spleen cell precursors (Figure III-10A). Primary osteoblasts derived from transgenic and nontransgenic mice were differentiated for 15 days and then cocultured with wild-type osteoclast precursor cells in the presence of dexamethasone and $1,25(OH)_2D_3$. In the absence of $1,25(OH)_2D_3$, no osteoclastogenesis was observed in the coculture using transgenic or nontransgenic osteoblasts (data not shown). At the presence of 10 nM or 100

nM 1,25$(OH)_2D_3$, significantly higher numbers of multinucleated, tartrate-resistant acid phosphatase (TRAP)-positive cells indicative of osteoclasts formed in the cocultures with transgenic osteoblasts compared to those with nontransgenic osteoblasts (Figure III-10A). These *in vitro* data support the *in vivo* observation that overexpression of SEMA3B in osteoblasts stimulates osteoclastogenesis.

To investigate the potential mechanistic basis for the increased osteoclastogenesis supported by the SEMA3B-expressing osteoblasts, we determined the expression levels of several osteoblast-derived factors that impact osteoclastogenesis, including RANKL, osteoprotegerin, M-CSF, IL-1β, IL-6, and TNFα, in the transgenic and nontransgenic primary osteoblast cultures. However, overt differences in transcript levels for these factors were not apparent in the transgenic and nontransgenic osteoblasts (Figure III-10B and data not shown), suggesting that osteoblast-targeted SEMA3B does not alter the expression of RANKL or other key osteoclastogenic factors in primary osteoblasts. Instead, SEMA3B signaling within osteoclast progenitor cells may enhance the RANK-RANKL pathway and promote osteoclastogenesis. This possibility is supported by studies depicted in Figure III-11B using the RAW 264.7 osteoclast progenitor cell line. This murine macrophage cell line responds to RANKL stimulation *in vitro* by forming TRAP-positive, multinucleated, fully differentiated osteoclasts. In this model, although recombinant SEMA3B alone had no effect on osteoclastogenesis, it dramatically enhanced RANKL-mediated osteoclast differentiation of the RAW 264.7 progenitor cell line. Thus, these data support a positive role for SEMA3B signaling in the RANK-RANKL pathway that

is required for differentiation of osteoclast precursors into mature, multinucleated, bone-resorbing cells.

Discussion

In the present study, we show that SEMA3B is a $1,25(OH)_2D_3$-induced gene in osteoblastic cells and provide evidence, through targeted expression of SEMA3B in mouse osteoblasts, that osteoblast-derived SEMA3B results in reduced bone mineral density. These studies are the first to demonstrate a potential biological role for SEMA3B in skeletal homeostasis. The primary role of the vitamin D endocrine system is to tightly control serum concentrations of mineral ions by driving intestinal absorption of calcium and phosphate. However, when dietary sources of calcium are lacking, $1,25(OH)_2D_3$ stimulates bone resorption by increasing osteoclastogenesis and osteoclast activity (232). The effects of $1,25(OH)_2D_3$ on osteoclasts are thought to be mediated by signaling through osteoblasts. Specifically, $1,25(OH)_2D_3$ stimulates osteoblasts to express RANKL (240), a cytokine that is essential for osteoclastogenesis and osteoclast activity (170, 178). However, beyond increasing RANKL signaling, the precise mechanisms governing osteoblast-osteoclast communication by $1,25(OH)_2D_3$ are not well understood. Here, our studies established SEMA3B signaling as another mediator for $1,25(OH)_2D_3$-stimulated, osteoblast supported osteoclastogenesis.

SEMA3B transcripts are strongly induced (up to 25-fold) by 1,25$(OH)_2D_3$ in a time- and dose-dependent manner in MG-63 osteoblastic cells (Figure III-1). Although the precise regulatory mechanisms remain unclear, our studies indicate that 1,25$(OH)_2D_3$ does not regulate SEMA3B mRNA stability (Figure III-2A and -2B). Instead, this is a transcriptional response to 1,25$(OH)_2D_3$ in osteoblastic cells that requires ongoing RNA and protein synthesis (Figure III-2C). Detailed promoter analysis is required to rigorously address the mechanism of regulation by 1,25$(OH)_2D_3$. In this regard, putative VDREs were identified downstream of the transcriptional start site in the human SEMA3B gene (at positions +1907 - +2029) and chromatin immunoprecipitation studies indicated a 1,25$(OH)_2D_3$-dependent recruitment of native VDR to this region in the SCC25 squamous carcinoma cell line (258). However, the functional relevance of this region of the human SEMA3B gene has not as yet been addressed. In our hands, this region of the SEMA3B gene does not drive VDR/1,25$(OH)_2D_3$-dependent expression of the heterologous TK promoter in a manner similar to established DR-3 VDREs from the rat osteocalcin or 24-hydroxylase genes (data not shown). This, combined with the atypical VDRE sequences identified in this region (258), suggests the potential for alternative mechanisms of regulation. Our actinomycin D and cycloheximide data suggest that the regulation of SEMA3B may be wholly mediated by another 1,25$(OH)_2D_3$-induced transcription factor(s) or that a newly synthesized factor(s) cooperates with VDR to stimulate SEMA3B expression in osteoblastic cells, perhaps through these downstream VDR binding sites. Defining the mechanisms involved in 1,25$(OH)_2D_3$-mediated expression of

SEMA3B transcripts in osteoblasts is an important goal, particularly in light of the impact that osteoblast-driven SEMA3B expression has on overall *in vivo* skeletal homeostasis.

Most reports on semaphorins focus on the role of these signaling proteins in axon guidance and neural development. Only recently has the role of semaphorins in other important physiological and pathological systems been reported (209, 299). Studies addressing the expression or role of semaphorins in skeleton are limited. Previous reports showed that SEMA3B transcripts as well as transcripts for many other semaphorin family members, their neuropilin receptors, and plexin co-receptors are expressed in osteoblast-enriched cell populations obtained from periodontal and gingival isolates *in vitro* (230). SEMA3A and its receptors have distinct expression patterns during endochondral ossification (227, 300). SEMA3A deletion in mice leads to wide-spread skeletal abnormalities, including vertebral fusions, rib duplications, and a thickened sternum (227, 300). This indicates a role for SEMA3A in skeletal development and patterning. SEMA7A is another family member whose expression is regulated by osteoblast differentiation *in vitro* (228, 301). In contrast to SEMA3B, SEMA7A expression is down regulated during the differentiation of primary osteoblasts and MC3T3-E1 cells, implying that each type of semaphorin glycoprotein plays a distinct role in bone development and homeostasis. In support of such functions, a SEMA7A polymorphism was shown to be associated with low bone mineral density and high fracture risk in women (228, 301).

The SEMA3B protein is expressed *in vivo* in osteoblasts, mature osteocytes, and a select population of chondrocytes (Figure III-5). In contrast, SEMA3A has been shown to be present in osteoblasts, osteoclasts, and prehypertrophic and hypertrophic chondrocytes (227, 300). SEMA3B was characteristically absent from the hypertrophic chondrocyte layer of the growth plate (Figure III-5B). Although we cannot exclude osteoclast expression of SEMA3B, strong staining for SEMA3B was not observed in multinucleated cells (osteoclasts) lining the mineralized matrix. Osteoblast and chondrocyte expression of these semaphorins suggest that signaling by secreted semaphorin may be important for skeletal development and homeostasis. The SEMA3B-expressing transgenic mouse provides important support for this possibility.

Osteoblast-directed expression of SEMA3B in mice led to decreased longitudinal bone growth (Figure III-6), and undermineralized cortical and trabecular bone (Figure III-7), the latter two most likely the result of increased osteoclast number (Figure III-8). Consistent with these findings, *in vitro* coculture studies showed that transgenic osteoblasts have higher ability to support $1,25(OH)_2D_3$-stimulated osteoclastogenesis as compared to nontransgenic osteoblasts (Figure III-10A). Taken together, these data suggest that the osteopenia observed in SEMA3B transgenic mice was due not to impaired osteoblast function but rather a result of increased osteoclastogenesis and osteoclast activity. These findings are analogous to the situation in transgenic mice expressing Runx2 (120), a transcription factor essential for osteoblast differentiation (116, 118). Runx2-overexpressing mice display normal mineral

apposition rates, but they have increased osteoclastogenic parameters *in vivo,* leading to low bone mass (120). Furthermore, osteoblasts derived from these Runx2-animals support the osteoclast formation *in vitro* to a greater extent than nontransgenic osteoblasts (120). Although the mechanisms remain unclear, this phenotype in Runx2-transgenic model is correlated with enhanced expression of RANKL.

In contrast to the Runx2 transgenic mouse, expression levels of RANKL and numerous other osteoblast-derived osteoclastogenic factors (including IL-1β, IL-6, osteoprotegerin, and M-CSF) do not differ in the SEMA3B-expressing osteoblasts compared with nontransgenic controls (Figure III-10B). Yet, SEMA3B-expressing osteoblasts showed increased ability to promote osteoclastogenesis in the coculture system (Figure III-10A). These data suggest that the osteoclastogenic effect of SEMA3B may be direct. Indeed, osteoclasts express neuropilin-1, one of the receptors for secreted semaphorins (291). Recent studies have shown that rac1, an effector of semaphorin signaling (302), is required for osteoclast differentiation and bone resorption (303, 304). Thus, SEMA3B may bind neuropilin-1 expressed on the surface of osteoclast precursors and signal through rac1 to directly promote osteoclastogenesis. We tested this potential mechanism in the more defined RAW 246.7 cell system (Figure III-11B). Here, direct stimulation of RAW 246.7 cells with conditioned medium (CM) containing recombinant SEMA3B showed no induction of osteoclast formation, arguing against direct stimulation of osteoclastogenesis via the semaphorin/neuropilin signaling system. However, recombinant SEMA3B

dramatically enhanced RANKL-stimulated osteoclastogenesis of RAW 246.7 cells. Cumulatively, these data support a mechanism involving SEMA3B-activated signaling cascades in osteoclast precursors that impinge upon and positively affect the RANKL pathway to promote osteoclast differentiation.

In osteoblastic cells, the basal level of SEMA3B and its responsiveness to $1,25(OH)_2D_3$ vary among the different lines examined (Figure III-1, -3 and -4). It is possible that each osteoblastic cell line represents a distinct stage of osteoblast cell differentiation. Indeed, we observed a dramatic increase in SEMA3B transcript levels as MC3T3-E1, ST-2, and primary osteoblasts differentiated into more mature osteoblasts, indicating that the process of osteoblast differentiation increases the level of native SEMA3B transcript expression. RANKL-mediated osteoclastogenesis is thought to be a primary action of early-stage osteoblasts. Thus, increased expression of SEMA3B in more differentiated, late-stage osteoblasts may not be entirely consistent with this pathway. However, the $1,25(OH)_2D_3$-activated expression of RANKL and SEMA3B in early-stage osteoblasts is consistent with the putative role of SEMA3B in the $1,25(OH)_2D_3$-stimulated, RANKL-activated osteoclastogenesis. Moreover, high-level expression of SEMA3B in more differentiated osteoblasts points to alternative roles for SEMA3B in other osteoblastic functions, perhaps influencing the late-stage differentiation process itself to generate mineralized matrix-producing cells. Neuropilin-1 receptors for SEMA3B also are expressed on osteoblasts (291), suggesting that SEMA3B might act in an autocrine fashion to induce osteoblast differentiation and function. This may be involved in the

enhanced expression of osteoblast differentiation markers such as alkaline phosphatase in the SEMA3B-expressing transgenic osteoblasts *in vitro*. A more thorough understanding of semaphorin signaling in osteoblasts and osteoclasts is required to decipher the mechanisms through which SEMA3B stimulates osteoclast formation and bone resorption.

In summary, our data show that SEMA3B is a target gene of $1,25(OH)_2D_3$ in osteoblastic cells and that osteoblast-derived SEMA3B impacts bone cell activities *in vitro* and skeletal homeostasis *in vivo*. Moreover, this study indicates that a member of the secreted semaphorin family exerts a biological effect on bone mineral density *in vivo* and uncovers a potential role for SEMA3B in modulating osteoclastogenesis and bone resorption.

Figure III-1

$1,25(OH)_2D_3$ induces SEMA3B expression in MG-63 osteoblastic cells.

A, MG-63 cells were treated for the indicated times with 10 nM $1,25(OH)_2D_3$ or 10 nM cholecalciferol (Chol). B, MG-63 cells were treated with ethanol vehicle control (0) or 0.1-100 nM $1,25(OH)_2D_3$ for 6 hours The mRNA expression of SEMA3B and β-actin was analyzed by Northern blots. C, MG-63 cells were treated with ethanol vehicle control (-) or 10 nM $1,25(OH)_2D_3$ (+) for 24 hours or 48 hours. The protein expression of SEMA3B and β-actin was analyzed by Western Blot analysis. Lane "Con" contains the lysate of COS-7 cells expressing recombinant SEMA3B as a positive control.

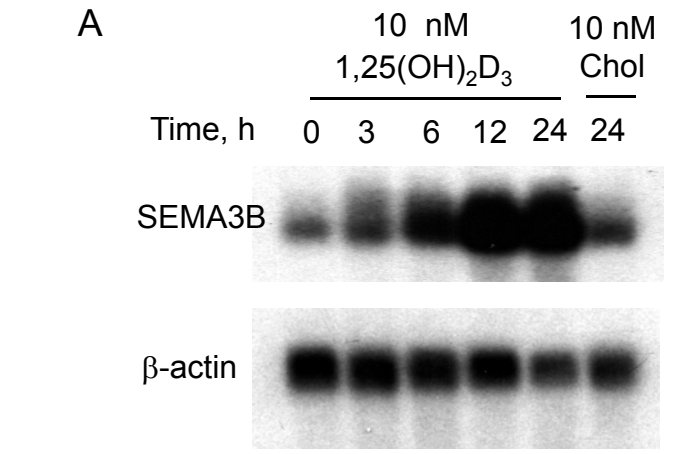
A
10 nM
1,25(OH)2D3
10 nM
Chol
Time, h
0 3 6 12 24 24
SEMA3B
β-actin

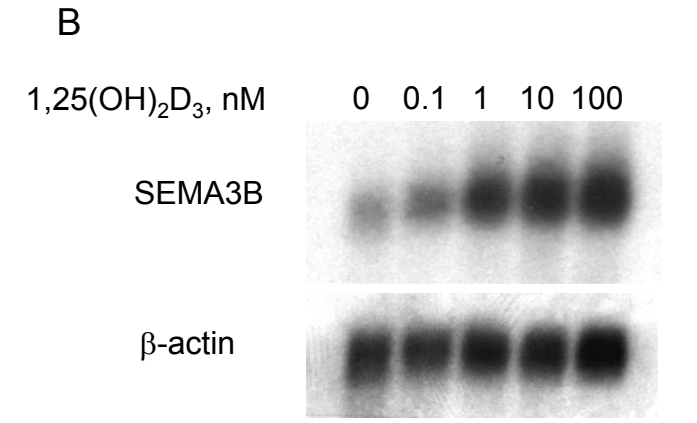
B
1,25(OH)2D3, nM
0 0.1 1 10 100
SEMA3B
β-actin

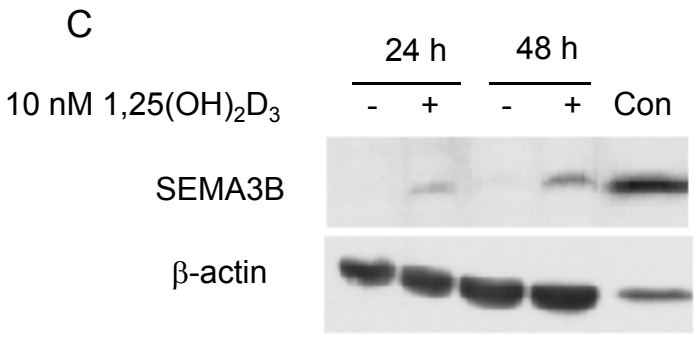
C
24 h
48 h
10 nM 1,25(OH)2D3
- + - + Con
SEMA3B
β-actin

Figure III-2

The mechanism of SEMA3B regulation in MG-63 cells.

A, MG-63 cells were treated with ethanol vehicle control or 10 nM 1,25$(OH)_2D_3$ for 6 hours, and further incubated with 1 μg/ml actinomycin D for the indicated times. The mRNA expression of SEMA3B and GAPDH was analyzed by Northern blot. B, The quantitation of SEMA3B mRNA levels normalized by GAPDH. C, MG-63 cells were pretreated with ethanol vehicle control, 1 μg/ml actinomycin D, or 10 μg/ml cycloheximide for 1 hour. Cells were then treated with ethanol control (-) or 10 nM 1,25$(OH)_2D_3$ (+) for 12 hours. The mRNA expression of MN1 and GAPDH was analyzed by Northern blots.

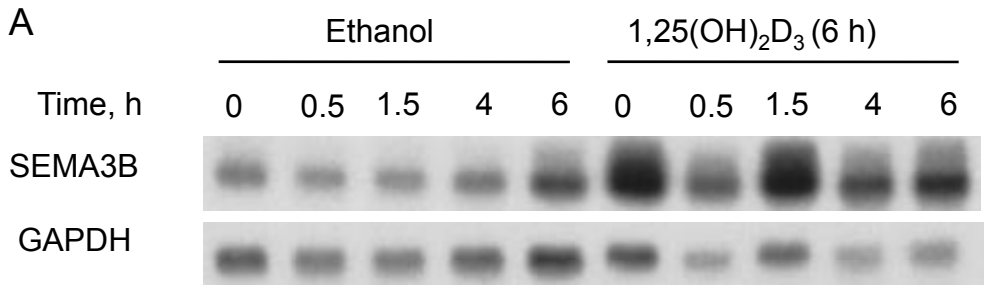
A
Ethanol
1,25(OH)2D3 (6 h)
Time, h
0 0.5 1.5 4 6 0 0.5 1.5 4 6
SEMA3B
GAPDH

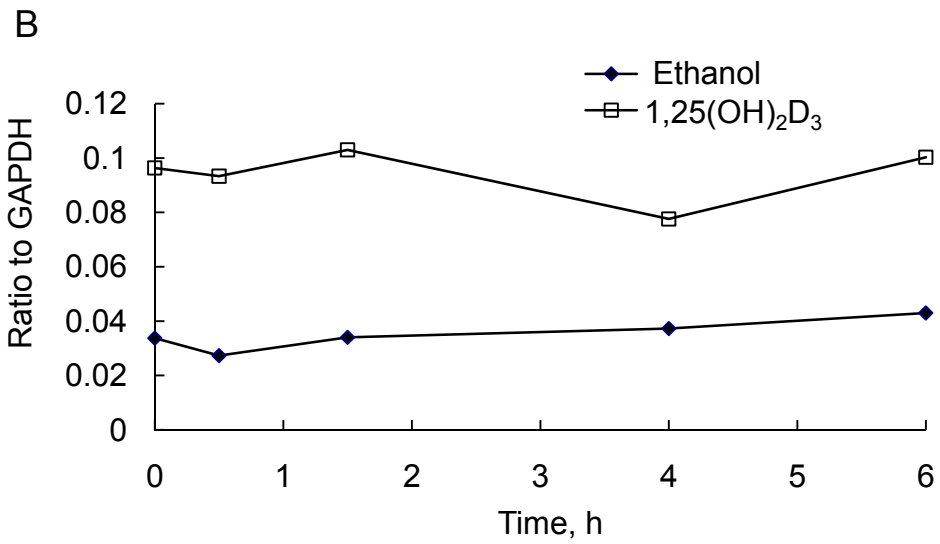
B
Ethanol
1,25(OH)2D3
Ratio to GAPDH
0.12
0.1
0.08
0.06
0.04
0.02
0
0 1 2 3 4 5 6
Time, h

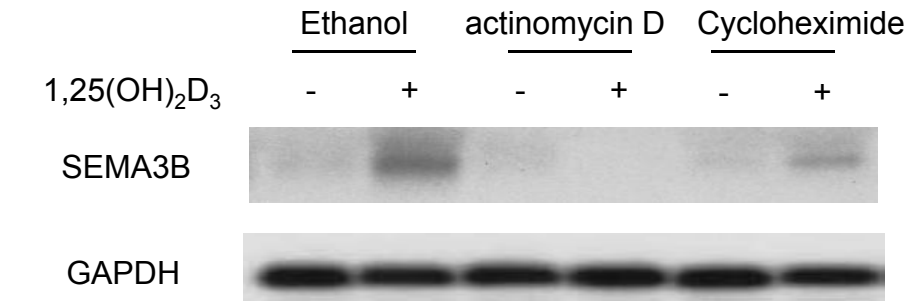
C
Ethanol
actinomycin D
Cycloheximide
1,25(OH)2D3
- + - + - +
SEMA3B
GAPDH

Figure III-3

SEMA3B is induced by 1,25$(OH)_2D_3$ and by osteoblastic differentiation in ST-2 bone marrow stromal cells.

A, Subconfluent ST-2 cells were treated with 10 nM 1,25$(OH)_2D_3$ for the indicated times. B, Subconfluent (Prolifer.) ST-2 cells were prepared in growth media or confluent cells were differentiated for 14 days (Differen.). Proliferating or differentiating cells were treated with ethanol control (-) or 10 nM 1,25$(OH)_2D_3$ (+) for 24 hours. The expression of SEMA3B, 24-hydroxylase, RANKL, and GAPDH was determined by Northern blot analysis.

A

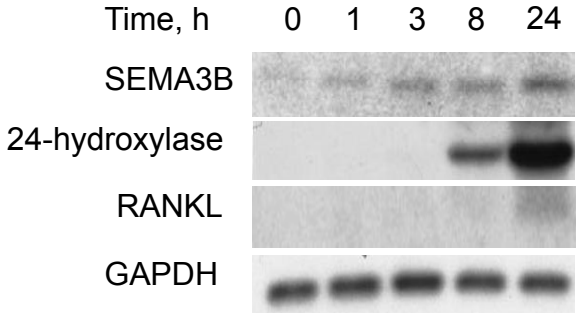
Time, h
0
1
3
8
24
SEMA3B
24-hydroxylase
RANKL
GAPDH

B

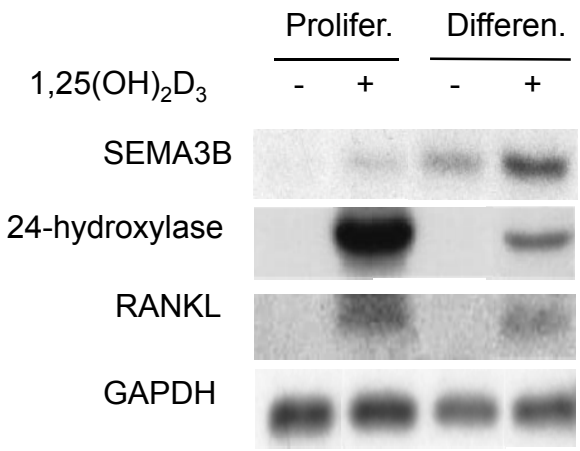
Prolifer.
Differen.
1,25(OH)2D3
-
+
-
+
SEMA3B
24-hydroxylase
RANKL
GAPDH

Figure III-4

SEMA3B is induced by 1,25$(OH)_2D_3$ and by differentiation in MC3T3-E1 cells and primary osteoblasts.

Subconfluent (Prolifer.) MC3T3-E1 cells (panel A) or primary osteoblasts (panel B) were prepared in growth media or confluent cells were differentiated for 14 days (Differen.). Proliferating or differentiating cells were treated with ethanol control (-) or 10 nM 1,25$(OH)_2D_3$ (+) for 24 hours. The expression of SEMA3B, 24-hydroxylase, and GAPDH was determined by Northern blot analysis. In panel B, two exposures of the blot probed with SEMA3B were performed to highlight the induction in differentiating cells (short exposure) and proliferating cells (long exposure).

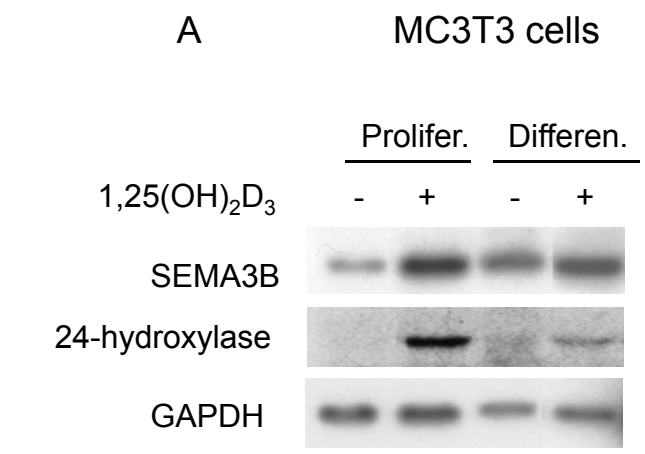
A
MC3T3 cells
Prolifer.
Differen.
1,25(OH)2D3
- + - +
SEMA3B
24-hydroxylase
GAPDH

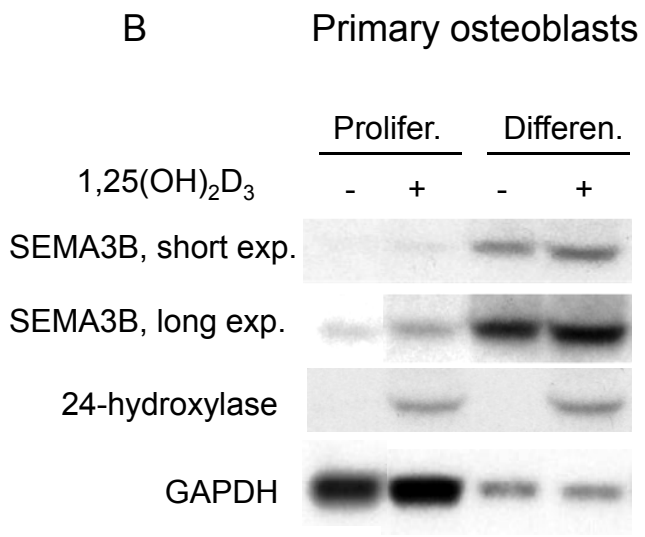
B
Primary osteoblasts
Prolifer.
Differen.
1,25(OH)2D3
- + - +
SEMA3B, short exp.
SEMA3B, long exp.
24-hydroxylase
GAPDH

Figure III-5

SEMA3B is expressed in the long bones of mice.

A, Total RNA was extracted from the indicated tissues of wild-type C57BL/6J mice, and SEMA3B expression was determined by Northern blot analysis. Ethidium bromide staining of 18S/28S ribosomal RNA was used to ensure the equal loading of the RNA. B-F, Tibias from wild-type 8-week-old male mice were formalin-fixed, decalcified in formic acid, embedded in paraffin, and sectioned. Serial sections were stained with hematoxylin and eosin (H & E in panels B and E) or immunostained using rabbit IgG control (IgG in panel C) or an affinity purified rabbit anti-SEMA3B antibody (α-SEMA3B in panels D and F). PC, prehypertrophic chondrocyte layer. C.B., cortical bone. HC, hypertrophic chondrocyte layer. M, marrow space. Arrow, osteocyte.

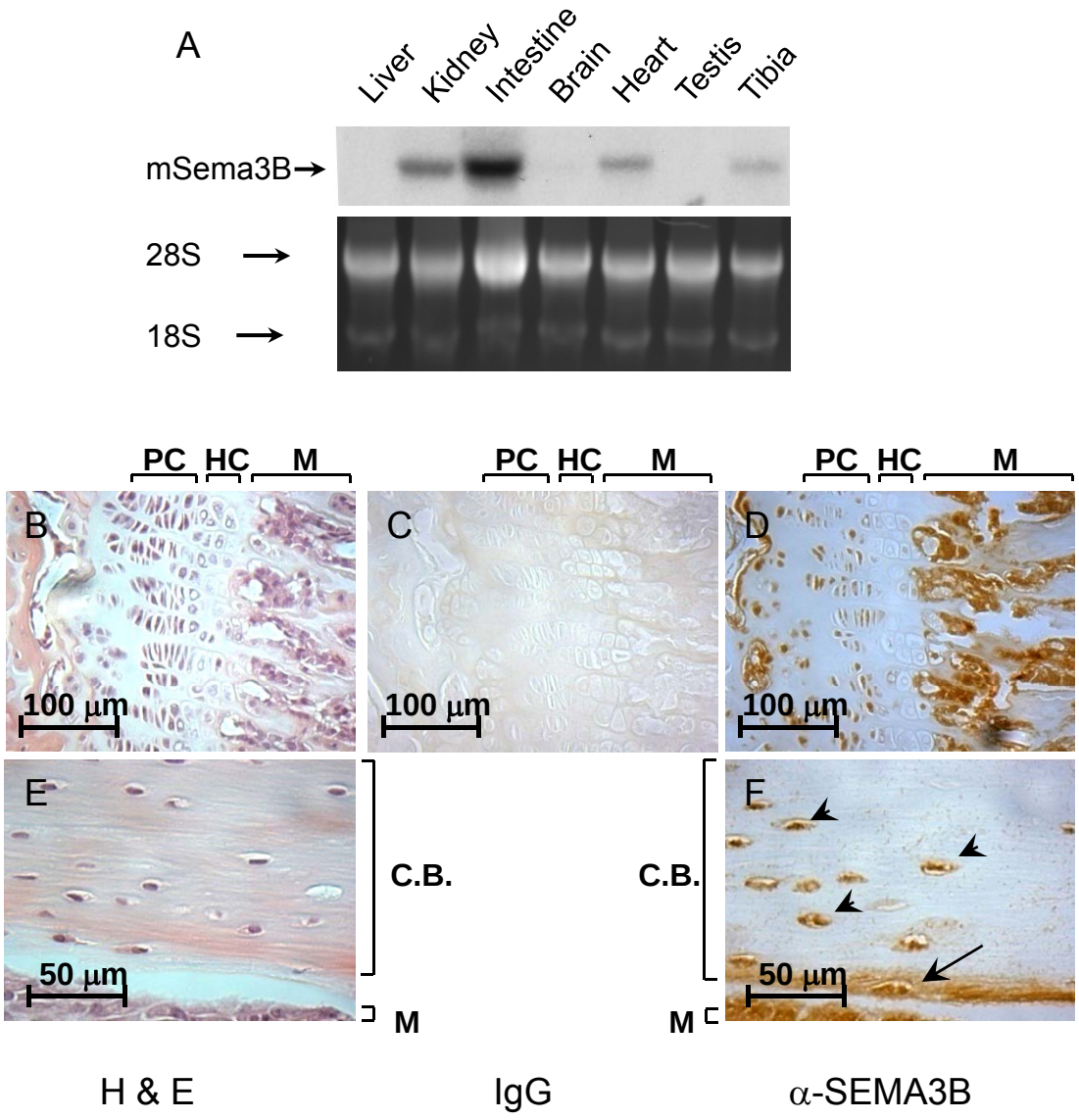
A
Liver
Kidney
Intestine
Brain
Heart
Testis
Tibia
mSema3B
28S
18S
PC
HC
M
B
C
D
100 μm
E
F
C.B.
50 μm
H & E
IgG
α-SEMA3B

Figure III-6

Transgenic mice with targeted osteoblast-selective expression of SEMA3B have reduced body weight and shorter bones.

A, Total RNA was isolated from the indicated organs of non-transgenic (NTG) or SEMA3B transgenic (TG) mice. The transgene expression was analyzed by Northern blot probed with human SEMA3B cDNA. Equal RNA loading was normalized by the band intensity of ethidium bromide-stained 18S/28S ribosomal RNA. B, Growth curve of male NTG and TG mice. Data represent the mean ±SEM ($n \geq 5$). C, pQCT measurement of left tibia length ($n = 8$).

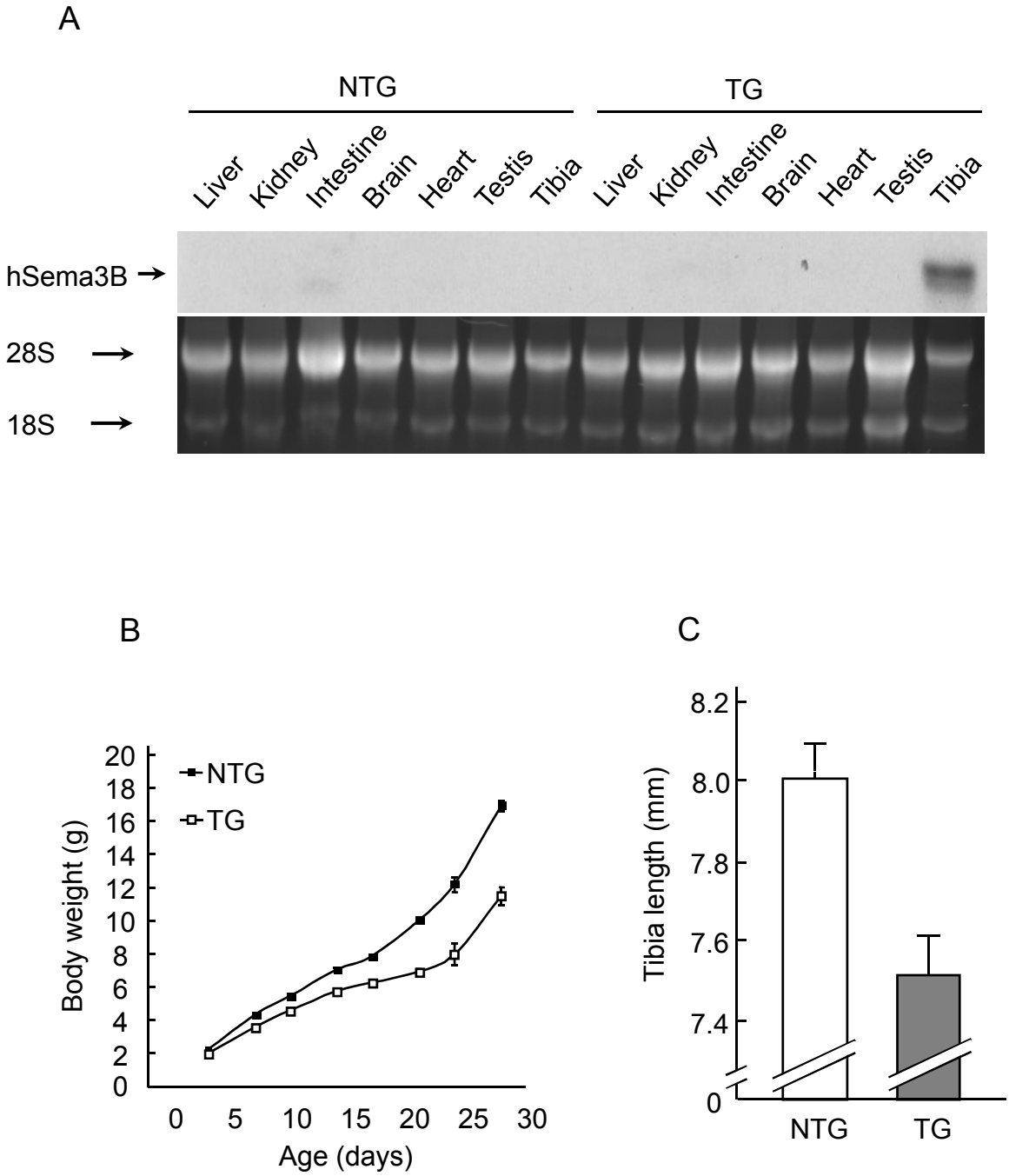
A
NTG
TG
Liver
Kidney
Intestine
Brain
Heart
Testis
Tibia
hSema3B
28S
18S
B
Body weight (g)
NTG
TG
Age (days)
C
Tibia length (mm)
NTG
TG

Figure III-7

SEMA3B-expressing transgenic mice have decreased bone mineral density and diminished trabecular bone.

A, pQCT analysis of total, trabecular, and cortical bone density of tibias from 31-day-old male non-transgenic (NTG) and SEMA3B transgenic (TG) littermates. Data represent the mean ± SEM (n = 7-8). B, μCT cross-sectional images of representative tibias from 31-day-old male NTG and TG littermates.

A

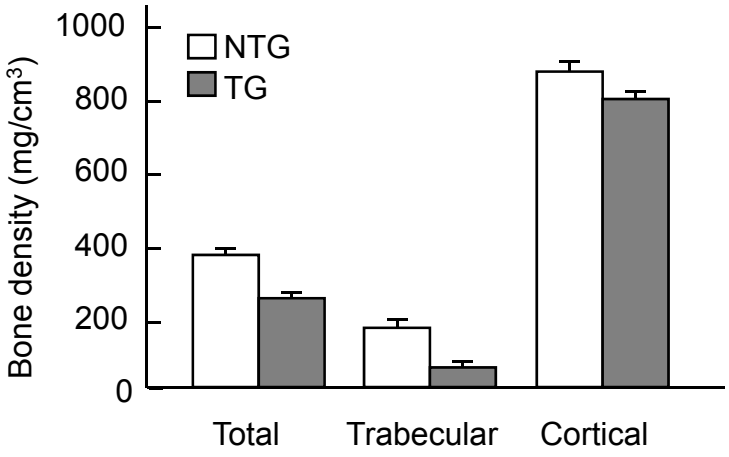
Bone density (mg/cm3)
1000
800
600
400
200
0
NTG
TG
Total
Trabecular
Cortical

B

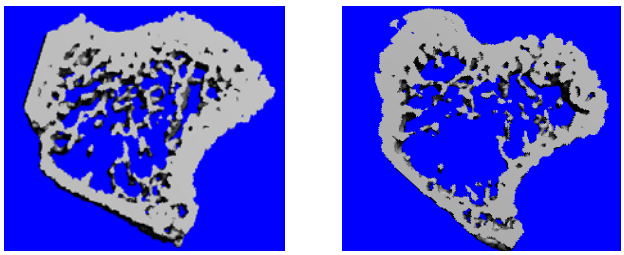
NTG
TG

Figure III-8

Transgenic bones have normal osteoblasts but increased osteoclasts.

Histomorphometry measurements were performed on sections of tibia from non-transgenic (NTG) and SEMA3B transgenic (TG) 31-day-old male mice that had been double-labeled with calcein and tetracycline. A, No. OBs/BS, number of osteoblasts per mm of bone surface. B, MAR, mineral apposition rate. C, No. OCs/BS, number of osteoclasts per mm of bone surface. D, ES/BS, percentage of bone surface involved in resorption. Data represent the mean ± SEM (n = 10).

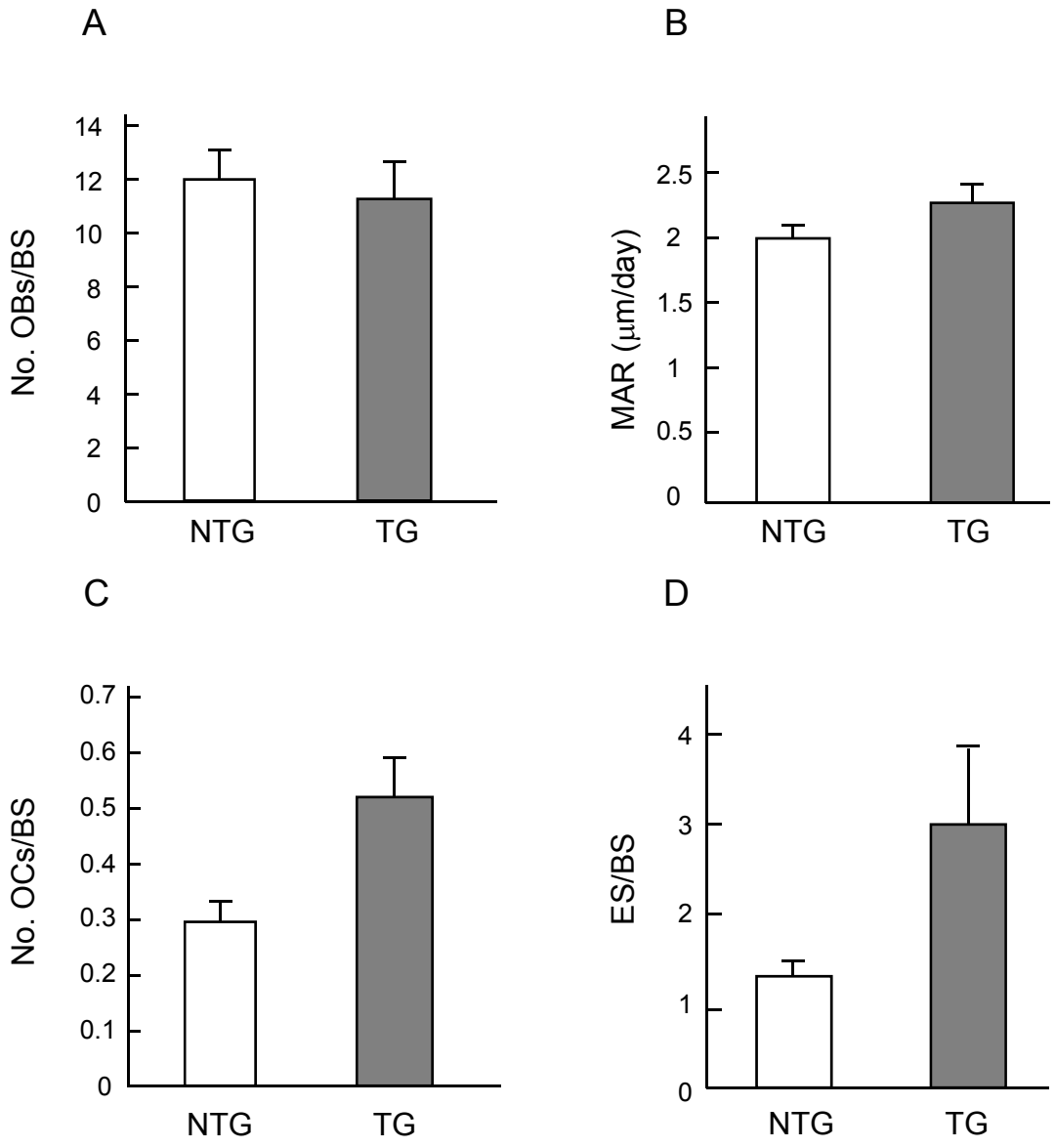
A
No. OBs/BS
14
12
10
8
6
4
2
0
NTG
TG
B
MAR (μm/day)
2.5
2
1.5
1
0.5
0
NTG
TG
C
No. OCs/BS
0.7
0.6
0.5
0.4
0.3
0.2
0.1
0
NTG
TG
D
ES/BS
4
3
2
1
0
NTG
TG

Figure III-9

SEMA3B transgenic osteoblasts exhibit increased differentiation and mineralization *in vitro.*

A, Primary osteoblasts isolated from the calvaria of newborn non-transgenic (NTG) and transgenic (TG) mice were differentiated as described in “Materials and Methods”. Total RNA was isolated at the indicated stages [proliferation (Prolif.), day 6; and differentiation (Differen.), day 15] and analyzed for SEMA3B and β-actin expression by Northern blot. B, Primary osteoblasts from TG and NTG animals were differentiated and alkaline phosphatase (ALP) activity was determined at the indicated stages [Prolif., day 6; Differen., day 15; and mineralization (Mineral.), day 25] by measuring conversion of p-nitrophenyl phosphate to p-nitrophenol. ALP activity was normalized to protein concentration. Data represent the mean ± SEM (n = 3). C, Primary osteoblasts from TG and NTG animals were differentiated for 31 days. The cells were stained with Alizarin Red S and the mineralized nodules were counted. Data represent the mean ± SEM (n = 3).

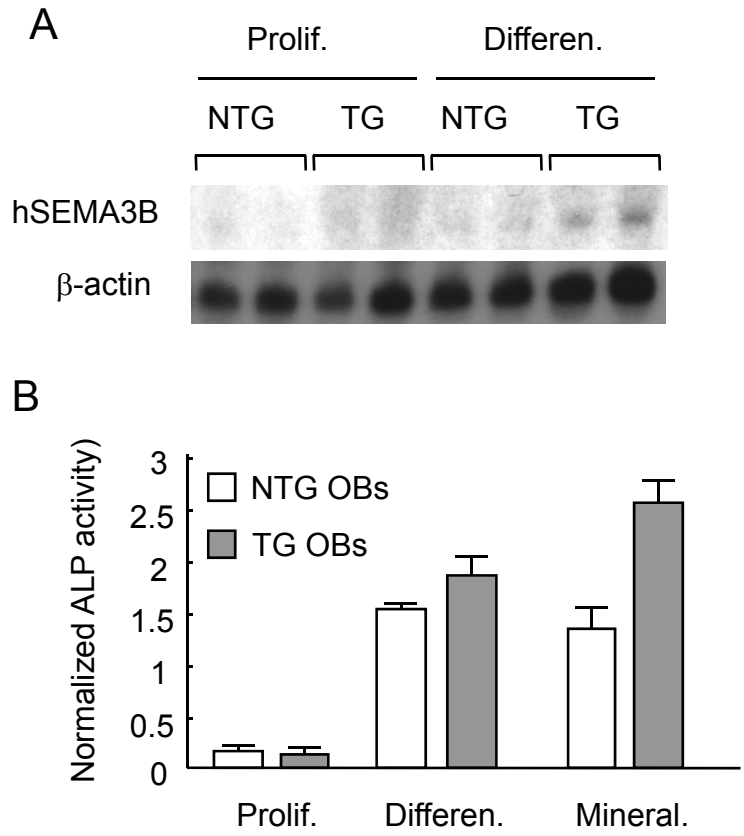
A
Prolif.
Differen.
NTG
TG
NTG
TG
hSEMA3B
β-actin
B
Normalized ALP activity)
3
2.5
2
1.5
1
0.5
0
NTG OBs
TG OBs
Prolif.
Differen.
Mineral.
C
Number of nodules
5
4
3
2
1
0
NTG
TG

Figure III-10

SEMA3B transgenic osteoblasts have increased ability to support $1,25(OH)_2D_3$-stimulated osteoclastogenesis.

A, Osteoclastogenic co-culture analysis was performed as described in “Materials and Methods” using SEMA3B transgenic (TG) and non-transgenic (NTG) osteoblasts. Multinucleated osteoclasts were visualized by staining for TRAP activity as described in “Materials and Methods”. The numbers of TRAP-positive multinucleated (≥ 3 nuclei) cells were counted. Data represent the mean ± SD (n = 3). B, Differentiating primary osteoblasts derived from non-transgenic (NTG) or transgenic (TG) mice were treated with 100 nM $1,25(OH)_2D_3$ for the indicated times, and the expression levels of RANKL, 24-hydroxylase, and GAPDH was determined by Northern blot analysis.

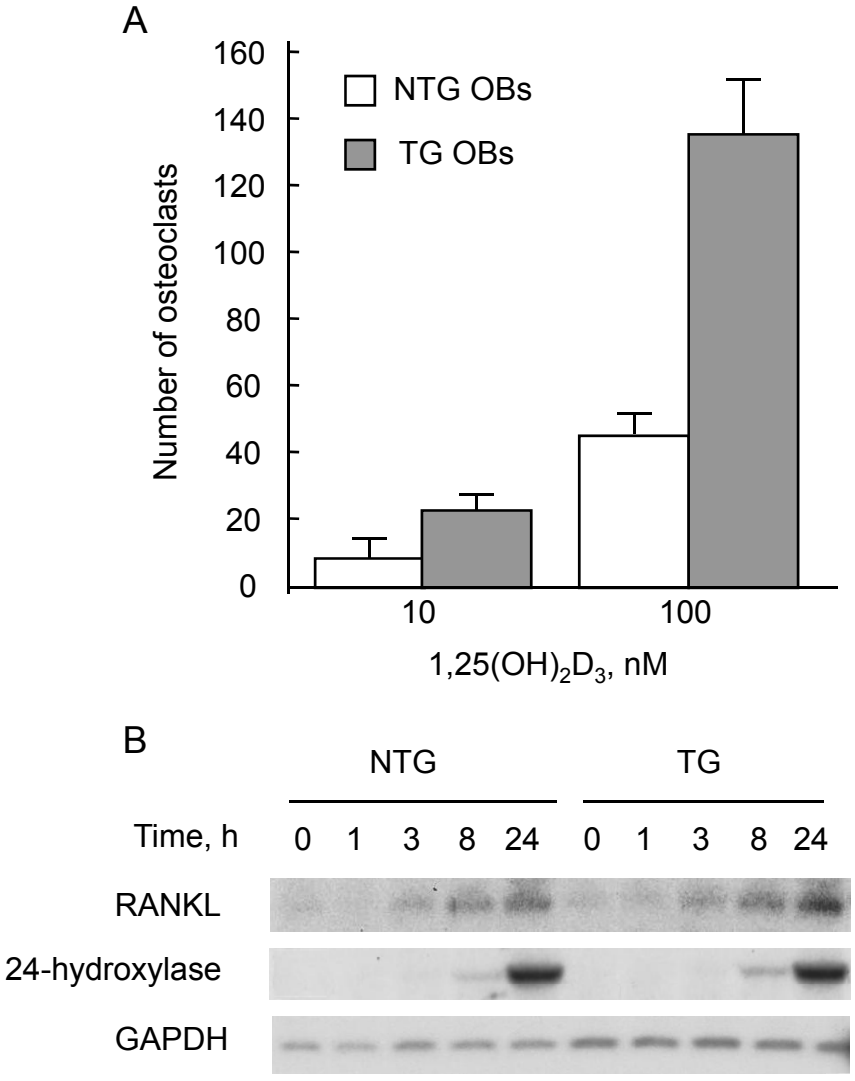
A
160
140
120
100
80
60
40
20
0
Number of osteoclasts
NTG OBs
TG OBs
10
100
1,25(OH)2D3, nM
B
NTG
TG
Time, h
0 1 3 8 24 0 1 3 8 24
RANKL
24-hydroxylase
GAPDH

Figure III-11

SEMA3B promotes osteoclast differentiation in RAW 264.7 cells.

A, SEMA3B-containing conditioned media (CM-SEMA3B) and control media (CM-control) were prepared by transfecting COS-7 cells with pcDNA-SEMA3B (for CM-SEMA3B) or pcDNA empty vector (for CM-control) as described in “Materials and Methods”. The expression of SEMA3B in conditioned media and COS-7 cells was examined by Western blot analysis. B, RAW 264.7 cells were cultured in 50% of indicated conditioned media in the absence or presence of 20 ng/ml RANKL for 72 hours and stained for TRAP. The numbers of TRAP positive multinucleated (≥ 3 nuclei) cells in each well were counted. Data represent the mean ± SD (n = 3).

A

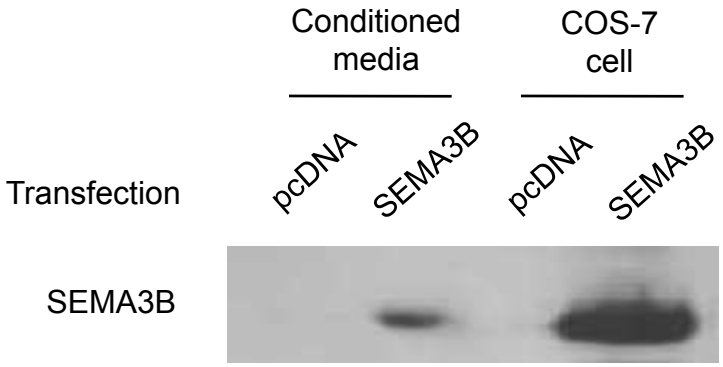
Conditioned media
COS-7 cell
Transfection
pcDNA
SEMA3B
pcDNA
SEMA3B
SEMA3B

B

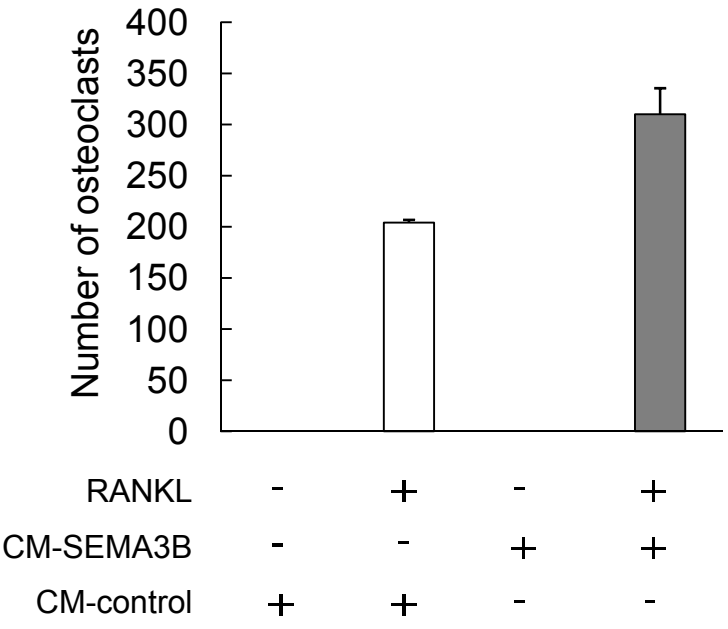
Number of osteoclasts
400
350
300
250
200
150
100
50
0
RANKL - + - +
CM-SEMA3B - - + +
CM-control + + - -

CHAPTER IV

SUMMARY AND FUTURE DIRECTIONS

This project investigated the regulation and functions of MN1 and SEMA3B, which are two novel 1,25$(OH)_2D_3$ target genes in osteoblasts. We characterized that both MN1 and SEMA3B are induced by 1,25$(OH)_2D_3$ in multiple osteoblastic models. Moreover, differentiation of osteogenic cells enhanced their expression, pointing to the active roles of these two genes in osteogenesis and the significance of 1,25$(OH)_2D_3$ in generating appropriate gene profiles for osteoblast activities. Before our study, there were evidences suggesting that MN1 and SEMA3B are involved in skeletal homeostasis, but their roles in bone cells were largely unknown. Using *in vitro* analysis and animal models, our studies revealed the unrecognized significance of MN1 and SEMA3B in bone remodeling.

MN1 is a coactivator for 1,25$(OH)_2D_3$/VDR-mediated gene transcription and shows selectivity for VDR. MN1 not only possesses autonomous transactivity, but also cooperates with SRC coactivators to potentiate 1,25$(OH)_2D_3$-stimulated transcription. MN1 knockout osteoblasts exhibit reduced 1,25$(OH)_2D_3$ activation for VDRE-driven reporter gene as well as for endogenous 24-hydroxylase expression, confirming that MN1 is required for optimal

$1,25(OH)_2D_3$ response. Functional assays revealed that ablation of MN1 results in a variety of defects in osteoblasts. Primary calvarial osteoblasts derived from MN1 knockout mice display altered morphology, attenuated motility, reduced growth rate, decreased differentiation marker (ALP) expression, and impaired calcium deposition. Importantly, the proliferation and mineralization defects were also observed in MN1 knockout calvaria tissue, indicating that MN1 is required for maintaining normal functions of osteoblasts both *in vitro* and *in vivo*. Strikingly, MN1 knockout calvarial osteoblasts cultures have high levels of oil red O-stained lipid droplets and high expression of adipocyte marker genes, including PPARγ, FABP4, LPL, and adiponectin, indicating an important role for MN1 in maintaining the appropriate balance between osteogenesis and adipogenesis from their mesenchymal precursor cells. In addition, MN1 null osteoblasts have decreased ability to support $1,25(OH)_2D_3$-stimulated osteoclastogenesis in spleenocyte coculture studies. Mechanistic studies reveal that MN1 activates RANKL promoter and stimulates RANKL transcription, and MN1 knockout osteoblasts show marked reduction of RANKL:OPG ratio. Taken together, our studies uncovered the essential roles of MN1 in gene transcription, osteoblast function, and osteoblast-supported osteoclastogenesis. These discoveries suggest the functional significance of MN1 in bone remodeling and provide the cellular mechanism that may partially account for the cranial skeleton defects in MN1 knockout mouse.

SEMA3B is a secreted protein that can potentially function in a paracrine or endocrine manner. Using a transgenic mouse model with targeted SEMA3B

overexpression in osteoblasts, we analyzed the impact of osteoblast-derived SEMA3B on global skeletal homeostasis in intact animals. Furthermore, we investigated the cellular mechanism by analyzing the properties of SEMA3B-overexpressing calvarial osteoblasts derived from transgenic animals. In cell culture, we observed that SEMA3B transgenic osteoblasts display enhanced ALP activity and calcium deposition, indicating the stimulatory roles of SEMA3B in osteoblast differentiation and mineralization. Moreover, SEMA3B transgenic osteoblasts exhibit enhanced capability to stimulate osteoclastogenesis in an osteoblast-spleenocyte coculture system, while mechanistic studies did not reveal expression changes in RANKL:OPG ratio. Using an osteoblast-independent RAW 264.7 macrophage model, we showed that recombinant SEMA3B is able to promote the RANKL-stimulated osteoclastogenesis, indicating the existence of paracrine pathway through which osteoblast-secreted SEMA3B activates the signaling cascades within osteoclast precursors. Although SEMA3B promotes both osteoblast and osteoclast differentiation *in vitro*, osteoblast-derived SEMA3B primarily enhances osteoclast formation *in vivo*. SEMA3B transgenic mice develop osteopenia, with decreased body weight, reduced bone mineral density, and aberrant trabecular structure compared to their nontransgenic littermate controls. Histomorphometry studies revealed that SEMA3B transgenic mice have normal osteoblast numbers and bone formation rate, but increased osteoclast numbers and bone erosion. Therefore, this study established that osteoblast-derived SEMA3B is a novel regulator of bone mass

that may function in a paracrine manner to stimulate osteoclastogenesis and bone resorption.

Collectively, our studies support the novel roles for MN1 and SEMA3B as $1,25(OH)_2D_3$-induced proteins that regulate bone cell activities and skeletal homeostasis. These data established the significance of MN1 and SEMA3B in promoting osteoblast differentiation and osteoclastogenesis. These activities are consistent with the recognized roles of $1,25(OH)_2D_3$ in bone remodeling, indicating that MN1 and SEMA3B are important mediators of the activity of $1,25(OH)_2D_3$ biologies in osteoblasts. Thus, these discoveries provide further insights about the molecular mechanisms underlying the direct actions of $1,25(OH)_2D_3$ in skeletal system. Further studies are proposed to investigate other *in vivo* activities of MN1 and SEMA3B, and focus more on elucidating the mechanisms of their functions.

MN1

Identify MN1-interacting proteins and DNA element(s)

Our data show that MN1 promotes VDR-mediated transcription and functions in concert with SRC proteins (Figure II-4, -5, and -6). However, the transcription factors that potentially mediate the transactivity of MN1 have not been characterized. To explore the underlying mechanism, it is important to identify the MN1-interacting proteins. We have used co-immunoprecipitation,

GST-pull down, and yeast-two-hybrid assays to examine whether MN1 interacts with VDR, SRC-1, or SRC-2, but no such interaction was identified (data not shown). It is possible that the binding of MN1 with these transcription factors is indirect, and cannot be detected under our experimental conditions. Therefore, MN1-interacting proteins should be identified through an unbiased screening. For example, a pull-down assay with GST-MN1 or a co-immunoprecipitation assay with FLAG-tagged MN1 can be used to isolate MN1-interacting proteins, which can be recognized by mass spectrometry. These experiments will require a large-scale preparation in the cell lines where MN1 has high transactivity, such as COS-7 cells.

MN1 is a large protein (136 kDa). It is expected that many interacting proteins will be identified via the screening assay using full-length MN1. One advantage of this approach is that potentially it will reveal the novel functions of MN1 in other cellular pathways. However, to focus on its transcription stimulatory activity, the functional domain(s) can be identified through structural-functional analysis and used in the screening assays. Our data suggest that MN1 235-750 (by amino acid number) has high transactivity when it is fused with GAL4-DBD (data not shown). Thus, this region may have chromatin remodeling activity or interact with chromatin remodeling factors, but MN1 235-750 alone is not able to stimulate VDR-mediated transcription. Indeed, removal of MN1 1-235 completely destroys the activation of VDR (data not shown), implying that MN1 1-235 may be critical for recruiting MN1 to the transcription complex. Therefore,

using MN1 1-235 in the screening analysis will possibly identify the proteins that are important for the recruitment of MN1 to transcriptional machinery.

Furthermore, as a transcriptional coactivator, MN1 may function through certain DNA element(s) at gene promoter regions. Such responsive element(s) will reveal the mechanisms of MN1 functions and other MN1-regulated gene targets. VDRE is a candidate DNA sequence, but no binding of MN1 with VDRE was identified using chromatin immunoprecipitation (ChIP) or EMSA analysis (data not shown). It is possible that MN1 does not bind VDRE directly or MN1 functions through different DNA elements. Indeed, it is reported that MN1 binds to a CACCC element to stimulate the activity of IGFBP-5 promoter (260). Figure II-15 shows that MN1 also activates human RANKL promoter, which does not contain a VDRE. Therefore, the putative MN1-interacting DNA element(s) should be identified through a blind screen, such as ChIP assay followed by sequencing MN1-bound DNA. The highly redundant DNA elements are possibly the MN1-binding sites.

Determine the in situ expression of MN1 and explore its signaling pathway

Our studies reveal that MN1 mRNA is expressed in osteoblastic cell lines, primary calvarial osteoblasts, and bone extracts. However, its *in situ* expression in bone structures, such as epiphyseal growth plate and cortical bone, should be determined to further elucidate its functions in skeletal physiology. We have tried to investigate the expression of endogenous MN1 protein through

immunohistochemistry, but it did not prove technically feasible using current MN1 antibody (data not shown). Another MN1 antibody is required to perform immunohistochemistry analysis, or alternatively, *in situ* hybridization can be used to determine the mRNA expression of MN1. Moreover, Northern blot detected the expression of MN1 transcripts in other tissues (Figure II-3D), such as heart and brain, where the functions of MN1 have not been well-described. Therefore, the *in situ* expression analysis for MN1 mRNA or protein should not be limited to bone, but in multiple tissues, for example, using whole embryo sections. This possibly will identify unrecognized MN1 target tissues and cells, and provide further insights into the functions of MN1 *in vivo*.

As discussed in Chapter II, the restricted craniofacial phenotype of MN1 knockout model suggests the roles of MN1 in neural crest cell migration and/or differentiation. MN1 knockout mice exhibit partially overlapping phenotypes with some homeobox gene knockout models, such as Prx1/2$^{-/-}$, Msx1$^{-/-}$ and Dlx2$^{-/-}$ mice (305-307). Certain cranial skeleton components in these homeobox gene knockout models exhibit similar agenesis or hypomineralization as those in MN1 knockout mice. Homeobox genes are transcription factors that are critical for patterning. Each homeobox gene has a unique expression profile during development and plays a distinct role in regulating organogenesis. As a transcriptional factor, MN1 can be upstream, downstream, or a cofactor of homeobox genes that are key to craniofacial development. Such candidate homeobox genes can be identified by comparing the spatial and temporal distribution of MN1 with well-characterized homeobox genes. Moreover, the

significance of MN1 in homeobox signaling can be further investigated by analyzing the expression of candidate homeobox genes in wild-type and MN1 knockout mice.

Gene expression analysis of MN1 knockout model

Our data and another report (207) show that ablation of MN1 causes dramatic defects in osteoblast differentiation *in vitro* and in skeletal development *in vivo*, but only limited numbers of MN1 target genes have been characterized (Figure II-12C, -13C and -14C). These genes mediate part of MN1 activities, but their expression changes cannot completely explain the phenotypes of MN1 knockout model. To further explore the molecular mechanisms of MN1 activities and elicit other possible functions of MN1 in osteoblasts, the gene expression profiles in wild-type and MN1 knockout primary osteoblasts should be investigated by microarray analysis, which will characterize the impact of MN1 on gene expression at specific differentiation stages and on the gene expression change during osteoblast differentiation.

Based on current knowledge, it is expected that MN1 knockout primary osteoblasts will express decreased levels of osteoblast marker genes and increased levels of adipocyte marker genes, but it will be important to investigate how the osteogenesis/adipogenesis-controlling genes are regulated. This will reveal whether MN1 is an upstream regulating factor or a downstream responsive gene in the mesenchymal stem cell differentiation pathways.

Furthermore, because MN1 knockout osteoblasts have a decreased proliferation rate, the growth-regulating genes, especially at proliferation stage, may have different expression levels in MN1 null cells. This possibly will provide mechanistic insights about how MN1 regulates cell growth. In addition, the altered cell morphology in MN1 knockout osteoblasts suggests that MN1 may regulate cell migration or adhesion. We found that cadherin-11 is down regulated by MN1 ablation (Figure II-13C). Gene expression analysis possibly will reveal whether other related signaling components are changed. Moreover, the expression changes of certain homeobox genes and/or their signaling pathway components will help to identify the candidate homeobox signals- in which MN1 is involved. Finally, by analyzing gene expression profiles, some novel functions or target genes of MN1 in osteoblasts may be recognized.

Examine the significance of MN1 in postnatal bone development by conditional knockout model

Our data indicate that MN1 is essential for maintaining normal osteoblast proliferation and differentiation, but the postnatal lethality of MN1 knockout mice restricts the bone development analysis to embryonic stages. Although deletion of MN1 causes cranial skeleton abnormalities and osteogenesis defects, comprehensive microCT analysis to examine bone mineral density and bone volume in E16.5 and E18.5 tibia did not reveal significant difference of appendicular bone development in MN1 knockout embryos (data not shown). It is important to note that ablation of bone-regulating genes does not always cause

obvious phenotypes at embryonic stages. For example, 1,25$(OH)_2D_3$ signaling is essential for bone mineralization, while neither VDR nor 1α-hydroxylase knockout mice display skeletal defects at embryos (89, 195). The ERα-mediated pathway plays significant roles in maintaining bone density. However, ERα knockout mice exhibit normal skeleton development before the early pubertal period (31 day after birth) (308). SRC-1 is a coactivator for ER-mediated transcription and is required for the skeletal response to estrogen, but SRC-1 knockout mice exhibit osteopenia only at 3 months of age (309, 310). These models indicate that osteoblast activities have significant impact on postnatal bone development and regeneration. Thus, a postnatally viable MN1 knockout model is required to fully understand the functions of MN1 in the skeleton. For example, the time-specific knockout of MN1 can be achieved by Cre/loxP system, in which the expression of Cre recombinase is under control of a tetracycline-responsive promoter. Then ablation of MN1 gene can be induced at an appropriate time through tetracycline administration.

Investigate the roles of MN1 in adipogenesis

Our data show that MN1 knockout calvarial osteoblast cultures have higher levels of adipogenesis (Figure II-13). In contrast to the up-regulation of MN1 during osteogenesis, MN1 expression was down-regulated when 3T3-L1 pre-adipocytes differentiate into more mature stages (data not shown). These data suggest that MN1 might block the differentiation of adipocytes from mesenchymal precursors. Osteoblasts and adipocytes may originate from

common mesenchymal stem cells, and the differentiation of these two lineages is believed to be inversely correlated (272, 273). It has been suggested that increased adipogenesis in bone marrow is associated with osteopenic bone disorders (274, 275). Importantly, other reports have shown that $1,25(OH)_2D_3$/VDR signaling inhibits adipogenesis in multiple models, including 3T3-L1 cells, bone marrow stromal cells, and primary cultures (280, 281, 311). $1,25(OH)_2D_3$ induces MN1 in 3T3-L1 cells at both proliferating and differentiating stages (data not shown), supporting that MN1 might mediate the regulation of $1,25(OH)_2D_3$ on adipogenesis. Therefore, the expression and $1,25(OH)_2D_3$ regulation of MN1 should be examined in additional adipocyte models, such as adipose tissue and adipogenic cultures from VDR knockout models.

The MN1 knockout model also can be used to explore the functional significance of MN1 in adipocyte differentiation and in $1,25(OH)_2D_3$/VDR signaling. The development of white/brown fat in wild-type and MN1 knockout mice can be analyzed via direct weight measurement of fat tissue or via indirect histological analysis of oil accumulation. The expression of adipocytic marker genes and adipogenesis controlling genes in fat tissue from wild-type and MN1 knockout mice can be determined by immunohistochemistry and/or mRNA analysis. Furthermore, the bone marrow cells, fibroblasts and mesenchymal stem cells (MSCs) that contains adipocyte precursors, and primary adipocytes in fat pads can be isolated from wild-type and MN1 knockout mice, and their adipocytic differentiation and the response to $1,25(OH)_2D_3$ can be analyzed using *in vitro* culture systems. Altered adipogenesis *in vitro* and/or fat accumulation *in*

vivo in MN1 knockout model will further support the significance of MN1 in regulating adipocyte differentiation.

Explore the functions of MN1 in osteoblasts using inducible overexpression system

Using MN1 knockout model, we have shown that ablation of MN1 leads to impaired osteoblast functions. As a complementary approach to further support the significance of MN1, the impact of ectopic MN1 on osteoblast/adipocyte differentiation should be analyzed. These cellular assays require long-term (10-30 days) of post-confluent culture and a high efficiency of MN1 expression. However, in our hands, transient transfection has a low efficiency (<5% in most osteoblasts used in this study) and a short expression time (3-4 day under our experimental conditions), and retroviral or lentiviral transduction did not provide higher efficiency (data not shown). Moreover, MN1 overexpression suppresses the growth of subconfluent osteoblasts. Although ectopic MN1 does not induce apoptosis (data not shown) and its impact on the survival of postconfluent cells are still unknown, MN1 overexpression inhibits BrdU incorporation and colony formation in proliferating osteoblasts (data not shown). Thus, an MN1 stable line cannot be established through transient transfection and subsequent selection of MN1-expressing cells. As an alternative approach, the tetracycline-inducible gene expression system can potentially overcome the anti-proliferative effects of MN1. With this inducible system, osteoblasts/adipocytes can be grown to confluence, and MN1 expression can be induced at specific differentiation stages

and for appropriate times. Then the direct impact of MN1 on osteoblast/adipocyte differentiation can be analyzed. Furthermore, by using such an inducible stable expression system that has high efficiency, the MN1 target genes can be identified, e.g., through microarray analysis.

SEMA3B

Investigate the roles of SEMA3B in RANKL-RANK signaling

Our studies show that recombinant SEMA3B promotes osteoblast-independent osteoclastogenesis in the RAW 264.7 macrophage model (Figure III-11B), suggesting that SEMA3B can directly target osteoclast precursors and stimulate their differentiation. However, RAW 264.7 is a transformed cell line, which represents only a limited window of osteoclast precursors. Thus, the direct impact of secreted SEMA3B should be examined in primary bone marrow cells or in spleen cells. Most osteoclastogenesis regulating factors alter the RANKL:OPG ratio in osteoblasts, while SEMA3B does not affect that (Figure III-10B and data not shown). To conclude that SEMA3B represents a novel signaling pathway on regulating osteoclast differentiation, the protein expression of RANKL/OPG should be examined in SEMA3B transgenic and non-transgenic osteoblasts. Even though SEMA3B does not regulate the synthesis of RANKL, it may modulate the activity of RANKL/RANK signaling within osteoclast precursors because SEMA3B requires the presence of RANKL to stimulate osteoclastogenesis in RAW 264.7 cells (Figure III-11B). Therefore, the impact of

SEMA3B on RANK-initiated intracellular pathways, such as the association of RANK with TRAF6, and the activation of NF-κB, JNK, and p38 MAPK, should be determined.

Identify the receptor(s), co-receptor(s), and intracellular signaling of SEMA3B in osteoclasts

SEMA3 molecules are secreted proteins that signal through neuropilin receptors and plexin co-receptors (213-216). Plexin-A1 is expressed in both isolated primary osteoclasts and *in vitro* induced osteoclasts (312). Plexin-A1$^{-/-}$ bone marrow cells exhibit reduced *in vitro* osteoclastogenesis when they are treated with RANKL and M-CSF, and plexin-A1 knockout mice develop osteopetrosis due to the decreased osteoclast formation (312). In addition, rac1, an effector of semaphorin signaling (302), is required for osteoclast differentiation and bone resorption (303, 304). These findings further support the active roles of SEMA3B signaling in regulating the formation and activity of osteoclasts.

To understand the mechanism of SEMA3B activities in osteoclasts, it is important to identify the functional SEMA3B receptor(s) or co-receptor(s), and to investigate the intracellular signaling cascades in osteoclast precursors and mature osteoclasts. For example, because plexin-A1 is essential for osteoclastogenesis (312), the activation of plexin-A1 signaling by SEMA3B should be examined. In addition, the osteoclastic expression of other subtypes of plexins and neuropilins should be determined. The significance of identified

plexins and neuropilins in SEMA3B-regulated osteoclastogenesis can be evaluated by siRNA knockdown or genetic knockout approaches. To identify the molecular targets of SEMA3B in osteoclasts, microarray analysis can be performed in primary osteoclasts isolated from SEMA3B transgenic and nontransgenic mice. The gene expression profiles will possibly uncover the intracellular signaling pathway of SEMA3B within osteoclasts.

Gene expression analysis of SEMA3B transgenic osteoblasts

It has been shown that transcripts for SEMA3B as well as some other semaphorin family members, their neuropilin receptors, and plexin co-receptors are expressed *in vitro* in osteoblast-enriched cell populations obtained from periodontal and gingival isolates (230). The presence of neuropilin receptors and plexin co-receptors suggests that SEMA3B may play active roles in osteoblasts. Our studies reveal that SEMA3B promotes osteoblast differentiation and mineralization *in vitro* (Figure III-9), while the mechanisms of these regulations are not described. Thus, microarray analysis can be performed to compare the gene expression profiles in SEMA3B transgenic and nontransgenic osteoblasts. Based on current knowledge, it is expected that certain osteoblast marker genes will show increased expression in SEMA3B transgenic osteoblasts, but it is important to examine whether SEMA3B regulates the osteogenesis controlling genes. Moreover, SEMA3B may have other unknown functions in osteoblasts. These novel activities of SEMA3B might be revealed by gene profile analysis.

Examine the bone development in SEMA3B knockout mice

Using the SEMA3B transgenic mouse model, our studies have shown that osteoblast-derived SEMA3B plays important roles in osteoclast formation and skeleton development. However, the roles of SEMA3B may not be completely depicted by this transgenic approach because gene deficiency might reveal unrecognized gene functions. Furthermore, genetic disorders are more frequently correlated with loss-of-function. Indeed, loss-of-heterozygosity of SEMA3B has been described in cancer patients, but the skeletal homeostasis was not examined (220, 221, 313). Thus, the SEMA3B knockout model will be useful to further understand the significance of SEMA3B in bone development.

Two independent groups reported that SEMA3B knockout mice are viable and largely normal, but the skeletal phenotype was not analyzed (224, 225). Although SEMA3B transgene primarily promotes osteoclast activity *in vivo*, the *in vitro* differentiation of both osteoblasts and osteoclasts is stimulated by SEMA3B. Thus, it is expected that SEMA3B knockout mice will exhibit coupled reduction of bone formation and bone resorption, but the overall outcome cannot be predicted without examining animal models. Unexpectedly, no viable SEMA3B knockout mice were generated by the $SEMA3B^{+/-}$ breeding in our lab. We are now trying to examine the genotypes of offspring in early embryonic stage and to explore the possible developmental defects in the SEMA3B knockout mice in our lab.

Determine the in situ expression of SEMA3B, its receptor(s) and co-receptor(s)

We have examined the *in situ* expression of SEMA3B at the epithyseal growth plate in adult mice (Figure III-5D), where SEMA3B was selectively expressed in proliferating chondrocytes within the prehypertrophic zone, but not in cells within the hypertrophic chondrocyte zone. The cell-stage specific expression of SEMA3B suggests its potential significance in growth plate formation, which is essential for endochondral ossification and forms most fetal bones. Thus, the expression of SEMA3B, its receptor(s) and co-receptor(s) in the embryonic skeleton should be determined to investigate the significance of SEMA3B signaling during early bone formation.

Even though SEMA3B is reported to be correlated with neural guidance and liver tumorigenesis (221, 224), tissue distribution analysis did not reveal strong expression of SEMA3B in brain or liver. In contrast, other organs such as intestine, heart, and kidney express higher levels of SEMA3B (Figure III-5A), but its functions in these tissues are undetermined. Thus, the current knowledge of SEMA3B remains limited. To further explore the physiological roles and the target cells of SEMA3B, the expression of SEMA3B, its receptor(s), and co-receptor(s) also should be determined in other organs during development. The temporal and spatial expression patterns of SEMA3B signaling will provide more insights about its *in vivo* functions.

Examine the involvement of SEMA3B in endocrine pathway

SEMA3B is a secreted protein and can function in a paracrine or endocrine manner. Our data revealed a paracrine pathway, in which osteoblast-synthesized SEMA3B regulates osteoclast differentiation. Therefore, it is important to examine whether osteoblast-secreted SEMA3B can target other tissues, and whether the SEMA3B secreted by other tissues can target osteoclasts/osteoblasts. For example, to determine the impact of circulating SEMA3B on bone cells, recombinant SEMA3B can be injected into mice and the effects on bone remodeling can be analyzed. To investigate whether osteoblast-derived SEMA3B enters the circulation, the plasma concentration of SEMA3B can be compared in SEMA3B transgenic and nontransgenic mice. If the serum level of SEMA3B is correlated with bone remodeling, it will be important to examine whether the expression of SEMA3B is altered in osteoporosis or osteopetrosis conditions. These changes will directly point to the diagnostic and therapeutic roles of SEMA3B in bone disorders.

Explore the therapeutic role of SEMA3B in treating bone disorders

Studies of SEMA3B transgenic mice indicate that osteoblast-secreted SEMA3B promotes osteoclastogenesis without altering osteoblast activity *in vivo.* This selective effect suggests a therapeutic role of SEMA3B in treating bone disorders. Biologically active SEMA3B can be achieved by purifying and/or concentrating SEMA3B-containing media that are prepared from bacteria or mammalian cells. Importantly, we have shown that recombinant SEMA3B can stimulate osteoclast differentiation *in vitro* (Figure III-11B). Next, it will be

important to investigate whether the recombinant SEMA3B is able to reverse the osteopetrosis *in vivo*, for example, using the OPG transgenic mouse model. In contrast, because SEMA3B promotes osteoclastogenesis, inhibiting SEMA3B signaling is a possible approach to treat osteopenia or osteoporosis. The putative targets can be SEMA3B, its receptor(s), co-receptor(s), or the downstream intracellular pathway.

However, these applications require further knowledge about SEMA3B activities. For example, it is important examine the impact of high doses of SEMA3B in other organs to evaluate the possible toxicity. Furthermore, it will be important to recognize the functional domain of SEMA3B by structural-functional analysis. The active SEMA3B fragment can be an alternative for the full-length recombinant SEMA3B or be a target against which to develop SEMA3B inhibitors. The dominant negative form of SEMA3B or competitive peptide can be directly used to suppress SEMA3B signaling.

In addition, there is evidence showing that SEMA3B functions through distinctive receptor/co-receptor complexes in different situations. Neuropilin-1 is required for SEMA3B to suppress the growth of breast and lung cancer cells (314), while neuropilin-1 expression was not detected in anterior commisure; instead, it is proposed that SEMA3B associates with neuropilin-2 to regulate the positioning of the anterior commisure (224). If certain receptor/co-receptor(s) that selectively mediate SEMA3B signaling in osteoclast can be identified, these

receptor/co-receptor(s) will be better therapeutic targets to modulate SEMA3B signaling so that the side effects in other tissues can be reduced.

Reference List

1. Wharton B, Bishop N 2003 Rickets. Lancet 362:1389-1400

2. Rajakumar K 2003 Vitamin D, cod-liver oil, sunlight, and rickets: a historical perspective. Pediatrics 112:e132-135

3. Carpenter KJ, Zhao L 1999 Forgotten mysteries in the early history of vitamin D. The Journal of nutrition 129:923-927

4. Wolf G 2004 The discovery of vitamin D: the contribution of Adolf Windaus. The Journal of nutrition 134:1299-1302

5. Norman AW 1998 Sunlight, season, skin pigmentation, vitamin D, and 25-hydroxyvitamin D: integral components of the vitamin D endocrine system. The American journal of clinical nutrition 67:1108-1110

6. Holick MF 2004 Sunlight and vitamin D for bone health and prevention of autoimmune diseases, cancers, and cardiovascular disease. The American journal of clinical nutrition 80:1678S-1688S

7. Jones G, Strugnell SA, DeLuca HF 1998 Current understanding of the molecular actions of vitamin D. Physiological reviews 78:1193-1231

8. Yoshida T, Monkawa T, Tenenhouse HS, Goodyer P, Shinki T, Suda T, Wakino S, Hayashi M, Saruta T 1998 Two novel 1alpha-hydroxylase mutations in French-Canadians with vitamin D dependency rickets type I1. Kidney international 54:1437-1443

9. Kitanaka S, Takeyama K, Murayama A, Sato T, Okumura K, Nogami M, Hasegawa Y, Niimi H, Yanagisawa J, Tanaka T, Kato S 1998 Inactivating mutations in the 25-hydroxyvitamin D3 1alpha-hydroxylase gene in patients with pseudovitamin D-deficiency rickets. The New England journal of medicine 338:653-661

10. Fu GK, Lin D, Zhang MY, Bikle DD, Shackleton CH, Miller WL, Portale AA 1997 Cloning of human 25-hydroxyvitamin D-1 alpha-hydroxylase and mutations causing vitamin D-dependent rickets type 1. Molecular endocrinology (Baltimore, Md 11:1961-1970

11. Sutton AL, MacDonald PN 2003 Vitamin D: more than a "bone-a-fide" hormone. Molecular endocrinology (Baltimore, Md 17:777-791

12. Hewison M, Zehnder D, Chakraverty R, Adams JS 2004 Vitamin D and barrier function: a novel role for extra-renal 1 alpha-hydroxylase. Molecular and cellular endocrinology 215:31-38

13. Shinki T, Shimada H, Wakino S, Anazawa H, Hayashi M, Saruta T, DeLuca HF, Suda T 1997 Cloning and expression of rat 25-hydroxyvitamin D3-1alpha-hydroxylase cDNA. Proceedings of the National Academy of Sciences of the United States of America 94:12920-12925

14. Bushinsky DA, Nalbantian-Brandt C, Favus MJ 1989 Elevated Ca2+ does not inhibit the 1,25(OH)2D3 response to phosphorus restriction. The American journal of physiology 256:F285-289

15. Schiavi SC, Kumar R 2004 The phosphatonin pathway: new insights in phosphate homeostasis. Kidney international 65:1-14

16. Shimada T, Urakawa I, Yamazaki Y, Hasegawa H, Hino R, Yoneya T, Takeuchi Y, Fujita T, Fukumoto S, Yamashita T 2004 FGF-23 transgenic mice demonstrate hypophosphatemic rickets with reduced expression of sodium phosphate cotransporter type IIa. Biochemical and biophysical research communications 314:409-414

17. Chen KS, DeLuca HF 1995 Cloning of the human 1 alpha,25-dihydroxyvitamin D-3 24-hydroxylase gene promoter and identification of two vitamin D-responsive elements. Biochimica et biophysica acta 1263:1-9

18. Takeyama K, Kitanaka S, Sato T, Kobori M, Yanagisawa J, Kato S 1997 25-Hydroxyvitamin D3 1alpha-hydroxylase and vitamin D synthesis. Science (New York, NY 277:1827-1830

19. Dusso AS, Brown AJ, Slatopolsky E 2005 Vitamin D. American journal of physiology 289:F8-28

20. 1999 A unified nomenclature system for the nuclear receptor superfamily. Cell 97:161-163

21. Jurutka PW, Remus LS, Whitfield GK, Thompson PD, Hsieh JC, Zitzer H, Tavakkoli P, Galligan MA, Dang HT, Haussler CA, Haussler MR 2000 The polymorphic N terminus in human vitamin D receptor isoforms influences transcriptional activity by modulating interaction with transcription factor IIB. Molecular endocrinology (Baltimore, Md 14:401-420

22. Shaffer PL, Gewirth DT 2002 Structural basis of VDR-DNA interactions on direct repeat response elements. The EMBO journal 21:2242-2252

23. Warnmark A, Treuter E, Wright AP, Gustafsson JA 2003 Activation functions 1 and 2 of nuclear receptors: molecular strategies for transcriptional activation. Molecular endocrinology (Baltimore, Md 17:1901-1909

24. Moras D, Gronemeyer H 1998 The nuclear receptor ligand-binding domain: structure and function. Current opinion in cell biology 10:384-391

25. Masuyama H, Brownfield CM, St-Arnaud R, MacDonald PN 1997 Evidence for ligand-dependent intramolecular folding of the AF-2 domain in vitamin D receptor-activated transcription and coactivator interaction. Molecular endocrinology (Baltimore, Md 11:1507-1517

26. Mangelsdorf DJ, Thummel C, Beato M, Herrlich P, Schutz G, Umesono K, Blumberg B, Kastner P, Mark M, Chambon P, Evans RM 1995 The nuclear receptor superfamily: the second decade. Cell 83:835-839

27. Danielian PS, White R, Lees JA, Parker MG 1992 Identification of a conserved region required for hormone dependent transcriptional activation by steroid hormone receptors. The EMBO journal 11:1025-1033

28. Haussler MR, Whitfield GK, Haussler CA, Hsieh JC, Thompson PD, Selznick SH, Dominguez CE, Jurutka PW 1998 The nuclear vitamin D receptor: biological and molecular regulatory properties revealed. J Bone Miner Res 13:325-349

29. Carlberg C, Polly P 1998 Gene regulation by vitamin D3. Critical reviews in eukaryotic gene expression 8:19-42

30. Toell A, Polly P, Carlberg C 2000 All natural DR3-type vitamin D response elements show a similar functionality in vitro. The Biochemical journal 352 Pt 2:301-309

31. Noda M, Vogel RL, Craig AM, Prahl J, DeLuca HF, Denhardt DT 1990 Identification of a DNA sequence responsible for binding of the 1,25-dihydroxyvitamin D3 receptor and 1,25-dihydroxyvitamin D3 enhancement of mouse secreted phosphoprotein 1 (SPP-1 or osteopontin) gene expression. Proceedings of the National Academy of Sciences of the United States of America 87:9995-9999

32. Zierold C, Darwish HM, DeLuca HF 1994 Identification of a vitamin D-response element in the rat calcidiol (25-hydroxyvitamin D3) 24-hydroxylase gene. Proceedings of the National Academy of Sciences of the United States of America 91:900-902

33. Kremer R, Sebag M, Champigny C, Meerovitch K, Hendy GN, White J, Goltzman D 1996 Identification and characterization of 1,25-dihydroxyvitamin D3-responsive repressor sequences in the rat parathyroid hormone-related peptide gene. The Journal of biological chemistry 271:16310-16316

34. Ozono K, Liao J, Kerner SA, Scott RA, Pike JW 1990 The vitamin D-responsive element in the human osteocalcin gene. Association with a

nuclear proto-oncogene enhancer. The Journal of biological chemistry 265:21881-21888

35. Rhodes SJ, Chen R, DiMattia GE, Scully KM, Kalla KA, Lin SC, Yu VC, Rosenfeld MG 1993 A tissue-specific enhancer confers Pit-1-dependent morphogen inducibility and autoregulation on the pit-1 gene. Genes & development 7:913-932

36. Morrison NA, Shine J, Fragonas JC, Verkest V, McMenemy ML, Eisman JA 1989 1,25-dihydroxyvitamin D-responsive element and glucocorticoid repression in the osteocalcin gene. Science (New York, NY 246:1158-1161

37. Kahlen JP, Carlberg C 1994 Identification of a vitamin D receptor homodimer-type response element in the rat calcitriol 24-hydroxylase gene promoter. Biochemical and biophysical research communications 202:1366-1372

38. Schrader M, Kahlen JP, Carlberg C 1997 Functional characterization of a novel type of 1 alpha,25-dihydroxyvitamin D3 response element identified in the mouse c-fos promoter. Biochemical and biophysical research communications 230:646-651

39. Schrader M, Nayeri S, Kahlen JP, Muller KM, Carlberg C 1995 Natural vitamin D3 response elements formed by inverted palindromes: polarity-directed ligand sensitivity of vitamin D3 receptor-retinoid X receptor heterodimer-mediated transactivation. Molecular and cellular biology 15:1154-1161

40. Quack M, Szafranski K, Rouvinen J, Carlberg C 1998 The role of the T-box for the function of the vitamin D receptor on different types of response elements. Nucleic acids research 26:5372-5378

41. Carlberg C 1995 Mechanisms of nuclear signalling by vitamin D3. Interplay with retinoid and thyroid hormone signalling. European journal of biochemistry / FEBS 231:517-527

42. Fretz JA, Zella LA, Kim S, Shevde NK, Pike JW 2007 1,25-Dihydroxyvitamin D3 induces expression of the Wnt signaling co-regulator LRP5 via regulatory elements located significantly downstream of the gene's transcriptional start site. The Journal of steroid biochemistry and molecular biology 103:440-445

43. Kim S, Yamazaki M, Zella LA, Meyer MB, Fretz JA, Shevde NK, Pike JW 2007 Multiple enhancer regions located at significant distances upstream of the transcriptional start site mediate RANKL gene expression in response to 1,25-dihydroxyvitamin D3. The Journal of steroid biochemistry and molecular biology 103:430-434

44. Meyer MB, Watanuki M, Kim S, Shevde NK, Pike JW 2006 The human transient receptor potential vanilloid type 6 distal promoter contains multiple vitamin D receptor binding sites that mediate activation by 1,25-dihydroxyvitamin D3 in intestinal cells. Molecular endocrinology (Baltimore, Md 20:1447-1461

45. Heery DM, Kalkhoven E, Hoare S, Parker MG 1997 A signature motif in transcriptional co-activators mediates binding to nuclear receptors. Nature 387:733-736

46. Darimont BD, Wagner RL, Apriletti JW, Stallcup MR, Kushner PJ, Baxter JD, Fletterick RJ, Yamamoto KR 1998 Structure and specificity of nuclear receptor-coactivator interactions. Genes & development 12:3343-3356

47. Shiau AK, Barstad D, Loria PM, Cheng L, Kushner PJ, Agard DA, Greene GL 1998 The structural basis of estrogen receptor/coactivator recognition and the antagonism of this interaction by tamoxifen. Cell 95:927-937

48. Jurutka PW, Hsieh JC, Remus LS, Whitfield GK, Thompson PD, Haussler CA, Blanco JC, Ozato K, Haussler MR 1997 Mutations in the 1,25-dihydroxyvitamin D3 receptor identifying C-terminal amino acids required for transcriptional activation that are functionally dissociated from hormone binding, heterodimeric DNA binding, and interaction with basal transcription factor IIB, in vitro. The Journal of biological chemistry 272:14592-14599

49. Savkur RS, Burris TP 2004 The coactivator LXXLL nuclear receptor recognition motif. J Pept Res 63:207-212

50. Hong H, Kohli K, Trivedi A, Johnson DL, Stallcup MR 1996 GRIP1, a novel mouse protein that serves as a transcriptional coactivator in yeast for the hormone binding domains of steroid receptors. Proceedings of the National Academy of Sciences of the United States of America 93:4948-4952

51. Li H, Gomes PJ, Chen JD 1997 RAC3, a steroid/nuclear receptor-associated coactivator that is related to SRC-1 and TIF2. Proceedings of the National Academy of Sciences of the United States of America 94:8479-8484

52. Voegel JJ, Heine MJ, Zechel C, Chambon P, Gronemeyer H 1996 TIF2, a 160 kDa transcriptional mediator for the ligand-dependent activation function AF-2 of nuclear receptors. The EMBO journal 15:3667-3675

53. Spencer TE, Jenster G, Burcin MM, Allis CD, Zhou J, Mizzen CA, McKenna NJ, Onate SA, Tsai SY, Tsai MJ, O'Malley BW 1997 Steroid receptor coactivator-1 is a histone acetyltransferase. Nature 389:194-198

54. Sadoul K, Boyault C, Pabion M, Khochbin S 2008 Regulation of protein turnover by acetyltransferases and deacetylases. Biochimie 90:306-312

55. Xu J, Qiu Y, DeMayo FJ, Tsai SY, Tsai MJ, O'Malley BW 1998 Partial hormone resistance in mice with disruption of the steroid receptor coactivator-1 (SRC-1) gene. Science (New York, NY 279:1922-1925

56. Torchia J, Rose DW, Inostroza J, Kamei Y, Westin S, Glass CK, Rosenfeld MG 1997 The transcriptional co-activator p/CIP binds CBP and mediates nuclear-receptor function. Nature 387:677-684

57. Goldman PS, Tran VK, Goodman RH 1997 The multifunctional role of the co-activator CBP in transcriptional regulation. Recent progress in hormone research 52:103-119; discussion 119-120

58. Ikeda M, Kawaguchi A, Takeshita A, Chin WW, Endo T, Onaya T 1999 CBP-dependent and independent enhancing activity of steroid receptor coactivator-1 in thyroid hormone receptor-mediated transactivation. Molecular and cellular endocrinology 147:103-112

59. Chakravarti D, LaMorte VJ, Nelson MC, Nakajima T, Schulman IG, Juguilon H, Montminy M, Evans RM 1996 Role of CBP/P300 in nuclear receptor signalling. Nature 383:99-103

60. Imhof A, Yang XJ, Ogryzko VV, Nakatani Y, Wolffe AP, Ge H 1997 Acetylation of general transcription factors by histone acetyltransferases. Curr Biol 7:689-692

61. Rachez C, Suldan Z, Ward J, Chang CP, Burakov D, Erdjument-Bromage H, Tempst P, Freedman LP 1998 A novel protein complex that interacts with the vitamin D3 receptor in a ligand-dependent manner and enhances VDR transactivation in a cell-free system. Genes & development 12:1787-1800

62. Rachez C, Lemon BD, Suldan Z, Bromleigh V, Gamble M, Naar AM, Erdjument-Bromage H, Tempst P, Freedman LP 1999 Ligand-dependent transcription activation by nuclear receptors requires the DRIP complex. Nature 398:824-828

63. Fondell JD, Ge H, Roeder RG 1996 Ligand induction of a transcriptionally active thyroid hormone receptor coactivator complex. Proceedings of the National Academy of Sciences of the United States of America 93:8329-8333

64. Bourbon HM, Aguilera A, Ansari AZ, Asturias FJ, Berk AJ, Bjorklund S, Blackwell TK, Borggrefe T, Carey M, Carlson M, Conaway JW, Conaway RC, Emmons SW, Fondell JD, Freedman LP, Fukasawa T, Gustafsson CM, Han M, He X, Herman PK, Hinnebusch AG, Holmberg S, Holstege

FC, Jaehning JA, Kim YJ, Kuras L, Leutz A, Lis JT, Meisterernest M, Naar AM, Nasmyth K, Parvin JD, Ptashne M, Reinberg D, Ronne H, Sadowski I, Sakurai H, Sipiczki M, Sternberg PW, Stillman DJ, Strich R, Struhl K, Svejstrup JQ, Tuck S, Winston F, Roeder RG, Kornberg RD 2004 A unified nomenclature for protein subunits of mediator complexes linking transcriptional regulators to RNA polymerase II. Molecular cell 14:553-557

65. Ge K, Guermah M, Yuan CX, Ito M, Wallberg AE, Spiegelman BM, Roeder RG 2002 Transcription coactivator TRAP220 is required for PPAR gamma 2-stimulated adipogenesis. Nature 417:563-567

66. Ito M, Okano HJ, Darnell RB, Roeder RG 2002 The TRAP100 component of the TRAP/Mediator complex is essential in broad transcriptional events and development. The EMBO journal 21:3464-3475

67. Blazek E, Mittler G, Meisterernst M 2005 The mediator of RNA polymerase II. Chromosoma 113:399-408

68. Rachez C, Gamble M, Chang CP, Atkins GB, Lazar MA, Freedman LP 2000 The DRIP complex and SRC-1/p160 coactivators share similar nuclear receptor binding determinants but constitute functionally distinct complexes. Molecular and cellular biology 20:2718-2726

69. Yang XJ, Ogryzko VV, Nishikawa J, Howard BH, Nakatani Y 1996 A p300/CBP-associated factor that competes with the adenoviral oncoprotein E1A. Nature 382:319-324

70. Blanco JC, Minucci S, Lu J, Yang XJ, Walker KK, Chen H, Evans RM, Nakatani Y, Ozato K 1998 The histone acetylase PCAF is a nuclear receptor coactivator. Genes & development 12:1638-1651

71. Korzus E, Torchia J, Rose DW, Xu L, Kurokawa R, McInerney EM, Mullen TM, Glass CK, Rosenfeld MG 1998 Transcription factor-specific requirements for coactivators and their acetyltransferase functions. Science (New York, NY 279:703-707

72. Kwon H, Imbalzano AN, Khavari PA, Kingston RE, Green MR 1994 Nucleosome disruption and enhancement of activator binding by a human SW1/SNF complex. Nature 370:477-481

73. Ryan MP, Jones R, Morse RH 1998 SWI-SNF complex participation in transcriptional activation at a step subsequent to activator binding. Molecular and cellular biology 18:1774-1782

74. Zhang C, Baudino TA, Dowd DR, Tokumaru H, Wang W, MacDonald PN 2001 Ternary complexes and cooperative interplay between NCoA-62/Ski-interacting protein and steroid receptor coactivators in vitamin D receptor-

mediated transcription. The Journal of biological chemistry 276:40614-40620

75. Zhang C, Dowd DR, Staal A, Gu C, Lian JB, van Wijnen AJ, Stein GS, MacDonald PN 2003 Nuclear coactivator-62 kDa/Ski-interacting protein is a nuclear matrix-associated coactivator that may couple vitamin D receptor-mediated transcription and RNA splicing. The Journal of biological chemistry 278:35325-35336

76. MacDonald PN, Dowd DR, Zhang C, Gu C 2004 Emerging insights into the coactivator role of NCoA62/SKIP in Vitamin D-mediated transcription. The Journal of steroid biochemistry and molecular biology 89-90:179-186

77. Demay MB, Kiernan MS, DeLuca HF, Kronenberg HM 1992 Sequences in the human parathyroid hormone gene that bind the 1,25-dihydroxyvitamin D3 receptor and mediate transcriptional repression in response to 1,25-dihydroxyvitamin D3. Proceedings of the National Academy of Sciences of the United States of America 89:8097-8101

78. Pike JW, Yamamoto H, Shevde NK 2002 Vitamin D receptor-mediated gene regulation mechanisms and current concepts of vitamin D analog selectivity. Advances in renal replacement therapy 9:168-174

79. Rachez C, Freedman LP 2000 Mechanisms of gene regulation by vitamin D(3) receptor: a network of coactivator interactions. Gene 246:9-21

80. Jurutka PW, Whitfield GK, Hsieh JC, Thompson PD, Haussler CA, Haussler MR 2001 Molecular nature of the vitamin D receptor and its role in regulation of gene expression. Reviews in endocrine & metabolic disorders 2:203-216

81. Kato S, Fujiki R, Kitagawa H 2004 Vitamin D receptor (VDR) promoter targeting through a novel chromatin remodeling complex. The Journal of steroid biochemistry and molecular biology 89-90:173-178

82. Leong GM, Subramaniam N, Issa LL, Barry JB, Kino T, Driggers PH, Hayman MJ, Eisman JA, Gardiner EM 2004 Ski-interacting protein, a bifunctional nuclear receptor coregulator that interacts with N-CoR/SMRT and p300. Biochemical and biophysical research communications 315:1070-1076

83. Dunlop TW, Vaisanen S, Frank C, Carlberg C 2004 The genes of the coactivator TIF2 and the corepressor SMRT are primary 1alpha,25(OH)2D3 targets. The Journal of steroid biochemistry and molecular biology 89-90:257-260

84. Norman AW, Mizwicki MT, Norman DP 2004 Steroid-hormone rapid actions, membrane receptors and a conformational ensemble model. Nature reviews 3:27-41

85. Huhtakangas JA, Olivera CJ, Bishop JE, Zanello LP, Norman AW 2004 The vitamin D receptor is present in caveolae-enriched plasma membranes and binds 1 alpha,25(OH)2-vitamin D3 in vivo and in vitro. Molecular endocrinology (Baltimore, Md 18:2660-2671

86. Nemere I, Dormanen MC, Hammond MW, Okamura WH, Norman AW 1994 Identification of a specific binding protein for 1 alpha,25-dihydroxyvitamin D3 in basal-lateral membranes of chick intestinal epithelium and relationship to transcaltachia. The Journal of biological chemistry 269:23750-23756

87. Nemere I, Farach-Carson MC, Rohe B, Sterling TM, Norman AW, Boyan BD, Safford SE 2004 Ribozyme knockdown functionally links a 1,25(OH)2D3 membrane binding protein (1,25D3-MARRS) and phosphate uptake in intestinal cells. Proceedings of the National Academy of Sciences of the United States of America 101:7392-7397

88. Falzon M 1996 DNA sequences in the rat parathyroid hormone-related peptide gene responsible for 1,25-dihydroxyvitamin D3-mediated transcriptional repression. Molecular endocrinology (Baltimore, Md 10:672-681

89. Li YC, Pirro AE, Amling M, Delling G, Baron R, Bronson R, Demay MB 1997 Targeted ablation of the vitamin D receptor: an animal model of vitamin D-dependent rickets type II with alopecia. Proceedings of the National Academy of Sciences of the United States of America 94:9831-9835

90. Bouillon R, Van Cromphaut S, Carmeliet G 2003 Intestinal calcium absorption: Molecular vitamin D mediated mechanisms. Journal of cellular biochemistry 88:332-339

91. van Abel M, Hoenderop JG, van der Kemp AW, van Leeuwen JP, Bindels RJ 2003 Regulation of the epithelial Ca2+ channels in small intestine as studied by quantitative mRNA detection. American journal of physiology 285:G78-85

92. Van Cromphaut SJ, Dewerchin M, Hoenderop JG, Stockmans I, Van Herck E, Kato S, Bindels RJ, Collen D, Carmeliet P, Bouillon R, Carmeliet G 2001 Duodenal calcium absorption in vitamin D receptor-knockout mice: functional and molecular aspects. Proceedings of the National Academy of Sciences of the United States of America 98:13324-13329

93. Zelinski JM, Sykes DE, Weiser MM 1991 The effect of vitamin D on rat intestinal plasma membrane CA-pump mRNA. Biochemical and biophysical research communications 179:749-755

94. Wasserman RH, Smith CA, Brindak ME, De Talamoni N, Fullmer CS, Penniston JT, Kumar R 1992 Vitamin D and mineral deficiencies increase the plasma membrane calcium pump of chicken intestine. Gastroenterology 102:886-894

95. Yagci A, Werner A, Murer H, Biber J 1992 Effect of rabbit duodenal mRNA on phosphate transport in Xenopus laevis oocytes: dependence on 1,25-dihydroxy-vitamin-D3. Pflugers Arch 422:211-216

96. Li YC, Amling M, Pirro AE, Priemel M, Meuse J, Baron R, Delling G, Demay MB 1998 Normalization of mineral ion homeostasis by dietary means prevents hyperparathyroidism, rickets, and osteomalacia, but not alopecia in vitamin D receptor-ablated mice. Endocrinology 139:4391-4396

97. Panda DK, Miao D, Bolivar I, Li J, Huo R, Hendy GN, Goltzman D 2004 Inactivation of the 25-hydroxyvitamin D 1alpha-hydroxylase and vitamin D receptor demonstrates independent and interdependent effects of calcium and vitamin D on skeletal and mineral homeostasis. The Journal of biological chemistry 279:16754-16766

98. Campbell KP, Leung AT, Sharp AH 1988 The biochemistry and molecular biology of the dihydropyridine-sensitive calcium channel. Trends in neurosciences 11:425-430

99. Hadjidakis DJ, Androulakis, II 2006 Bone remodeling. Annals of the New York Academy of Sciences 1092:385-396

100. Ortega N, Behonick DJ, Werb Z 2004 Matrix remodeling during endochondral ossification. Trends in cell biology 14:86-93

101. Mackie EJ, Ahmed YA, Tatarczuch L, Chen KS, Mirams M 2008 Endochondral ossification: how cartilage is converted into bone in the developing skeleton. The international journal of biochemistry & cell biology 40:46-62

102. Ducy P, Schinke T, Karsenty G 2000 The osteoblast: a sophisticated fibroblast under central surveillance. Science (New York, NY 289:1501-1504

103. Suda T, Ueno Y, Fujii K, Shinki T 2003 Vitamin D and bone. Journal of cellular biochemistry 88:259-266

104. Mackie EJ 2003 Osteoblasts: novel roles in orchestration of skeletal architecture. The international journal of biochemistry & cell biology 35:1301-1305

105. Ducy P, Desbois C, Boyce B, Pinero G, Story B, Dunstan C, Smith E, Bonadio J, Goldstein S, Gundberg C, Bradley A, Karsenty G 1996 Increased bone formation in osteocalcin-deficient mice. Nature 382:448-452

106. Rodan GA, Martin TJ 2000 Therapeutic approaches to bone diseases. Science 289:1508-1514

107. van Driel M, Pols HA, van Leeuwen JP 2004 Osteoblast differentiation and control by vitamin D and vitamin D metabolites. Current pharmaceutical design 10:2535-2555

108. Knothe Tate ML, Adamson JR, Tami AE, Bauer TW 2004 The osteocyte. The international journal of biochemistry & cell biology 36:1-8

109. Franz-Odendaal TA, Hall BK, Witten PE 2006 Buried alive: how osteoblasts become osteocytes. Dev Dyn 235:176-190

110. Vaananen HK, Zhao H, Mulari M, Halleen JM 2000 The cell biology of osteoclast function. Journal of cell science 113 (Pt 3):377-381

111. Teitelbaum SL 2000 Bone resorption by osteoclasts. Science (New York, NY 289:1504-1508

112. Bianco P, Riminucci M, Gronthos S, Robey PG 2001 Bone marrow stromal stem cells: nature, biology, and potential applications. Stem cells (Dayton, Ohio) 19:180-192

113. Ducy P, Zhang R, Geoffroy V, Ridall AL, Karsenty G 1997 Osf2/Cbfa1: a transcriptional activator of osteoblast differentiation. Cell 89:747-754

114. Ducy P, Karsenty G 1995 Two distinct osteoblast-specific cis-acting elements control expression of a mouse osteocalcin gene. Molecular and cellular biology 15:1858-1869

115. Lecka-Czernik B, Gubrij I, Moerman EJ, Kajkenova O, Lipschitz DA, Manolagas SC, Jilka RL 1999 Inhibition of Osf2/Cbfa1 expression and terminal osteoblast differentiation by PPARgamma2. Journal of cellular biochemistry 74:357-371

116. Otto F, Thornell AP, Crompton T, Denzel A, Gilmour KC, Rosewell IR, Stamp GW, Beddington RS, Mundlos S, Olsen BR, Selby PB, Owen MJ 1997 Cbfa1, a candidate gene for cleidocranial dysplasia syndrome, is

essential for osteoblast differentiation and bone development. Cell 89:765-771

117. Lee B, Thirunavukkarasu K, Zhou L, Pastore L, Baldini A, Hecht J, Geoffroy V, Ducy P, Karsenty G 1997 Missense mutations abolishing DNA binding of the osteoblast-specific transcription factor OSF2/CBFA1 in cleidocranial dysplasia. Nature genetics 16:307-310

118. Komori T, Yagi H, Nomura S, Yamaguchi A, Sasaki K, Deguchi K, Shimizu Y, Bronson RT, Gao YH, Inada M, Sato M, Okamoto R, Kitamura Y, Yoshiki S, Kishimoto T 1997 Targeted disruption of Cbfa1 results in a complete lack of bone formation owing to maturational arrest of osteoblasts. Cell 89:755-764

119. Ducy P, Starbuck M, Priemel M, Shen J, Pinero G, Geoffroy V, Amling M, Karsenty G 1999 A Cbfa1-dependent genetic pathway controls bone formation beyond embryonic development. Genes & development 13:1025-1036

120. Geoffroy V, Kneissel M, Fournier B, Boyde A, Matthias P 2002 High bone resorption in adult aging transgenic mice overexpressing cbfa1/runx2 in cells of the osteoblastic lineage. Mol Cell Biol 22:6222-6233

121. Acampora D, Merlo GR, Paleari L, Zerega B, Postiglione MP, Mantero S, Bober E, Barbieri O, Simeone A, Levi G 1999 Craniofacial, vestibular and bone defects in mice lacking the Distal-less-related gene Dlx5. Development (Cambridge, England) 126:3795-3809

122. Wuyts W, Reardon W, Preis S, Homfray T, Rasore-Quartino A, Christians H, Willems PJ, Van Hul W 2000 Identification of mutations in the MSX2 homeobox gene in families affected with foramina parietalia permagna. Human molecular genetics 9:1251-1255

123. Satokata I, Ma L, Ohshima H, Bei M, Woo I, Nishizawa K, Maeda T, Takano Y, Uchiyama M, Heaney S, Peters H, Tang Z, Maxson R, Maas R 2000 Msx2 deficiency in mice causes pleiotropic defects in bone growth and ectodermal organ formation. Nature genetics 24:391-395

124. Yamaguchi A, Komori T, Suda T 2000 Regulation of osteoblast differentiation mediated by bone morphogenetic proteins, hedgehogs, and Cbfa1. Endocrine reviews 21:393-411

125. Udagawa N, Takahashi N, Akatsu T, Sasaki T, Yamaguchi A, Kodama H, Martin TJ, Suda T 1989 The bone marrow-derived stromal cell lines MC3T3-G2/PA6 and ST2 support osteoclast-like cell differentiation in cocultures with mouse spleen cells. Endocrinology 125:1805-1813

126. Kawasaki K, Aihara M, Honmo J, Sakurai S, Fujimaki Y, Sakamoto K, Fujimaki E, Wozney JM, Yamaguchi A 1998 Effects of recombinant human bone morphogenetic protein-2 on differentiation of cells isolated from human bone, muscle, and skin. Bone 23:223-231

127. Katagiri T, Yamaguchi A, Komaki M, Abe E, Takahashi N, Ikeda T, Rosen V, Wozney JM, Fujisawa-Sehara A, Suda T 1994 Bone morphogenetic protein-2 converts the differentiation pathway of C2C12 myoblasts into the osteoblast lineage. The Journal of cell biology 127:1755-1766

128. Storm EE, Kingsley DM 1999 GDF5 coordinates bone and joint formation during digit development. Developmental biology 209:11-27

129. Hee CK, Nicoll SB 2008 Endogenous bone morphogenetic proteins mediate 1alpha, 25-dihydroxyvitamin D(3)-induced expression of osteoblast differentiation markers in human dermal fibroblasts. J Orthop Res

130. Sodek J, Chen J, Nagata T, Kasugai S, Todescan R, Jr., Li IW, Kim RH 1995 Regulation of osteopontin expression in osteoblasts. Annals of the New York Academy of Sciences 760:223-241

131. Owen TA, Aronow MS, Barone LM, Bettencourt B, Stein GS, Lian JB 1991 Pleiotropic effects of vitamin D on osteoblast gene expression are related to the proliferative and differentiated state of the bone cell phenotype: dependency upon basal levels of gene expression, duration of exposure, and bone matrix competency in normal rat osteoblast cultures. Endocrinology 128:1496-1504

132. Ishida H, Bellows CG, Aubin JE, Heersche JN 1993 Characterization of the 1,25-(OH)2D3-induced inhibition of bone nodule formation in long-term cultures of fetal rat calvaria cells. Endocrinology 132:61-66

133. Viereck V, Siggelkow H, Tauber S, Raddatz D, Schutze N, Hufner M 2002 Differential regulation of Cbfa1/Runx2 and osteocalcin gene expression by vitamin-D3, dexamethasone, and local growth factors in primary human osteoblasts. Journal of cellular biochemistry 86:348-356

134. Fraser JD, Otawara Y, Price PA 1988 1,25-Dihydroxyvitamin D3 stimulates the synthesis of matrix gamma-carboxyglutamic acid protein by osteosarcoma cells. Mutually exclusive expression of vitamin K-dependent bone proteins by clonal osteoblastic cell lines. The Journal of biological chemistry 263:911-916

135. Gardiner EM, Baldock PA, Thomas GP, Sims NA, Henderson NK, Hollis B, White CP, Sunn KL, Morrison NA, Walsh WR, Eisman JA 2000 Increased formation and decreased resorption of bone in mice with elevated vitamin

D receptor in mature cells of the osteoblastic lineage. Faseb J 14:1908-1916

136. Heberden C, Denis I, Pointillart A, Mercier T 1998 TGF-beta and calcitriol. General pharmacology 30:145-151

137. Wu Y, Haugen JD, Zinsmeister AR, Kumar R 1997 1 alpha,25-Dihydroxyvitamin D3 increases transforming growth factor and transforming growth factor receptor type I and II synthesis in human bone cells. Biochemical and biophysical research communications 239:734-739

138. Wu Y, Craig TA, Lutz WH, Kumar R 1999 Identification of 1 alpha,25-dihydroxyvitamin D3 response elements in the human transforming growth factor beta 2 gene. Biochemistry 38:2654-2660

139. Finkelman RD, Linkhart TA, Mohan S, Lau KH, Baylink DJ, Bell NH 1991 Vitamin D deficiency causes a selective reduction in deposition of transforming growth factor beta in rat bone: possible mechanism for impaired osteoinduction. Proceedings of the National Academy of Sciences of the United States of America 88:3657-3660

140. Staal A, Van Wijnen AJ, Desai RK, Pols HA, Birkenhager JC, Deluca HF, Denhardt DT, Stein JL, Van Leeuwen JP, Stein GS, Lian JB 1996 Antagonistic effects of transforming growth factor-beta on vitamin D3 enhancement of osteocalcin and osteopontin transcription: reduced interactions of vitamin D receptor/retinoid X receptor complexes with vitamin E response elements. Endocrinology 137:2001-2011

141. Gurlek A, Kumar R 2001 Regulation of osteoblast growth by interactions between transforming growth factor-beta and 1alpha,25-dihydroxyvitamin D3. Critical reviews in eukaryotic gene expression 11:299-317

142. Gurlek A, Pittelkow MR, Kumar R 2002 Modulation of growth factor/cytokine synthesis and signaling by 1alpha,25-dihydroxyvitamin D(3): implications in cell growth and differentiation. Endocrine reviews 23:763-786

143. Yanagisawa J, Yanagi Y, Masuhiro Y, Suzawa M, Watanabe M, Kashiwagi K, Toriyabe T, Kawabata M, Miyazono K, Kato S 1999 Convergence of transforming growth factor-beta and vitamin D signaling pathways on SMAD transcriptional coactivators. Science (New York, NY 283:1317-1321

144. Borton AJ, Frederick JP, Datto MB, Wang XF, Weinstein RS 2001 The loss of Smad3 results in a lower rate of bone formation and osteopenia through dysregulation of osteoblast differentiation and apoptosis. J Bone Miner Res 16:1754-1764

145. Shima DT, Kuroki M, Deutsch U, Ng YS, Adamis AP, D'Amore PA 1996 The mouse gene for vascular endothelial growth factor. Genomic structure, definition of the transcriptional unit, and characterization of transcriptional and post-transcriptional regulatory sequences. The Journal of biological chemistry 271:3877-3883

146. Dai J, Rabie AB 2007 VEGF: an essential mediator of both angiogenesis and endochondral ossification. Journal of dental research 86:937-950

147. Maes C, Carmeliet P, Moermans K, Stockmans I, Smets N, Collen D, Bouillon R, Carmeliet G 2002 Impaired angiogenesis and endochondral bone formation in mice lacking the vascular endothelial growth factor isoforms VEGF164 and VEGF188. Mechanisms of development 111:61-73

148. Zelzer E, McLean W, Ng YS, Fukai N, Reginato AM, Lovejoy S, D'Amore PA, Olsen BR 2002 Skeletal defects in VEGF(120/120) mice reveal multiple roles for VEGF in skeletogenesis. Development (Cambridge, England) 129:1893-1904

149. Wang DS, Miura M, Demura H, Sato K 1997 Anabolic effects of 1,25-dihydroxyvitamin D3 on osteoblasts are enhanced by vascular endothelial growth factor produced by osteoblasts and by growth factors produced by endothelial cells. Endocrinology 138:2953-2962

150. Mayr-Wohlfart U, Waltenberger J, Hausser H, Kessler S, Gunther KP, Dehio C, Puhl W, Brenner RE 2002 Vascular endothelial growth factor stimulates chemotactic migration of primary human osteoblasts. Bone 30:472-477

151. Midy V, Plouet J 1994 Vasculotropin/vascular endothelial growth factor induces differentiation in cultured osteoblasts. Biochemical and biophysical research communications 199:380-386

152. Schlaeppi JM, Gutzwiller S, Finkenzeller G, Fournier B 1997 1,25-Dihydroxyvitamin D3 induces the expression of vascular endothelial growth factor in osteoblastic cells. Endocrine research 23:213-229

153. Soriano P, Montgomery C, Geske R, Bradley A 1991 Targeted disruption of the c-src proto-oncogene leads to osteopetrosis in mice. Cell 64:693-702

154. Li YP, Chen W, Liang Y, Li E, Stashenko P 1999 Atp6i-deficient mice exhibit severe osteopetrosis due to loss of osteoclast-mediated extracellular acidification. Nature genetics 23:447-451

155. Gowen M, Lazner F, Dodds R, Kapadia R, Feild J, Tavaria M, Bertoncello I, Drake F, Zavarselk S, Tellis I, Hertzog P, Debouck C, Kola I 1999

Cathepsin K knockout mice develop osteopetrosis due to a deficit in matrix degradation but not demineralization. J Bone Miner Res 14:1654-1663

156. Myint YY, Miyakawa K, Naito M, Shultz LD, Oike Y, Yamamura K, Takahashi K 1999 Granulocyte/macrophage colony-stimulating factor and interleukin-3 correct osteopetrosis in mice with osteopetrosis mutation. The American journal of pathology 154:553-566

157. Wu X, McKenna MA, Feng X, Nagy TR, McDonald JM 2003 Osteoclast apoptosis: the role of Fas in vivo and in vitro. Endocrinology 144:5545-5555

158. Yamashita DS, Dodds RA 2000 Cathepsin K and the design of inhibitors of cathepsin K. Current pharmaceutical design 6:1-24

159. Visentin L, Dodds RA, Valente M, Misiano P, Bradbeer JN, Oneta S, Liang X, Gowen M, Farina C 2000 A selective inhibitor of the osteoclastic V-H(+)-ATPase prevents bone loss in both thyroparathyroidectomized and ovariectomized rats. The Journal of clinical investigation 106:309-318

160. Yamamoto M, Fisher JE, Gentile M, Seedor JG, Leu CT, Rodan SB, Rodan GA 1998 The integrin ligand echistatin prevents bone loss in ovariectomized mice and rats. Endocrinology 139:1411-1419

161. Ross FP 2006 M-CSF, c-Fms, and signaling in osteoclasts and their precursors. Annals of the New York Academy of Sciences 1068:110-116

162. Yoshida H, Hayashi S, Kunisada T, Ogawa M, Nishikawa S, Okamura H, Sudo T, Shultz LD, Nishikawa S 1990 The murine mutation osteopetrosis is in the coding region of the macrophage colony stimulating factor gene. Nature 345:442-444

163. Dai XM, Ryan GR, Hapel AJ, Dominguez MG, Russell RG, Kapp S, Sylvestre V, Stanley ER 2002 Targeted disruption of the mouse colony-stimulating factor 1 receptor gene results in osteopetrosis, mononuclear phagocyte deficiency, increased primitive progenitor cell frequencies, and reproductive defects. Blood 99:111-120

164. Marks SC, Jr., Mackay CA, Jackson ME, Larson EK, Cielinski MJ, Stanley ER, Aukerman SL 1993 The skeletal effects of colony-stimulating factor-1 in toothless (osteopetrotic) rats: persistent metaphyseal sclerosis and the failure to restore subepiphyseal osteoclasts. Bone 14:675-680

165. Marks SC, Jr., Wojtowicz A, Szperl M, Urbanowska E, MacKay CA, Wiktor-Jedrzejczak W, Stanley ER, Aukerman SL 1992 Administration of colony stimulating factor-1 corrects some macrophage, dental, and skeletal defects in an osteopetrotic mutation (toothless, tl) in the rat. Bone 13:89-93

166. Teitelbaum SL, Ross FP 2003 Genetic regulation of osteoclast development and function. Nature reviews 4:638-649

167. Darnay BG, Haridas V, Ni J, Moore PA, Aggarwal BB 1998 Characterization of the intracellular domain of receptor activator of NF-kappaB (RANK). Interaction with tumor necrosis factor receptor-associated factors and activation of NF-kappab and c-Jun N-terminal kinase. The Journal of biological chemistry 273:20551-20555

168. Galibert L, Tometsko ME, Anderson DM, Cosman D, Dougall WC 1998 The involvement of multiple tumor necrosis factor receptor (TNFR)-associated factors in the signaling mechanisms of receptor activator of NF-kappaB, a member of the TNFR superfamily. The Journal of biological chemistry 273:34120-34127

169. Kim HH, Lee DE, Shin JN, Lee YS, Jeon YM, Chung CH, Ni J, Kwon BS, Lee ZH 1999 Receptor activator of NF-kappaB recruits multiple TRAF family adaptors and activates c-Jun N-terminal kinase. FEBS letters 443:297-302

170. Kong YY, Yoshida H, Sarosi I, Tan HL, Timms E, Capparelli C, Morony S, Oliveira-dos-Santos AJ, Van G, Itie A, Khoo W, Wakeham A, Dunstan CR, Lacey DL, Mak TW, Boyle WJ, Penninger JM 1999 OPGL is a key regulator of osteoclastogenesis, lymphocyte development and lymph-node organogenesis. Nature 397:315-323

171. Lomaga MA, Yeh WC, Sarosi I, Duncan GS, Furlonger C, Ho A, Morony S, Capparelli C, Van G, Kaufman S, van der Heiden A, Itie A, Wakeham A, Khoo W, Sasaki T, Cao Z, Penninger JM, Paige CJ, Lacey DL, Dunstan CR, Boyle WJ, Goeddel DV, Mak TW 1999 TRAF6 deficiency results in osteopetrosis and defective interleukin-1, CD40, and LPS signaling. Genes & development 13:1015-1024

172. Franzoso G, Carlson L, Xing L, Poljak L, Shores EW, Brown KD, Leonardi A, Tran T, Boyce BF, Siebenlist U 1997 Requirement for NF-kappaB in osteoclast and B-cell development. Genes & development 11:3482-3496

173. Dougall WC, Glaccum M, Charrier K, Rohrbach K, Brasel K, De Smedt T, Daro E, Smith J, Tometsko ME, Maliszewski CR, Armstrong A, Shen V, Bain S, Cosman D, Anderson D, Morrissey PJ, Peschon JJ, Schuh J 1999 RANK is essential for osteoclast and lymph node development. Genes & development 13:2412-2424

174. Yasuda H, Shima N, Nakagawa N, Yamaguchi K, Kinosaki M, Mochizuki S, Tomoyasu A, Yano K, Goto M, Murakami A, Tsuda E, Morinaga T, Higashio K, Udagawa N, Takahashi N, Suda T 1998 Osteoclast differentiation factor is a ligand for osteoprotegerin/osteoclastogenesis-inhibitory factor and is identical to TRANCE/RANKL. Proceedings of the

National Academy of Sciences of the United States of America 95:3597-3602

175. Grigoriadis AE, Wang ZQ, Cecchini MG, Hofstetter W, Felix R, Fleisch HA, Wagner EF 1994 c-Fos: a key regulator of osteoclast-macrophage lineage determination and bone remodeling. Science (New York, NY 266:443-448

176. Nosaka K, Miyamoto T, Sakai T, Mitsuya H, Suda T, Matsuoka M 2002 Mechanism of hypercalcemia in adult T-cell leukemia: overexpression of receptor activator of nuclear factor kappaB ligand on adult T-cell leukemia cells. Blood 99:634-640

177. Miyamoto T, Suda T 2003 Differentiation and function of osteoclasts. The Keio journal of medicine 52:1-7

178. Lacey DL, Timms E, Tan HL, Kelley MJ, Dunstan CR, Burgess T, Elliott R, Colombero A, Elliott G, Scully S, Hsu H, Sullivan J, Hawkins N, Davy E, Capparelli C, Eli A, Qian YX, Kaufman S, Sarosi I, Shalhoub V, Senaldi G, Guo J, Delaney J, Boyle WJ 1998 Osteoprotegerin ligand is a cytokine that regulates osteoclast differentiation and activation. Cell 93:165-176

179. Simonet WS, Lacey DL, Dunstan CR, Kelley M, Chang MS, Luthy R, Nguyen HQ, Wooden S, Bennett L, Boone T, Shimamoto G, DeRose M, Elliott R, Colombero A, Tan HL, Trail G, Sullivan J, Davy E, Bucay N, Renshaw-Gegg L, Hughes TM, Hill D, Pattison W, Campbell P, Sander S, Van G, Tarpley J, Derby P, Lee R, Boyle WJ 1997 Osteoprotegerin: a novel secreted protein involved in the regulation of bone density. Cell 89:309-319

180. Bucay N, Sarosi I, Dunstan CR, Morony S, Tarpley J, Capparelli C, Scully S, Tan HL, Xu W, Lacey DL, Boyle WJ, Simonet WS 1998 osteoprotegerin-deficient mice develop early onset osteoporosis and arterial calcification. Genes & development 12:1260-1268

181. Mizuno A, Amizuka N, Irie K, Murakami A, Fujise N, Kanno T, Sato Y, Nakagawa N, Yasuda H, Mochizuki S, Gomibuchi T, Yano K, Shima N, Washida N, Tsuda E, Morinaga T, Higashio K, Ozawa H 1998 Severe osteoporosis in mice lacking osteoclastogenesis inhibitory factor/osteoprotegerin. Biochemical and biophysical research communications 247:610-615

182. Amizuka N, Shimomura J, Li M, Seki Y, Oda K, Henderson JE, Mizuno A, Ozawa H, Maeda T 2003 Defective bone remodelling in osteoprotegerin-deficient mice. Journal of electron microscopy 52:503-513

183. Xing L, Boyce BF 2005 Regulation of apoptosis in osteoclasts and osteoblastic cells. Biochemical and biophysical research communications 328:709-720

184. Spelsberg TC, Subramaniam M, Riggs BL, Khosla S 1999 The actions and interactions of sex steroids and growth factors/cytokines on the skeleton. Molecular endocrinology (Baltimore, Md 13:819-828

185. Holliday LS, Welgus HG, Fliszar CJ, Veith GM, Jeffrey JJ, Gluck SL 1997 Initiation of osteoclast bone resorption by interstitial collagenase. The Journal of biological chemistry 272:22053-22058

186. Meikle MC, Bord S, Hembry RM, Compston J, Croucher PI, Reynolds JJ 1992 Human osteoblasts in culture synthesize collagenase and other matrix metalloproteinases in response to osteotropic hormones and cytokines. Journal of cell science 103 (Pt 4):1093-1099

187. Hoenderop JG, van Leeuwen JP, van der Eerden BC, Kersten FF, van der Kemp AW, Merillat AM, Waarsing JH, Rossier BC, Vallon V, Hummler E, Bindels RJ 2003 Renal Ca2+ wasting, hyperabsorption, and reduced bone thickness in mice lacking TRPV5. The Journal of clinical investigation 112:1906-1914

188. Jilka RL, Weinstein RS, Bellido T, Roberson P, Parfitt AM, Manolagas SC 1999 Increased bone formation by prevention of osteoblast apoptosis with parathyroid hormone. The Journal of clinical investigation 104:439-446

189. Schoppet M, Preissner KT, Hofbauer LC 2002 RANK ligand and osteoprotegerin: paracrine regulators of bone metabolism and vascular function. Arteriosclerosis, thrombosis, and vascular biology 22:549-553

190. Conover CA 2008 Insulin-like growth factor-binding proteins and bone metabolism. American journal of physiology 294:E10-14

191. Rosen CJ 1999 Serum insulin-like growth factors and insulin-like growth factor-binding proteins: clinical implications. Clinical chemistry 45:1384-1390

192. Amin S, Riggs BL, Atkinson EJ, Oberg AL, Melton LJ, 3rd, Khosla S 2004 A potentially deleterious role of IGFBP-2 on bone density in aging men and women. J Bone Miner Res 19:1075-1083

193. Eckstein F, Pavicic T, Nedbal S, Schmidt C, Wehr U, Rambeck W, Wolf E, Hoeflich A 2002 Insulin-like growth factor-binding protein-2 (IGFBP-2) overexpression negatively regulates bone size and mass, but not density, in the absence and presence of growth hormone/IGF-I excess in transgenic mice. Anatomy and embryology 206:139-148

194. Zhang M, Faugere MC, Malluche H, Rosen CJ, Chernausek SD, Clemens TL 2003 Paracrine overexpression of IGFBP-4 in osteoblasts of transgenic mice decreases bone turnover and causes global growth retardation. J Bone Miner Res 18:836-843

195. Dardenne O, Prud'homme J, Arabian A, Glorieux FH, St-Arnaud R 2001 Targeted inactivation of the 25-hydroxyvitamin D(3)-1(alpha)-hydroxylase gene (CYP27B1) creates an animal model of pseudovitamin D-deficiency rickets. Endocrinology 142:3135-3141

196. Lips P 2006 Vitamin D physiology. Progress in biophysics and molecular biology 92:4-8

197. Lekanne Deprez RH, Riegman PH, Groen NA, Warringa UL, van Biezen NA, Molijn AC, Bootsma D, de Jong PJ, Menon AG, Kley NA, et al. 1995 Cloning and characterization of MN1, a gene from chromosome 22q11, which is disrupted by a balanced translocation in a meningioma. Oncogene 10:1521-1528

198. Carella C, Bonten J, Sirma S, Kranenburg TA, Terranova S, Klein-Geltink R, Shurtleff S, Downing JR, Zwarthoff EC, Liu PP, Grosveld GC 2007 MN1 overexpression is an important step in the development of inv(16) AML. Leukemia 21:1679-1690

199. Heuser M, Argiropoulos B, Kuchenbauer F, Yung E, Piper J, Fung S, Schlenk RF, Dohner K, Hinrichsen T, Rudolph C, Schambach A, Baum C, Schlegelberger B, Dohner H, Ganser A, Humphries RK 2007 MN1 overexpression induces acute myeloid leukemia in mice and predicts ATRA resistance in patients with AML. Blood 110:1639-1647

200. Heuser M, Beutel G, Krauter J, Dohner K, von Neuhoff N, Schlegelberger B, Ganser A 2006 High meningioma 1 (MN1) expression as a predictor for poor outcome in acute myeloid leukemia with normal cytogenetics. Blood 108:3898-3905

201. Buijs A, van Rompaey L, Molijn AC, Davis JN, Vertegaal AC, Potter MD, Adams C, van Baal S, Zwarthoff EC, Roussel MF, Grosveld GC 2000 The MN1-TEL fusion protein, encoded by the translocation (12;22)(p13;q11) in myeloid leukemia, is a transcription factor with transforming activity. Molecular and cellular biology 20:9281-9293

202. Kawagoe H, Grosveld GC 2005 Conditional MN1-TEL knock-in mice develop acute myeloid leukemia in conjunction with overexpression of HOXA9. Blood 106:4269-4277

203. Kawagoe H, Grosveld GC 2005 MN1-TEL myeloid oncoprotein expressed in multipotent progenitors perturbs both myeloid and lymphoid growth and causes T-lymphoid tumors in mice. Blood 106:4278-4286

204. Carella C, Bonten J, Rehg J, Grosveld GC 2006 MN1-TEL, the product of the t(12;22) in human myeloid leukemia, immortalizes murine myeloid cells and causes myeloid malignancy in mice. Leukemia 20:1582-1592

205. Mrozek K, Dohner H, Bloomfield CD 2007 Influence of new molecular prognostic markers in patients with karyotypically normal acute myeloid leukemia: recent advances. Current opinion in hematology 14:106-114

206. Buijs A, Sherr S, van Baal S, van Bezouw S, van der Plas D, Geurts van Kessel A, Riegman P, Lekanne Deprez R, Zwarthoff E, Hagemeijer A, et al. 1995 Translocation (12;22) (p13;q11) in myeloproliferative disorders results in fusion of the ETS-like TEL gene on 12p13 to the MN1 gene on 22q11. Oncogene 10:1511-1519

207. Meester-Smoor MA, Vermeij M, van Helmond MJ, Molijn AC, van Wely KH, Hekman AC, Vermey-Keers C, Riegman PH, Zwarthoff EC 2005 Targeted disruption of the Mn1 oncogene results in severe defects in development of membranous bones of the cranial skeleton. Molecular and cellular biology 25:4229-4236

208. Neufeld G, Kessler O 2008 The semaphorins: versatile regulators of tumour progression and tumour angiogenesis. Nature reviews 8:632-645

209. Klagsbrun M, Eichmann A 2005 A role for axon guidance receptors and ligands in blood vessel development and tumor angiogenesis. Cytokine Growth Factor Rev 16:535-548

210. Geretti E, Shimizu A, Klagsbrun M 2008 Neuropilin structure governs VEGF and semaphorin binding and regulates angiogenesis. Angiogenesis 11:31-39

211. Tominaga M, Ogawa H, Takamori K 2008 Decreased production of semaphorin 3A in the lesional skin of atopic dermatitis. The British journal of dermatology 158:842-844

212. Casazza A, Fazzari P, Tamagnone L 2007 Semaphorin signals in cell adhesion and cell migration: functional role and molecular mechanisms. Advances in experimental medicine and biology 600:90-108

213. Kolodkin AL, Levengood DV, Rowe EG, Tai YT, Giger RJ, Ginty DD 1997 Neuropilin is a semaphorin III receptor. Cell 90:753-762

214. He Z, Tessier-Lavigne M 1997 Neuropilin is a receptor for the axonal chemorepellent Semaphorin III. Cell 90:739-751

215. Tamagnon L, Artigiani S, Chen H, He Z, Ming GI, Song H, Chedotal A, Winberg ML, Goodman CS, Poo M, Tessier-Lavigne M, Comoglio PM 1999 Plexins are a large family of receptors for transmembrane, secreted, and GPI-anchored semaphorins in vertebrates. Cell 99:71-80

216. Winberg ML, Noordermeer JN, Tamagnone L, Comoglio PM, Spriggs MK, Tessier-Lavigne M, Goodman CS 1998 Plexin A is a neuronal semaphorin receptor that controls axon guidance. Cell 23:903-916

217. Sekido Y, Bader S, Latif F, Chen JY, Duh FM, Wei MH, Albanesi JP, Lee CC, Lerman MI, Minna JD 1996 Human semaphorins A(V) and IV reside in the 3p21.3 small cell lung cancer deletion region and demonstrate distinct expression patterns. Proc Natl Acad Sci USA:4120-4125

218. Sekido Y, Bader S, Latif F, Chen JY, Duh FM, Wei MH, Albanesi JP, Lee CC, Lerman MI, Minna JD 1996 Human semaphorins A(V) and IV reside in the 3p21.3 small cell lung cancer deletion region and demonstrate distinct expression patterns. Proceedings of the National Academy of Sciences of the United States of America 93:4120-4125

219. Nair PN, McArdle L, Cornell J, Cohn SL, Stallings RL 2007 High-resolution analysis of 3p deletion in neuroblastoma and differential methylation of the SEMA3B tumor suppressor gene. Cancer genetics and cytogenetics 174:100-110

220. Kuroki T, Trapasso F, Yendamuri S, Matsuyama A, Alder H, Williams NN, Kaiser LR, Croce CM 2003 Allelic loss on chromosome 3p21.3 and promoter hypermethylation of semaphorin 3B in non-small cell lung cancer. Cancer research 63:3352-3355

221. Tischoff I, Markwarth A, Witzigmann H, Uhlmann D, Hauss J, Mirmohammadsadegh A, Wittekind C, Hengge UR, Tannapfel A 2005 Allele loss and epigenetic inactivation of 3p21.3 in malignant liver tumors. International journal of cancer 115:684-689

222. Tomizawa Y, Sekido Y, Kondo M, Gao B, Yokota J, Roche J, Drabkin H, Lerman MI, Gazdar AF, Minna JD 2001 Inhibition of lung cancer cell growth and induction of apoptosis after reexpression of 3p21.3 candidate tumor suppressor gene SEMA3B. Proc Natl Acad Sci U S A 98:13954-13959

223. Tse C, Xiang RH, Bracht T, Naylor SL 2002 Human Semaphorin 3B (SEMA3B) located at chromosome 3p21.3 suppresses tumor formation in an adenocarcinoma cell line. Cancer Res 62:542-546

224. Falk J, Bechara A, Fiore R, Nawabi H, Zhou H, Hoyo-Becerra C, Bozon M, Rougon G, Grumet M, Puschel AW, Sanes JR, Castellani V 2005 Dual functional activity of semaphorin 3B is required for positioning the anterior commissure. Neuron 48:63-75

225. van der Weyden L, Adams DJ, Harris LW, Tannahill D, Arends MJ, Bradley A 2005 Null and conditional semaphorin 3B alleles using a flexible puroDeltatk loxP/FRT vector. Genesis 41:171-178

226. Chung L, Yang TL, Huang HR, Hsu SM, Cheng HJ, Huang PH 2007 Semaphorin signaling facilitates cleft formation in the developing salivary gland. Development (Cambridge, England) 134:2935-2945

227. Behar O, Golden JA, Mashimo H, Schoen FJ, Fishman MC 1996 Semaphorin III is needed for normal patterning and growth of nerves, bones and heart. Nature 383:525-528

228. Koh JM, Oh B, Lee JY, Lee JK, Kimm K, Kim GS, Park BL, Cheong HS, Shin HD, Hong JM, Kim TH, Park EK, Kim SY 2006 Association study of semaphorin 7a (sema7a) polymorphisms with bone mineral density and fracture risk in postmenopausal Korean women. Journal of human genetics 51:112-117

229. Abe M, Inagaki S, Furuyama T, Iwamoto M, Wakisaka S 2008 Semaphorin 4D inhibits collagen synthesis of rat pulp-derived cells. Archives of oral biology 53:27-34

230. Lallier TE 2004 Semaphorin profiling of periodontal fibroblasts and osteoblasts. J Dent Res 83:677-682

231. Harper J, Gerstenfeld LC, Klagsbrun M 2001 Neuropilin-1 expression in osteogenic cells: down-regulation during differentiation of osteoblasts into osteocytes. Journal of cellular biochemistry 81:82-92

232. DeLuca HF 2004 Overview of general physiologic features and functions of vitamin D. Am J Clin Nutr 80:1689S-1696S

233. Asturias FJ, Jiang YW, Myers LC, Gustafsson CM, Kornberg RD 1999 Conserved structures of mediator and RNA polymerase II holoenzyme. Science (New York, NY 283:985-987

234. Sato S, Tomomori-Sato C, Banks CA, Sorokina I, Parmely TJ, Kong SE, Jin J, Cai Y, Lane WS, Brower CS, Conaway RC, Conaway JW 2003 Identification of mammalian Mediator subunits with similarities to yeast Mediator subunits Srb5, Srb6, Med11, and Rox3. The Journal of biological chemistry 278:15123-15127

235. Guglielmi B, van Berkum NL, Klapholz B, Bijma T, Boube M, Boschiero C, Bourbon HM, Holstege FC, Werner M 2004 A high resolution protein interaction map of the yeast Mediator complex. Nucleic acids research 32:5379-5391

236. Kassem M, Abdallah BM, Saeed H 2008 Osteoblastic cells: differentiation and trans-differentiation. Archives of biochemistry and biophysics 473:183-187

237. Aubin JE 1998 Bone stem cells. J Cell Biochem Suppl 30-31:73-82

238. Bord S, Ireland DC, Beavan SR, Compston JE 2003 The effects of estrogen on osteoprotegerin, RANKL, and estrogen receptor expression in human osteoblasts. Bone 32:136-141

239. Mrak E, Villa I, Lanzi R, Losa M, Guidobono F, Rubinacci A 2007 Growth hormone stimulates osteoprotegerin expression and secretion in human osteoblast-like cells. The Journal of endocrinology 192:639-645

240. Horwood NJ, Elliott J, Martin TJ, Gillespie MT 1998 Osteotropic agents regulate the expression of osteoclast differentiation factor and osteoprotegerin in osteoblastic stromal cells. Endocrinology 139:4743-4746

241. Sutton AL, Zhang X, Ellison TI, Macdonald PN 2005 The 1,25(OH)2D3-regulated transcription factor MN1 stimulates vitamin D receptor-mediated transcription and inhibits osteoblastic cell proliferation. Molecular endocrinology (Baltimore, Md 19:2234-2244

242. MacDonald PN, Dowd DR, Nakajima S, Galligan MA, Reeder MC, Haussler CA, Ozato K, Haussler MR 1993 Retinoid X receptors stimulate and 9-cis retinoic acid inhibits 1,25-dihydroxyvitamin D3-activated expression of the rat osteocalcin gene. Molecular and cellular biology 13:5907-5917

243. Masuyama H, Jefcoat SC, Jr., MacDonald PN 1997 The N-terminal domain of transcription factor IIB is required for direct interaction with the vitamin D receptor and participates in vitamin D-mediated transcription. Molecular endocrinology (Baltimore, Md 11:218-228

244. Baudino TA, Kraichely DM, Jefcoat SC, Jr., Winchester SK, Partridge NC, MacDonald PN 1998 Isolation and characterization of a novel coactivator protein, NCoA-62, involved in vitamin D-mediated transcription. The Journal of biological chemistry 273:16434-16441

245. Hsieh JC, Dang HT, Galligan MA, Whitfield GK, Haussler CA, Jurutka PW, Haussler MR 2004 Phosphorylation of human vitamin D receptor serine-182 by PKA suppresses 1,25(OH)2D3-dependent transactivation. Biochemical and biophysical research communications 324:801-809

246. Hsieh JC, Jurutka PW, Galligan MA, Terpening CM, Haussler CA, Samuels DS, Shimizu Y, Shimizu N, Haussler MR 1991 Human vitamin D receptor is selectively phosphorylated by protein kinase C on serine 51, a residue crucial to its trans-activation function. Proceedings of the National Academy of Sciences of the United States of America 88:9315-9319

247. Smith CL, Onate SA, Tsai MJ, O'Malley BW 1996 CREB binding protein acts synergistically with steroid receptor coactivator-1 to enhance steroid

receptor-dependent transcription. Proceedings of the National Academy of Sciences of the United States of America 93:8884-8888

248. Ding XF, Anderson CM, Ma H, Hong H, Uht RM, Kushner PJ, Stallcup MR 1998 Nuclear receptor-binding sites of coactivators glucocorticoid receptor interacting protein 1 (GRIP1) and steroid receptor coactivator 1 (SRC-1): multiple motifs with different binding specificities. Molecular endocrinology (Baltimore, Md 12:302-313

249. Bove PF, Hristova M, Wesley UV, Olson N, Lounsbury KM, van der Vliet A 2008 Inflammatory levels of nitric oxide inhibit airway epithelial cell migration by inhibition of the kinase ERK1/2 and activation of hypoxia-inducible factor-1 alpha. The Journal of biological chemistry 283:17919-17928

250. Divieti P, Lanske B, Kronenberg HM, Bringhurst FR 1998 Conditionally immortalized murine osteoblasts lacking the type 1 PTH/PTHrP receptor. J Bone Miner Res 13:1835-1845

251. Sutton AL, Zhang X, Dowd DR, Kharode YP, Komm BS, Macdonald PN 2008 Semaphorin 3B is a 1,25-Dihydroxyvitamin D3-induced gene in osteoblasts that promotes osteoclastogenesis and induces osteopenia in mice. Molecular endocrinology (Baltimore, Md 22:1370-1381

252. van Wely KH, Molijn AC, Buijs A, Meester-Smoor MA, Aarnoudse AJ, Hellemons A, den Besten P, Grosveld GC, Zwarthoff EC 2003 The MN1 oncoprotein synergizes with coactivators RAC3 and p300 in RAR-RXR-mediated transcription. Oncogene 22:699-709

253. Shin CS, Lecanda F, Sheikh S, Weitzmann L, Cheng SL, Civitelli R 2000 Relative abundance of different cadherins defines differentiation of mesenchymal precursors into osteogenic, myogenic, or adipogenic pathways. Journal of cellular biochemistry 78:566-577

254. Kawaguchi J, Kii I, Sugiyama Y, Takeshita S, Kudo A 2001 The transition of cadherin expression in osteoblast differentiation from mesenchymal cells: consistent expression of cadherin-11 in osteoblast lineage. J Bone Miner Res 16:260-269

255. Kii I, Amizuka N, Shimomura J, Saga Y, Kudo A 2004 Cell-cell interaction mediated by cadherin-11 directly regulates the differentiation of mesenchymal cells into the cells of the osteo-lineage and the chondro-lineage. J Bone Miner Res 19:1840-1849

256. Kawaguchi J, Azuma Y, Hoshi K, Kii I, Takeshita S, Ohta T, Ozawa H, Takeichi M, Chisaka O, Kudo A 2001 Targeted disruption of cadherin-11 leads to a reduction in bone density in calvaria and long bone metaphyses. J Bone Miner Res 16:1265-1271

257. Jiang F, Li P, Fornace AJ, Jr., Nicosia SV, Bai W 2003 G2/M arrest by 1,25-dihydroxyvitamin D3 in ovarian cancer cells mediated through the induction of GADD45 via an exonic enhancer. The Journal of biological chemistry 278:48030-48040

258. Wang TT, Tavera-Mendoza LE, Laperriere D, Libby E, MacLeod NB, Nagai Y, Bourdeau V, Konstorum A, Lallemant B, Zhang R, Mader S, White JH 2005 Large-scale in silico and microarray-based identification of direct 1,25-dihydroxyvitamin D3 target genes. Mol Endocrinol 19:2685-2695

259. Eelen G, Verlinden L, van Camp M, van Hummelen P, Marchal K, de Moor B, Mathieu C, Carmeliet G, Bouillon R, Verstuyf A 2004 The effects of 1alpha,25-dihydroxyvitamin D3 on the expression of DNA replication genes. J Bone Miner Res 19:133-146

260. Meester-Smoor MA, Molijn AC, Zhao Y, Groen NA, Groffen CA, Boogaard M, van Dalsum-Verbiest D, Grosveld GC, Zwarthoff EC 2007 The MN1 oncoprotein activates transcription of the IGFBP5 promoter through a CACCC-rich consensus sequence. Journal of molecular endocrinology 38:113-125

261. Meester-Smoor MA, Janssen MJ, Grosveld GC, de Klein A, van IWF, Douben H, Zwarthoff EC 2008 MN1 affects expression of genes involved in hematopoiesis and can enhance as well as inhibit RAR/RXR-induced gene expression. Carcinogenesis 29:2025-2034

262. Ritchie HH, Hughes MR, Thompson ET, Malloy PJ, Hochberg Z, Feldman D, Pike JW, O'Malley BW 1989 An ochre mutation in the vitamin D receptor gene causes hereditary 1,25-dihydroxyvitamin D3-resistant rickets in three families. Proceedings of the National Academy of Sciences of the United States of America 86:9783-9787

263. Kato S 1999 Genetic mutation in the human 25-hydroxyvitamin D3 1alpha-hydroxylase gene causes vitamin D-dependent rickets type I. Molecular and cellular endocrinology 156:7-12

264. Olsen BR, Reginato AM, Wang W 2000 Bone development. Annual review of cell and developmental biology 16:191-220

265. Liu W, Lan Y, Pauws E, Meester-Smoor MA, Stanier P, Zwarthoff EC, Jiang R 2008 The Mn1 transcription factor acts upstream of Tbx22 and preferentially regulates posterior palate growth in mice. Development (Cambridge, England) 135:3959-3968

266. Samee N, de Vernejoul MC, Levi G 2007 Role of DLX regulatory proteins in osteogenesis and chondrogenesis. Critical reviews in eukaryotic gene expression 17:173-186

267. Hassan MQ, Tare R, Lee SH, Mandeville M, Weiner B, Montecino M, van Wijnen AJ, Stein JL, Stein GS, Lian JB 2007 HOXA10 controls osteoblastogenesis by directly activating bone regulatory and phenotypic genes. Molecular and cellular biology 27:3337-3352

268. Dobreva G, Chahrour M, Dautzenberg M, Chirivella L, Kanzler B, Farinas I, Karsenty G, Grosschedl R 2006 SATB2 is a multifunctional determinant of craniofacial patterning and osteoblast differentiation. Cell 125:971-986

269. Lecanda F, Warlow PM, Sheikh S, Furlan F, Steinberg TH, Civitelli R 2000 Connexin43 deficiency causes delayed ossification, craniofacial abnormalities, and osteoblast dysfunction. The Journal of cell biology 151:931-944

270. Kawai S, Yamauchi M, Wakisaka S, Ooshima T, Amano A 2007 Zinc-finger transcription factor odd-skipped related 2 is one of the regulators in osteoblast proliferation and bone formation. J Bone Miner Res 22:1362-1372

271. Sanford LP, Ormsby I, Gittenberger-de Groot AC, Sariola H, Friedman R, Boivin GP, Cardell EL, Doetschman T 1997 TGFbeta2 knockout mice have multiple developmental defects that are non-overlapping with other TGFbeta knockout phenotypes. Development (Cambridge, England) 124:2659-2670

272. Beresford JN, Bennett JH, Devlin C, Leboy PS, Owen ME 1992 Evidence for an inverse relationship between the differentiation of adipocytic and osteogenic cells in rat marrow stromal cell cultures. Journal of cell science 102 (Pt 2):341-351

273. Dorheim MA, Sullivan M, Dandapani V, Wu X, Hudson J, Segarini PR, Rosen DM, Aulthouse AL, Gimble JM 1993 Osteoblastic gene expression during adipogenesis in hematopoietic supporting murine bone marrow stromal cells. Journal of cellular physiology 154:317-328

274. Nuttall ME, Gimble JM 2000 Is there a therapeutic opportunity to either prevent or treat osteopenic disorders by inhibiting marrow adipogenesis? Bone 27:177-184

275. Duque G 2003 Will reducing adopogenesis in bone increase bone mass?: PPARgamma2 as a key target in the treatment of age-related bone loss. Drug news & perspectives 16:341-346

276. Hong JH, Hwang ES, McManus MT, Amsterdam A, Tian Y, Kalmukova R, Mueller E, Benjamin T, Spiegelman BM, Sharp PA, Hopkins N, Yaffe MB 2005 TAZ, a transcriptional modulator of mesenchymal stem cell differentiation. Science (New York, NY 309:1074-1078

277. Lecka-Czernik B, Moerman EJ, Grant DF, Lehmann JM, Manolagas SC, Jilka RL 2002 Divergent effects of selective peroxisome proliferator-activated receptor-gamma 2 ligands on adipocyte versus osteoblast differentiation. Endocrinology 143:2376-2384

278. Sciaudone M, Gazzerro E, Priest L, Delany AM, Canalis E 2003 Notch 1 impairs osteoblastic cell differentiation. Endocrinology 144:5631-5639

279. Kobayashi H, Gao Y, Ueta C, Yamaguchi A, Komori T 2000 Multilineage differentiation of Cbfa1-deficient calvarial cells in vitro. Biochemical and biophysical research communications 273:630-636

280. Kong J, Li YC 2006 Molecular mechanism of 1,25-dihydroxyvitamin D3 inhibition of adipogenesis in 3T3-L1 cells. American journal of physiology 290:E916-924

281. Kelly KA, Gimble JM 1998 1,25-Dihydroxy vitamin D3 inhibits adipocyte differentiation and gene expression in murine bone marrow stromal cell clones and primary cultures. Endocrinology 139:2622-2628

282. Sutton AL, MacDonald PN 2003 Vitamin D: More Than a "Bone-a-Fide" Hormone. Mol Endocrinol 17:777-791

283. Malloy PJ, Pike JW, Feldman D 1999 The vitamin D receptor and the syndrome of hereditary 1,25- dihydroxyvitamin D-resistant rickets. Endocr Rev 20:156-188

284. van Leeuwen JP, van Driel M, van den Bemd GJ, Pols HA 2001 Vitamin D control of osteoblast function and bone extracellular matrix mineralization. Crit Rev Eukaryot Gene Expr 11:199-226

285. Shevde NK, Plum LA, Clagett-Dame M, Yamamoto H, Pike JW, DeLuca HF 2002 A potent analog of 1alpha,25-dihydroxyvitamin D3 selectively induces bone formation. Proc Natl Acad Sci U S A 99:13487-13491

286. Peleg S, Uskokovic M, Ahene A, Vickery B, Avnur Z 2002 Cellular and molecular events associated with the bone-protecting activity of the noncalcemic vitamin D analog Ro-26-9228 in osteopenic rats. Endocrinology 143:1625-1636

287. Prince CW, Butler WT 1987 1,25-Dihydroxyvitamin D3 regulates the biosynthesis of osteopontin, a bone-derived cell attachment protein, in clonal osteoblast-like osteosarcoma cells. Coll Relat Res 7:305-313

288. Yoon K, Buenaga R, Rodan GA 1987 Tissue specificity and developmental expression of rat osteopontin. Biochem Biophys Res Commun 148:1129-1136

289. Price PA, Baukol SA 1980 1,25-Dihydroxyvitamin D3 increases the synthesis of the vitamin K-dependent bone protein by osteosarcoma cells. J Biol Chem 255:11660-11663

290. Tamagnone L, Comoglio PM 2004 To move or not to move? Semaphorin signalling in cell migration. EMBO Rep 5:356-361

291. Harper J, Gerstenfeld LC, Klagsbrun M 2001 Neuropilin-1 expression in osteogenic cells: down-regulation during differentiation of osteoblasts into osteocytes. J Cell Biochem 81:82-92

292. Rossert J, Eberspaecher H, de Crombrugghe B 1995 Separate cis-acting DNA elements of the mouse pro-alpha 1(I) collagen promoter direct expression of reporter genes to different type I collagen-producing cells in transgenic mice. The Journal of cell biology 129:1421-1432

293. Turgeman G, Zilberman Y, Zhou S, Kelly P, Moutsatsos IK, Kharode YP, Borella LE, Bex FJ, Komm BS, Bodine PV, Gazit D 2002 Systemically administered rhBMP-2 promotes MSC activity and reverses bone and cartilage loss in osteopenic mice. Journal of cellular biochemistry 86:461-474

294. Babij P, Zhao W, Small C, Kharode Y, Yaworsky PJ, Bouxsein ML, Reddy PS, Bodine PV, Robinson JA, Bhat B, Marzolf J, Moran RA, Bex F 2003 High bone mass in mice expressing a mutant LRP5 gene. J Bone Miner Res 18:960-974

295. Erlebacher A, Filvaroff EH, Ye JQ, Derynck R 1998 Osteoblastic responses to TGF-beta during bone remodeling. Molecular biology of the cell 9:1903-1918

296. Parfitt AM, Drezner MK, Glorieux FH, Kanis JA, Malluche H, Meunier PJ, Ott SM, Recker RR 1987 Bone histomorphometry: standardization of nomenclature, symbols, and units. Report of the ASBMR Histomorphometry Nomenclature Committee. J Bone Miner Res 2:595-610

297. Ragab AA, Lavish SA, Banks MA, Goldberg VM, Greenfield EM 1998 Osteoclast differentiation requires ascorbic acid. J Bone Miner Res 13:970-977

298. Zhao M, Qiao M, Harris SE, Oyajobi BO, Mundy GR, Chen D 2004 Smurf1 inhibits osteoblast differentiation and bone formation in vitro and in vivo. J Biol Chem 279:12854-12859

299. Kumanogoh A, Kikutani H 2003 Roles of the semaphorin family in immune regulation. Adv Immunol 81:173-198

300. Gomez C, Burt-Pichat B, Mallein-Gerin F, Merle B, Delmas PD, Skerry TM, Vico L, Malaval L, Chenu C 2005 Expression of Semaphorin-3A and its receptors in endochondral ossification: potential role in skeletal development and innervation. Dev Dyn 234:393-403

301. Delorme G, Saltel F, Bonnelye E, Jurdic P, Machuca-Gayet I 2005 Expression and function of semaphorin 7A in bone cells. Biology of the cell / under the auspices of the European Cell Biology Organization 97:589-597

302. Liu BP, Strittmatter SM 2001 Semaphorin-mediated axonal guidance via Rho-related G proteins. Curr Opin Cell Biol 13:619-626

303. Lee NK, Choi YG, Baik JY, Han SY, Jeong DW, Bae YS, Kim N, Lee SY 2005 A crucial role for reactive oxygen species in RANKL-induced osteoclast differentiation. Blood 106:852-859

304. Razzouk S, Lieberherr M, Cournot G 1999 Rac-GTPase, osteoclast cytoskeleton and bone resorption. Eur J Cell Biol 78:249-255

305. ten Berge D, Brouwer A, Korving J, Martin JF, Meijlink F 1998 Prx1 and Prx2 in skeletogenesis: roles in the craniofacial region, inner ear and limbs. Development (Cambridge, England) 125:3831-3842

306. Qiu M, Bulfone A, Martinez S, Meneses JJ, Shimamura K, Pedersen RA, Rubenstein JL 1995 Null mutation of Dlx-2 results in abnormal morphogenesis of proximal first and second branchial arch derivatives and abnormal differentiation in the forebrain. Genes & development 9:2523-2538

307. Satokata I, Maas R 1994 Msx1 deficient mice exhibit cleft palate and abnormalities of craniofacial and tooth development. Nature genetics 6:348-356

308. Vidal O, Lindberg MK, Hollberg K, Baylink DJ, Andersson G, Lubahn DB, Mohan S, Gustafsson JA, Ohlsson C 2000 Estrogen receptor specificity in the regulation of skeletal growth and maturation in male mice. Proceedings of the National Academy of Sciences of the United States of America 97:5474-5479

309. Modder UI, Sanyal A, Xu J, O'Malley BW, Spelsberg TC, Khosla S 2008 The skeletal response to estrogen is impaired in female but not in male steroid receptor coactivator (SRC)-1 knock out mice. Bone 42:414-421

310. Modder UI, Sanyal A, Kearns AE, Sibonga JD, Nishihara E, Xu J, O'Malley BW, Ritman EL, Riggs BL, Spelsberg TC, Khosla S 2004 Effects of loss of steroid receptor coactivator-1 on the skeletal response to estrogen in mice. Endocrinology 145:913-921

311. Cianferotti L, Demay MB 2007 VDR-mediated inhibition of DKK1 and SFRP2 suppresses adipogenic differentiation of murine bone marrow stromal cells. Journal of cellular biochemistry 101:80-88

312. Takegahara N, Takamatsu H, Toyofuku T, Tsujimura T, Okuno T, Yukawa K, Mizui M, Yamamoto M, Prasad DV, Suzuki K, Ishii M, Terai K, Moriya M, Nakatsuji Y, Sakoda S, Sato S, Akira S, Takeda K, Inui M, Takai T, Ikawa M, Okabe M, Kumanogoh A, Kikutani H 2006 Plexin-A1 and its interaction with DAP12 in immune responses and bone homeostasis. Nature cell biology 8:615-622

313. Riquelme E, Tang M, Baez S, Diaz A, Pruyas M, Wistuba, II, Corvalan A 2007 Frequent epigenetic inactivation of chromosome 3p candidate tumor suppressor genes in gallbladder carcinoma. Cancer letters 250:100-106

314. Castro-Rivera E, Ran S, Brekken RA, Minna JD 2008 Semaphorin 3B inhibits the phosphatidylinositol 3-kinase/Akt pathway through neuropilin-1 in lung and breast cancer cells. Cancer research 68:8295-8303